RECONFIGURABLE ULTRA WIDEBAND ANTENNA DESIGN AND DEVELOPMENT FOR WIRELESS COMMUNICATION

(REKAAN DAN PEMBANGUNAN ANTENA JALUR LEBAR ULTRA BOLEH UBAH UNTUK KOMUNIKASI WAYARLES)

THAREK ABDUL RAHMAN

RESEARCH PROJECT VOT NO.:
79028

Wireless Communication Centre
Faculty of Electrical Engineering
Universiti Teknologi Malaysia

2008

ACKNOWLEDGEMENTS

Alhamdulillah. I praise and glorify be only to **Allah SWT** the Almighty, the Most Beneficent and the Most Merciful, whose blessings and guidance have helped me to be able to finish this project. I wish to thank the Ministry of Higher Education Malaysia and Research Management Centre, Universiti Teknologi Malaysia for their financial support during the full term of this research.

Many thanks to my colleague Dr. Razali Ngah, my Ph.D student Ms. Yusnita Rahayu and also to my research assistant Mr. Khomeini Abu for their support. This project will not be completed without their full encouragement and support as a solid team. This project is a Ph.D research work that has been done intensively by Ms. Yusnita through out her study.

Last but not least, I am grateful for the encouragement and support provided by the many friends in Wireless Communication Centre (WCC) UTM.

ABSTRACT

A few years after the early investigation on ultra wideband (UWB) wireless system, considerable research efforts have been put into the design of UWB antennas and systems for communications. These UWB antennas are essential for providing wireless wideband communications based on the use of very narrow pulses on the order of nanoseconds, covering a very wide bandwidth in the frequency domain, and over very short distances at very low power densities. In this project, new models of T, L and U slotted UWB antennas are proposed by studying their current distribution characteristics. The wideband behavior is due to the fact that the currents along the edges of the slots introduce an additional resonance, which, in conjunction with the resonance of the main patch, produce an overall broadband frequency response characteristic. These antennas are considerable small than others listed in the references, which their sizes are less than a wavelength, compact, and suitable for many UWB applications. The configuration of slots type for both patches and feeding strip are considered as a novelty and contribution in this project. The geometry of the antenna implies the current courses and makes it possible to identify active and neutral zones in the antenna, thus it will be possible to fix which elements will act on each characteristic. This project also investigated the ability of slotted UWB antennas to reject the interference from licensed Fix Wireless Access (FWA), High performance local area network (HIPERLAN) and wireless local area network (WLAN) within the same propagation environment. Inserting a half-wavelength slot structure with additional small patches gap attached have resulted frequency notched band characteristics. The small patches gap instead of switching. The measured return loss, radiation patterns, and phase agree well with the simulated results. The antenna provides an omnidirectional pattern with the return loss less than -10 dB and linear in phase.

Key researchers:

Prof. Dr. Tharek Abdul Rahman (Project Leader)
Dr Razali Ngah
Ms. Yusnita Rahayu
Mr. Khomeini Abu

E-mail : tharek@fke.utm.my
Tel. No. : 07-5536106
Vote No. : 79028

ABSTRAK

Beberapa tahun setelah peneraju asal pada sistem wayarles jalur sangat lebar (UWB), sokongan penyelidikan telah ditumpukan pada reka bentuk antena UWB dan sistem komunikasi. Antena UWB ini sangat diperlukan dalam penyediaan komunikasi jalur lebar berasaskan penggunaan denyut yang sangat sempit dalam kiraan nano saat, meliputi jalur yang sangat lebar dalam domain frekuensi, dan mencakupi jarak yang sangat pendek pada kerapatan tenaga yang sangat rendah. Dalam projek ini, model terbaru antena UWB terselot-T, L dan U di cadangkan dengan mengkaji karakteristik pengagihan arus. Perilaku jalur lebar disebabkan pada kenyataan bahawa arus disepanjang tepian selot memperkenalkan satu resonan tambahan, yang mana ianya berkaitan dengan resonan tampal asas, sehingga menghasilkan keseluruhan karakteristik sambutan frekuensi yang sangat lebar. Antena-antena ini berukuran lebih kecil bila diperbandingkan dengan antena lainnya yang tersenarai dalam rujukan, ukurannya lebih kecil daripada satu panjang gelombang, padat, dan sangat sesuai digunakan untuk pelbagai aplikasi UWB. Konfigurasi jenis selot pada kedua tampal dan jalur suapan adalah *novelty* dan sebagai kontribusi dalam projek ini. Geometri antena mempengaruhi arah arus dan dengan menentukan zon aktif dan neutral pada antenna, maka elemen yang sesuai dapat ditentukan bagi setiap karakteristik. Projek ini juga menkaji kemampuan antena UWB terselot untuk menolak gangguan isyarat daripada Capaian Wayarles Tetap (FWA), Rangkaian Kawasan Tempatan Berprestasi Tinggi (HIPERLAN) dan Rangkaian kawasan Tempatan Wayarles (WLAN) yang wujud dalam kawasan yang sama. Kemasukan sebuah struktur selot separuh panjang gelombang dengan penambahan sela tampal yang kecil berjaya menghasilkan karakteristik frekuensi *notched band*. Sela tampal yang kecil ini digunakan bagi mewakili suatu suis. Keputusan pengujian seperti kehilangan kembali, corak sinaran dan fasa didapati menepati keputusan simulasi. Antena ini memberikan corak sinaran semua arah dengan kehilangan kembali kurang daripada -10 dB dan mempunyai sambutan fasa yang linar.

Penyelidik Utama:

Prof. Dr. Tharek Abdul Rahma (Ketua Projek)
Dr. Razali Ngah
Ms. Yusnita Rahayu
Mr. Khomeini

E-mail : tharek@fke.utm.my
Tel. No. : 07-5536106
Vote No. : 79028

TABLE OF CONTENTS

LIST OF TABLES

LIST OF FIGURES

LIST OF ABBREVIATIONS

AUT		Antenna Under Test
CEPT		Conference of European Posts and Telecommunications
CATV		Cable Television
DS-UWB		Direct Sequence Ultra Wideband
DAA		Detect and Avoid
DC		Direct Current
ETSI	:	European Telecommunications Standard Institute
ECC	:	Electronic Communications Committee
ETRI		Electronics and Telecommunications Research Institute
FCC		Federal Communication Committee
FWA		Fixed Wireless Access
FDTD		Finite Difference Time Domain
FR4		Flame Resistant 4
GPS		Global Positioning System
HIPERLAN		High Performance Local Area Network
H-cut		Horizontal cut
IEEE		Institute of Electrical and Electronics Engineers
IDA		Infocomm Development Authority
IR		Impulse Radio
MIC		Ministry of Internal Affairs and Communications
MB		Multi Band
MCMC		Malaysian Communications and Multimedia Commissions
OFDM		Orthogonal Frequency Division Multiplexing
PDA		Personal Digital Assistance
PCB		Printed Circuit Board
RCS		Radar Cross Section
RF		Radio Frequency
SMA		SubMiniature version A
SRR		Split Ring Resonator
SB		Single Band
TEM		Transverse Electric Magnetic
TDMA		Time Division Multiple Access
UFZ		UWB Friendly Zone
UWB		Ultra Wideband
VSWR		Voltage Standing Wave Ratio
V-cut		Vertical cut
WPAN		Wireless Personal Area Network
WLAN		Wireless Local Area Network

LIST OF SYMBOLS

BW		Bandwidth
f_H		High frequency
f_L		Low frequency
f_C		Centre frequency
dBm		Decibel (milliwatt)
MHz		Megahertz
GHz		Gigahertz
P_{RX}		Antenna received power
P_{TX}		Antenna transmitted power
G_{TX}		Transmit antenna gain
G_{RX}		Receive antenna gain
A		Aperture
c		Speed of light
θ		Theta angle
φ		Phi angle
e_r		Reflection efficiency
P_{rad}		Radiated power
P_{in}		Input power
χ_n	-	Eigenvalue
J_n		Characteristic modes
w_s		Slot width
l_s		Slot length
r		Radius
λ		Wavelength
S_{11}		Return loss
R_e		Real part
I_m	-	Imaginary part
ε_r		Relative permittivity
E-plane		Electric plane
H-plane		Magnetic plane

LIST OF APPENDICES

CHAPTER 1

INTRODUCTION

1.1 Introduction

Ultra Wideband (UWB) is currently receiving special attention and is quite a hot topic in industry and academia. UWB short-range wireless communication is different from a traditional carrier wave system. UWB waveforms are short time duration and have some rather unique properties. The benefits of UWB technology are derived from its unique characteristics that are the reasons why it presents a more eloquent solution to wireless broadband than other technologies. The unique characteristics are listed below [1]:

Firstly, an inherent capability for integration in low cost, low power Integrated Circuit (IC) processes. UWB system based on impulse radio features low cost and low complexities which arise from the essentially base-band nature of the signal transmission. UWB does not modulate and demodulate a complex carrier waveform, so it does not require components such as mixers, filters, amplifiers and local oscillators.

Secondly, UWB has an ultra wide frequency bandwidth; it can achieve huge capacity as high as hundreds of Mbps or even several Gbps with distances of 1 to 10 meters [2]. Thus, the UWB is a promising technology for Wireless Personal Area Network (WPAN). In recent years, more interests have been put into WPAN technology worldwide. The future WPAN aims to provide reliable wireless connections between computers, portable devices and consumer electronics within a

short range. Furthermore, fast data storage and exchange between these devices will also be accomplished. This requires a data rate which is much higher than what can be achieved through currently existing wireless technologies.

Thirdly, UWB system is extremely fine time and range solution even through lossy, opaque media. And fourthly, UWB system has immunity from multipaths.

Fifthly, non-interfering operation with existing services. In spreading signals over very wide bandwidths, the UWB concept is especially attractive since it facilitates optimal sharing of a given bandwidth between different systems and applications. UWB systems are highly frequency adaptive, enabling them to be positioned anywhere within the RF spectrum. This feature avoids interference to existing services, while fully utilizing the available spectrum. UWB systems operate at extremely low power transmission levels. Therefore, UWB short-range radio technology complements other longer-range radio technologies such as Wireless Fidelity (WiFi), Worldwide Interoperability for Microwave Access (WiMAX), and cellular wide area communications.

Lastly, UWB has low probability of detection and interception. UWB provides high secure and high reliable communication solutions. Due to the low energy density, the UWB signal is noise-like, which makes unintended detection quite difficult. Furthermore, the “noise-like" signal has a particular shape; in contrast, real noise has no shape. For this reason, it is almost impossible for real noise to obliterate the pulse because interference would have to spread uniformly across the entire spectrum to obscure the pulse. Interference in only part of the spectrum reduces the amount of received signal, but the pulse still can be recovered to restore the signal. Hence UWB is perhaps the most secure means of wireless transmission ever previously available [3].

As with any technology, there are always applications that may be better served by other approaches. For example, for extremely high data rate (10’s of Gigabits/second and higher), point-to-point or point-to-multipoint applications, it is difficult today for UWB systems to compete with high capacity optical fiber or optical wireless communications systems. The high cost associated with optical fiber

installation and the inability of an optical wireless signal to penetrate a wall dramatically limits the applicability of optically-based systems for in-home or in-building applications. In addition, optical wireless systems have extremely precise pointing requirements, obviating their use in mobile environments.

1.2 Research Background

The UWB technology has experienced many significant developments in recent years. However, there are still challengers in making this technology live up to its full potential. One particular challenge is the UWB antenna design. UWB technology has had a substantial effect on antenna design. The UWB antennas have to be able to transmit pulses as accurately and efficiently as possible. The spectrum allocated certainly requires transmitters and receivers with wideband antennas.

Thorough literature survey, there are two vital design considerations in UWB radio systems. One is radiated power density spectrum shaping must comply with certain emission limit mask for coexistence with other electronic systems [4]. Another is that the design source pulses and transmitting/receiving antennas should be optimal for performance of overall systems [5]. Emission limits will be crucial considerations for the design of source pulses and antennas in UWB systems.

The main challenge in UWB antenna design is achieving the extremely wide impedance bandwidth while still maintaining high radiation efficiency. By definition, an UWB antenna must be operable over the entire 3.1 GHz - 10.6 GHz frequency range. Therefore, the UWB antenna must achieve almost a decade of impedance bandwidth, spanning 7.5 GHz. The high radiation efficiency is also required especially for UWB applications to ensure the transmit power spectral density requirement achieved. Conductor and dielectric losses should be minimized in order to maximize radiation efficiency. High radiation efficiency is imperative for an UWB antenna because the transmit power spectral density is excessively low. Therefore, any excessive losses incurred by the antenna could potentially compromise the functionality of the system.

Next, the performance of UWB antenna is required to have a constant group delay. Group delay is given by the derivative of the unwrapped phase of an antenna. If the phase is linear throughout the frequency range, the group delay will be constant for the frequency range. This is an important characteristic because it helps to indicate how well a UWB pulse will be transmitted and to what degree it may be distorted or dispersed. The antennas required to have a non-dispersive characteristic in time and frequency, providing a narrow, pulse duration to enhance a high data throughput. It is also a parameter that is not typically considered for narrowband antenna design because linear phase is naturally achieved for narrowband resonance.

In addition, a nearly omni-directional radiation pattern is desirable in that it enables freedom in the receiver and transmitter location. This implies maximizing the half power beam-width and minimizing directivity and gain. It is also highly desirable that the antenna feature low profile and compatibility for integration with printed circuit board (PCB) [6].

A good design of UWB antenna should be optimal for the performance of overall system. For example, the antenna should be designed such that the overall device (antenna and Radio Frequency (RF) front end) complies with the mandatory power emission mask given by the Federal Communication Committee (FCC) or other regulatory bodies [6]. But not the least important, a UWB antenna is required to achieve good time domain characteristics. Minimum pulse distortion in the received waveform, is a primary concern of a suitable UWB antenna because the signal is the carrier of useful information. For the narrow band case, it is approximated that an antenna has same performance over the entire bandwidth and the basic parameters, such as gain and return loss, have little variation across the operational band.

Today the state of the art of UWB antennas focuses in the microstrip, slot and planar monopole antennas with different matching techniques to improve the bandwidth ratio without loss of its radiation pattern properties [7]. The expected antennas are small size, omni directional patterns, and simple structure that produce low distortion but can provide large bandwidth [8].

In the past, one serious limitation of microstrip antennas was the narrow bandwidth characteristic, being 15% to 50% that of commonly used antenna elements such as dipoles, and slots [9]. This limitation was successfully removed achieving a matching impedance bandwidth of up 90%. To increase the matching impedance bandwidth ratio it was necessary to increase the size, height, volume or feeding and matching techniques [10]. Variety of matching techniques have been proposed in the literature reviews, such as the use of slot [11][12], bevel or taper at the bottom of patch [13], notch and partial ground plane [12]. There is a growing demand for small and low cost UWB antennas that can provide satisfactory performances in both frequency domain and time domain.

The planar monopole antennas are promising antennas for UWB applications due to their simple structure, low profile, easy to fabricate and UWB characteristics with nearly omni-directional radiation patterns [6][14][15]. Planar monopole antennas feature broad impedance bandwidth but somewhat suffer high cross-polarization radiation levels. The large lateral size or asymmetric geometry of the planar radiator causes the cross-polarized radiation. Fortunately, the purity of the polarization issue is not critical, particularly for the antennas used for portable devices [16]. There are several UWB planar antenna designs, including planar half-disk antenna [17], planar horn antenna [18], and metal plate antenna [19], have been reported.

Even though UWB is recommended by the FCC of United States (U.S) to operate with maximum in-band effective incident radiated power of -41.3 dBm/MHz within the band from 3.1 GHz to 10.6 GHz, there have been almost 1000 complaints logged against UWB deployment so far [20]. Evaluation of interference between Multiband Orthogonal Frequency Division Multiplexing (MB-OFDM) UWB and Wireless Local Area Network (WLAN) systems using a Gigahertz Transverse Electromagnetic (GTEM) cell has been proposed in [21]. As a result, when the frequencies of the MB-OFDM UWB corresponded to out-of-band radiation for 11a (Band #3), MB-OFDM UWM did not interfere with the WLAN system. In the other hand, when frequencies of the MB-OFDM UWB corresponded to in-band radiation for 11a (Band #4), although the interference power of MB-OFDM UWB was less than receiver noise, the MB-OFDM UWB systems interfered with the WLAN.

Evaluation of interference between Direct Sequence spread spectrum UWB (DS-UWB) and WLAN systems using a GTEM cell has already been presented a year before in [22]. Even if the UWB signal is smaller than the receiver noise of WLAN, the throughput characteristics deteriorate than those in case of the non-interference [22]. Therefore, recently the consideration of UWB antennas is not only focused on an extremely wide frequency bandwidth, but on the ability of rejecting the interference from WLAN 11.a (5725 - 5825 MHz) and High Performance Local Area Network (HIPERLAN) (5150 - 5350 MHz) within the same propagation environment [23].

To avoid the interference between the UWB, WLAN and HIPERLAN systems, a band-notch filter in UWB systems is necessary. However, the use of a filter will increase the complexity of the UWB systems [24]. One of the solutions proposed, as far as antennas are concerned, was to design frequency notched antenna. Therefore, several techniques used to introduce a notched band for rejecting the WLAN and HIPERLAN interference have been investigated, which include such as inserting a half-wavelength slot structure [23][25]-[29], slitting on the edges [30]-[31], utilizing fractal feeding structure [32], and parasitic quarter-wave patch [33] or parasitic open-circuit stub [34]. With the notched band characteristic, the antenna allows to reconfigurable its frequency that only responsive to other frequencies beyond the rejection bands within UWB bandwidth.

1.3 Problem Statements

One of the critical issues in this UWB antenna design is the size of the antenna for portable devices, because the size affects the gain and bandwidth greatly [35]. Therefore, to miniaturize the antennas capable of providing ultra wide bandwidth for impedance matching and acceptable gain will be a challenging task [5]. Planar monopole is used to reduce the size of the proposed antennas. Some novelty UWB planar monopole antennas are investigated in detail in order to understand their operations; find out the mechanism that leads to UWB

characteristics and to obtain some quantitative guidelines for designing of this type of antennas.

In order to obtain the ultra wide bandwidth and omni directional radiation pattern, four matching techniques are applied to the proposed UWB antennas, such as the use of slots, the use of bevels and notches at the bottom of patch, the truncation ground plane, and the slotted ground plane. All these techniques are applied to the small UWB antenna without degrading the required UWB antenna's performance. The size of slots, bevels and notches are critically affect to the impedance bandwidth. The distance between truncation ground plane to the bottom of the patch is as matching point, where it determines the resonance frequency. To ensure the broad bandwidth can be obtained, the proper designs on those parameters are required.

The theory characteristic modes are used to design and optimize the proposed UWB antennas as well as some new designs are studied. From the study of the behavior of characteristic modes, important information about the resonant frequency and the bandwidth of an antenna can be obtained. The current behaviors of the antenna are investigated in order to obtain several new slotted UWB antennas. High radiation efficiency and linear phase are also required.

A licensed Fix Wireless Access (FWA) for point to multipoint radio systems assigned by Malaysian Communications and Multimedia Commissions (MCMC) for 3.4 to 3.7 GHz is considered giving a potential interference to UWB application. This is due to the allocation frequency for this FWA within the UWB range. Thus, the proposed notched antenna is not only designed to reject interference from WLAN, HIPERLAN but also from FWA. In order to meet the goal, the previous designed UWB slotted antenna is chosen as a basic type of reconfigurable slotted UWB antennas. This is due to the slot antennas are good candidate to meet the needs for UWB communication and antenna size reduction due to their compact and broadband. To design this reconfigurable UWB slotted antenna with three notched bands characteristics by using a simple structure of antenna is very challenging task. In this thesis, this antenna is known as reconfigurable UWB slotted antenna. The reconfigurability characteristic means the ability of UWB slotted antenna to reject

certain frequencies by using some small gaps, instead of switches, without any degrading the radiation pattern. The controllable slot length by the gaps is intended to reject the required frequencies.

Finally, two types of UWB antennas have been designed and resulted in this thesis. One is slotted antenna type for general UWB applications. The second one is the reconfigurable UWB slotted antenna. This second type of antenna is used to reject the interference from existing wireless communication systems within the UWB range such as FWA, HIPERLAN, and WLAN bands. However this is still the newest issue, the existing publications mostly on UWB antenna with notched bands on HIPERLAN/WLAN bands. This thesis is working with an additional notched on FWA band in order to give contribution in UWB antenna development.

1.4 Research Objective

The main purpose of this research is to propose small novel types of reconfigurable UWB antennas. The proposed antennas have capability to reconfigurable their frequency to a narrower bandwidth over UWB bandwidth (3.1 GHz - 10.6 GHz) while excepting from interference with existing FWA, HIPERLAN, and WLAN bands with band notched characteristics.

1.5 Research Scope and Methodology

The research scope is focused on slotted UWB antennas designs which provide an ultra wide bandwidth. Truncation ground plane and notches/bevels techniques are added to improve the impedance matching. The reconfigurability antennas characteristics are achieved by varying the length of slots with on/off the small gaps, instead of switches. In order to achieve the objective, a number of activities have been identified, as outline below:

- Investigate characteristics of UWB antenna by means of simulation and numerical analysis.
- Simulate the UWB antenna design model using antenna simulation software before the actual prototype built.
- Integrate some small gaps into the proposed antenna to evaluate the reconfigurable characteristics performance.
- Develop a new design prototype of reconfigurable UWB antenna.
- Antenna performance evaluation and optimization.

1.6 Thesis Outline

The thesis is divided into six chapters. Following is an introductory chapter that defines the importance of this research, objective, and scope. The introduction of UWB technology, the challenges in UWB antenna design, the UWB notched band characteristics and the current issues are also highlighted. The review of UWB applications technology is given in Chapter 2. This chapter begins by the UWB history and definition of UWB signal with some international standardization on it. A wide variety of wideband antennas are presented as well. Some applications applied for this UWB technology such as communication system, radar system and positioning system are discussed. With UWB techniques, it becomes feasible to fuse these unique capabilities into a single system. The review of UWB antenna with notched band characteristics with capability to reject interference generated between other communication systems is presented. Finally, overview of short pulse generation and link performance are discussed.

The literature review examined a comprehensive background of other related research works and the fundamental antenna parameters that should be considered in designing UWB antenna, and potential technologies for physical construction given in Chapter 3. Design methodology applied in this proposed UWB antenna and reconfigurable UWB antenna is discussed in detail. The key differences and considerations for UWB antenna design are also discussed in depth as several

antennas are presented with these considerations in mind. Several bandwidth enhancement techniques such as various geometry perturbation and Genetic Algorithm will be highlighted in order to obtain optimization in size and performance.

Chapter 4 elaborates on the design methodology mentioned in the previous sections. Some new novelty slotted UWB antennas and reconfigurable UWB antennas are presented and design requirements, general strategy for the design are discussed in detail. By properly design the slots and gaps have provided band notched characteristics at 3.4 - 3.7 GHz and 5.150 - 5.850 GHz. The novelty is in term of the type of slots used and it is considered as a contribution in this thesis.

Chapter 5 presents the results and discussion. Simulated and measured results are compared. The experimental verification process is explained with numerical analysis given. The key contributions in this thesis are highlighted. Finally, some recommendations on further work as well as a concluding statement are given in Chapter 6.

CHAPTER 2

ULTRA WIDEBAND APPLICATIONS TECHNOLOGY

2.1 Introduction

Although often considered a recent breakthrough in broadband wireless technology, the concept of UWB dates back many decades. The early UWB systems, designed for the U.S military and government agencies, included such applications as covert (low probability of detection and intercept) radar and communication systems. Recent advancements in chip development have made UWB more viable for commercial and civilian use. Freescale Semiconductor was the first company to produce UWB chips in the world and its XS110 solution is the only commercially available UWB chipset to date [6]. It provides full wireless connectivity implementing DS-UWB. The chipset delivers more than 110 Mbps data transfer rate supporting applications such as streaming video, streaming audio, and high-rate data transfer at very low levels of power consumption.

Contributions to the development of a field addressing UWB RF signals commenced in the late 1960's on time-domain electromagnetic [37] as carrier-free, base-band or impulse technology [38] by the pioneering contributions of Harmuth at Catholic University of America, Ross and Robbins at Sperry Rand Corporation and Paul van Etten at the USAF's Rome Air Development Center. The Harmuth books and published papers, 1969 - 1984, placed in the public domain the basic design for UWB transmitters and receivers [39]-[45]. At approximately the same time and independently, the Ross and Robbins (R & R) patents, 1972 - 1987, pioneered the

use of UWB signals in a number of application areas, including communications and radar using coding schemes [46]-[53]. Ross' US Patent 3,728,632 dated 17th April, 1973, is a landmark patent in UWB communications [42]. Van Etten's empirical testing of UWB radar systems resulted in the development of system design and antenna concepts. In 1974, Morey designed a UWB radar system for penetrating the ground, which was to become a commercial success at Geophysical Survey Systems, Inc. (GSSI) [54].

By the early 1970s the basic designs for UWB signal systems were available and there remained no major impediment to progress in perfecting such systems. After the 1970s, the only innovations in the UWB field could come from improvements in particular instantiations of subsystems, but not in the system concept itself. The basic components known were pulse train generators, pulse train modulators, switching pulse train generators, detection receivers and wideband antennas. Moreover, particular instantiations of the subcomponents and methodologies known were avalanche transistor switches, light responsive switches, use of sub-carriers in coding pulse trains, leading edge detectors, ring demodulators, mono-stable multi-vibrator detectors, integration and averaging matched filters, template signal match detectors, correlation detectors, signal integrators, synchronous detectors and antennas driven by stepped amplitude input [38].

Through the late 1980's, UWB technology was referred to as base-band, carrier free or impulse technology, as the term ultra wideband was not used until 1989 by the U.S. Department of Defense. Until the recent FCC allocation of the UWB spectrum for unlicensed use, all UWB applications were permissible only under a special license. The interest seems to be growing exponentially now, precipitated by the FCC allocation in 2002 of the UWB spectrum, with several researchers exploring RF design, circuit design, system design and antenna design, all related to UWB applications.

2.2 UWB Definition

On February 14, 2002, a UWB frequency allocation has been made by the U.S FCC in the range from 1.99 GHz - 10.6 GHz, 3.1 GHz - 10.6 GHz, or below 960 MHz depending on the particular application [4] and work is underway by regulatory bodies to achieve the same in Europe and Asia [55]. Since then, UWB technology has been regarded as one of the most promising wireless technologies that promises to revolutionize high data rate transmission and enables the personal area networking industry leading to new innovations and greater quality of services to the end users.

The FCC has defined an UWB device as any device with a -10 dB fractional bandwidth, greater than 20% or occupying at least 500 MHz of the spectrum [4]. Most narrowband systems occupy less than 10% of the center frequency bandwidth, and are transmitted at far greater power levels. For example, if a radio system were to use the entire UWB spectrum from 3.1-10.6 GHz, and center about almost any frequency within that band, the bandwidth used would have to be greater than 100% of the center frequency in order to span the entire UWB frequency range. By contrast, the 802.11b radio system centers about 2.4 GHz with an operating bandwidth of 80 MHz. This communication system occupies a bandwidth of only 1% of the center frequency.

The FCC also regulated the spectral shape and maximum power spectral density (-41.3 dBm/MHz) of the UWB radiation in order to limit the interference with other communication systems. The power spectral density is the average power in the signal per unit bandwidth and hence provides important information on the distribution of power over the RF spectrum. The European Telecommunications Standard Institute (ETSI) regulations in European (EU) are expected to follow the FCC but with a more restrictive spectral shape, motivated by a different management of the available spectrum [56]-[57]. For the antenna this means that only one 500 MHz band need to be active at a time. The UWB spectral power density mask is shown in Figure 2.1.

From Figure 2.1, it shows the UWB spectral power density mask limited to -41.3 dBm by FCC and ETSI to ensure that the UWB emission levels exceedingly small. The blue and red lines from that figure present the emission levels for indoor and handheld UWB devices defined by FCC, and the green and violet lines by ETSI.

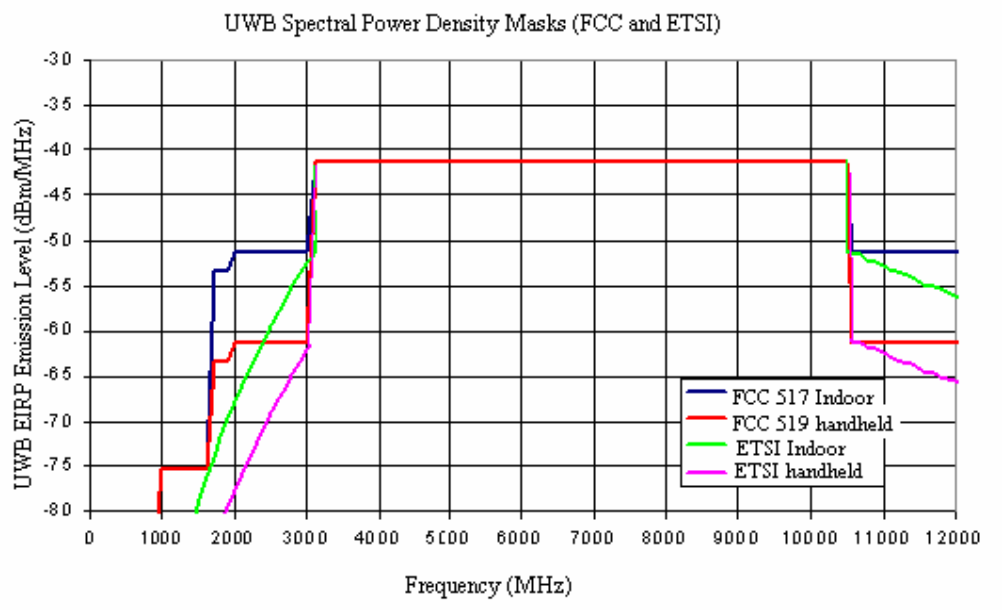

Figure 2.1: UWB spectral power density mask (FCC and ETSI) [4] [58]

Table 2.1 gives the summary of emission levels for indoor and handheld UWB devices defined by FCC. The emissions shall not exceed the average limits as shown in the table when measured using a resolution bandwidth of 1 MHz. UWB handheld devices are relatively small devices that do not employ a fixed infrastructure. Antennas may not be mounted on outdoor structures such as the outside of a building or on a telephone pole. Antennas may be mounted only on the handheld UWB devices. Handheld UWB devices may operate indoors or outdoors [55].

Table 2.1: FCC limits for indoor and handheld systems [55]

Frequency (MHz)	Indoor EIRP (dBm)	Handheld EIRP (dBm)
960-1.610	-75.3	-75.3
1.610-1.990	-53.3	-63.3
990-3.100	-51.3	-61.3
3.100-10.600	-41.3	-41.3
Above 10.600	-51.3	-61.3

The fractional bandwidth is measured at -10 dB points on either side of the peak emission. If these upper and lower frequencies are represented by f_H and f_L, respectively, the fractional bandwidth (BW) and center frequency (f_C) can be expressed as [55]:

$$BW = 2(f_H - f_L)/\ (f_H + f_L) \tag{2.1}$$

$$f_C = (f_H + f_L)/2 \tag{2.2}$$

This fractional bandwidth greatly exceeds that of other radio transmitters, which are generally confined to a narrow frequency band allocated for a specific service. As a consequence of occupying a large bandwidth, UWB devices can span a number of bands. However, as the level of emissions from UWB is very low and below the power floor of existing frequency users, they are able to share spectrum with existing services. By dividing the power of the signal across a huge frequency spectrum, the effect upon any frequency is below the acceptable noise floor [59], as illustrated in Figure 2.2.

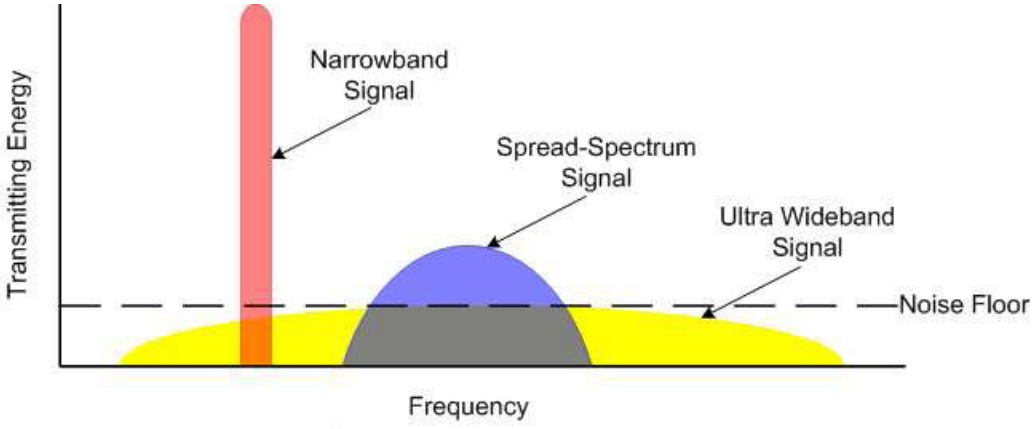

Figure 2.2: Ultra wideband communications spread transmitting energy across a wide spectrum of frequency (Reproduced from [59])

The large transmission bandwidth, from near direct current (dc) to a few GHz, has as result a higher immunity to interference effects and improved multipath fading robustness. Another direct consequence of the large bandwidth is the possibility to accommodate many users, even in multipath environments. Furthermore, the very low frequencies have good penetration properties through different materials, improving the coverage of the UWB radios.

UWB radio, operating with extremely large bandwidths, must coexist with many other interfering narrow-band signals (TV, GSM, UMTS, GPS, etc.). In the same time, these narrow-band systems must not suffer intolerable interference from the UWB radios. Regulatory considerations over such a wide bandwidth limit the radiated power. The low transmit power levels together with the ultra-fine time resolution of the system can increase considerably the synchronization acquisition time and the complexity of the receiver.

2.2.1 Regulations Worldwide

The regulatory bodies outside U.S. are also actively conducting studies to reach a decision on the UWB regulations now. They are heavily influenced by the FCC's decision, but will not necessarily fully adopt the FCC's regulations. In Europe, the Electronic Communications Committee (ECC) of the Conference of European Posts and Telecommunications (CEPT) completed the draft report on the protection requirement of radio communication systems from UWB applications [60]. In contrast to the FCC's single emission mask level over the entire UWB band, this report proposed two sub-bands with the low band ranging from 3.1 GHz to 4.8 GHz and the high band from 6 GHz to 8.5 GHz, respectively. The emission limit in the high band is -41.3 dBm/MHz.

In order to ensure co-existence with other systems that may reside in the low band, the ECC's proposal includes the requirement of Detect and Avoid (DAA) which is an interference mitigation technique [61]. The emission level within the frequency range from 3.1 GHz to 4.2 GHz is -41.3 dBm/MHz if the DAA protection mechanism is available. Otherwise, it should be lower than -70 dBm/MHz. Within the frequency range from 4.2 GHz to 4.8 GHz, there is no limitation until 2010 and the mask level is -41.3 dBm/MHz. The ECC proposed mask against the FCC one are plotted in Figure 2.3.

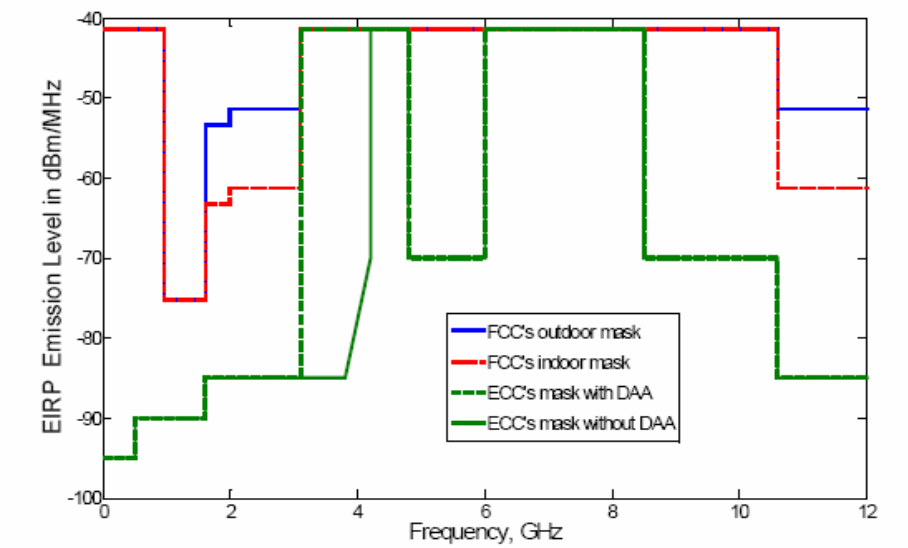

Figure 2.3: Proposed spectral mask of ECC [61]

In Japan, the Ministry of Internal Affairs & Communications (MIC) completed the proposal draft in 2005 [62]. Similar to ECC, the MIC proposal has two sub-bands, but the low band is from 3.4 GHz to 4.8 GHz and the high band from 7.25 GHz to 10.25 GHz. DAA protections is also required for the low band.

In Korea, Electronics and Telecommunications Research Institute (ETRI) recommended an emission mask at a much lower level than the FCC spectral mask.

Currently in Singapore the Infocomm Development Authority (IDA) permits UWB with a special experimental license. The UWB Friendly Zone (UFZ) is located within Science Park II, amidst the research, development, and engineering community in Singapore [55].

The UWB proposals in Japan, Korea and Singapore against the FCC one are illustrated in Figure 2.4.

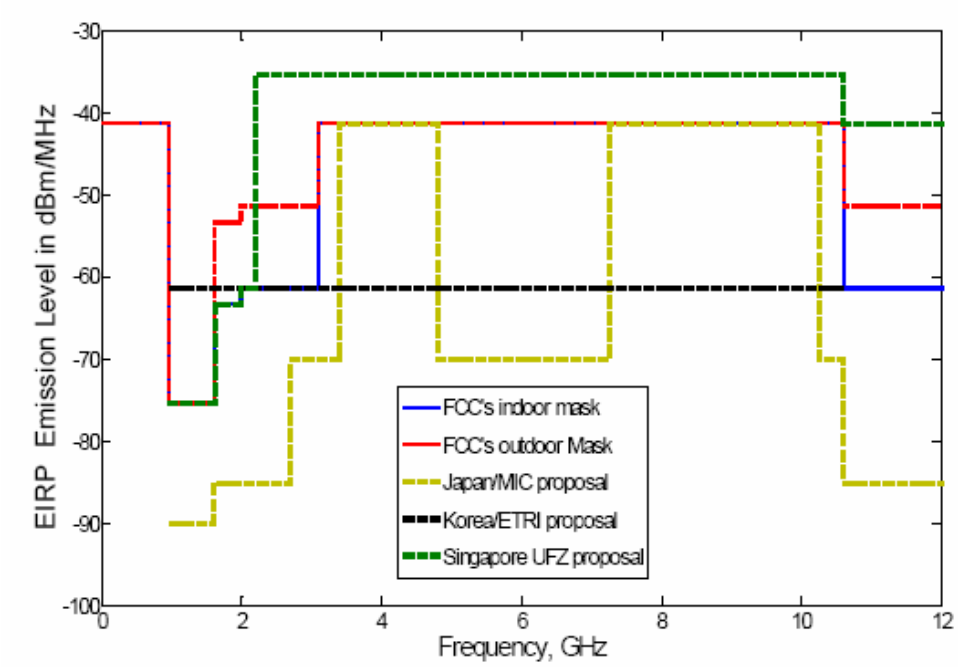

Figure 2.4: Proposed spectral mask in Asia [61]

In order to facilitate experimentation and encourage innovation, IDA issues trial licenses to companies permitting them operate UWB devices within the UFZ, subject to the emission limits given in Table 2.2. The emissions of Table 2.2 are measured in a resolution of 1 MHz. The limits are 6 dB less stringent, and have an expanded lower frequency band edge than what is permitted by the FCC.

Table 2.2: UWB limits for the Singapore UFZ

Frequency (MHz)	EIRP (dBm)
960-1.610	-75.3
1.610-1.990	-63.3
1.990-2.200	-61.3
2.200-10.600	-35.3
Above 10.600	-41.3

2.3 A Brief History of UWB Antenna

The demand for wireless wideband communications is rapidly increasing due to the need to support more users and to provide more information with higher data rates. Over the past few years, considerable research efforts have been put into the design of UWB antennas and systems for communications. These UWB antennas are essential for providing wireless wideband communications based on the use of very narrow pulses on the order of nanoseconds, covering a very wide bandwidth in the frequency domain, and over very short distance at very low power densities. In addition, the antennas required to have a non-dispersive characteristic in time and frequency, providing a narrow, pulse duration to enhance a high data throughput. A wide variety of antennas are suitable for use in UWB applications. Some of these are described elsewhere in a historical survey [63].

Before the decade 1990‘s, all proposed UWB antennas were based on general volumetric and partly on planar structures [64]. Basic wideband antenna structures have been investigated in 1939. Carter investigated biconical antenna and conical monopole by incorporating a tapered feed. Carter was among the first to take the key step of incorporating a broadband transition between a feed-line and radiating elements [65]-[66].

Stratton and Chu [67]-[68] proposed the spheroidal antenna in 1941. The spheroidal antenna was obtained by a straightforward solution of Maxwell’s equation. The zero reactance occurs when the antenna length is slightly less than a half wavelength for long thin wires. However, for thicker wires zero reactance may occur when the antenna length is greater than a half wavelength, thus makes the impedance curve broader and wider bandwidth.

In 1943 Schelkunoff proposed a biconical antenna, which presented analytical formulas for antenna impedance characteristics for several antenna shapes. The biconical antenna concept is based on the fact that thicker wire provides wider impedance bandwidth that that for a thin wire dipole antenna [69]. If the biconical antenna is flared out to infinity called as infinite biconical antenna, while the finite biconical antenna is formed by finite sections of the two infinite cones. This antenna is still widely used for wideband antenna applications and its variations, including the discone antenna and the bow-tie antenna, are popular antennas for wideband applications.

In 1947, a wideband antenna concept was proposed by the staff of the U.S. Radio Research Laboratory at Harvard University [70]. The concept of a wideband antenna evolves from a transmission line that gradually diverges while keeping the inner and outer conductors ratio constant. Several variations of the concept were developed, such as the teardrop antenna, sleeve antenna and inverted trapezoidal antenna.

However, those antennas mentioned above are large, non-planar and physically obtrusive, and therefore ruling them out as a possibility for use with small UWB integrated electronics [71]. Currently modern telecommunication systems require antennas with wider bandwidth and smaller dimensions than conventionally possible.

Comparison study between the UWB antennas with conventional antennas has been done in [8]. In that paper, the authors described a study of conventional antennas and why they are not suitable for a UWB system. One of the simplest practical resonant antennas is the dipole antenna. The antenna can only radiate sinusoidal waves on the resonant frequency. Thus, the dipole antennas are not suitable for UWB system. On the other hand, a non-resonant antenna can cover a wide frequency range, but special care must be taken in antenna design to achieve sufficient antenna efficiency. Moreover, the physical size of available non-resonant antenna is inappropriate for portable UWB devices. Even with appropriate size and sufficient efficiency, until now non-resonant antennas have not been suitable for UWB systems [8].

In 1950's, the spiral antennas were introduced in the class of frequency independent antennas. These Antennas whose mechanical dimensions are short compared to the operating wavelength is usually characterized by low radiation resistance and large reactance [72]. Due the effective source of the radiated fields varies with frequency, these antennas tend to be dispersive. The equiangular spiral and archimedean spiral antennas are the most well known spiral antennas. Spiral antennas have about a 10:1 bandwidth, providing circular polarization in low profile geometry [73].

Transverse electric magnetic (TEM) horns and frequency-independent antennas feature very broad well-matched bandwidths and have been widely studied and applied [74]–[80]. However, for the log-periodic antennas structures, such as planar log-periodic slot antennas, bidirectional log-periodic antennas, and log-periodic dipole arrays, frequency-dependant changes in their phase centers severely distort the waveforms of radiated pulses [81]. Biconical antennas are the earliest antennas used in wireless systems relatively stable phase centers with broad well-

matched bandwidths due to the excitation of TEM modes. The cylindrical antennas with resistive loading also feature broadband impedance characteristics [82]–[84]. However, the antennas mentioned above are seldom used in portable devices due to their bulky size or directional radiation, although they are widely used in electromagnetic measurements [16].

In 1982, R.H. Duhamel invented the sinuous antenna, which provides dual linear polarization plus wide bandwidth in a compact, low profile geometry [85]. The sinuous antenna is more complicated than the spiral antenna. However, it provides dual orthogonal linear polarizations so that it can be used for polarization diversity or for transmit/receive operation.

From 1992, several microstrip, slot and planar monopole antennas with simple structure have been proposed [14][86]-[89]. They produce very wide bandwidth with a simple structure such as circular, elliptical or trapezoidal shapes. The radiating elements are mounted orthogonal to a ground plane and are fed by a coaxial cable. The large ground plane mounted orthogonal to the patch made these antennas bulkier and are difficult to fit into small devices. On the other hand, research works on monopole and dipole UWB antennas in radiation and reception mode for some set of operation conditions including traveling and standing wave of exciting and induced currents in antenna was also reported in [90]. Some theoretical and experimental generalized data are obtained. The obtained theoretical is the more adequate approach to estimate performances of the UWB antennas in contrast to frequency domain technique due physical nature of solving problems.

A novel UWB antenna with combination of two antenna concepts: a slot-line circuit board antenna and a bowtie horn were introduced in 1992 [11]. These two antenna concepts are put together to form a novel antenna type that is wide band with easily controllable E- and H- plane beam-widths. The bowtie horn is known for its broadband radiation pattern; whereas, the slot-line antenna provides a broadband and balanced feed structure. However, a broadband balun is needed for the transition between the microstrip and slotline transmission line. The microstrip and slotline are

on opposite sides of the substrate. Proper design of broadband balun is crucial to improve the antenna bandwidth.

In 1998, Guillanton et al [13] proposed a new balanced antipodal vivaldi antenna for UWB application. The author extended the tapers of the balanced antipodal vivaldi to make the vivaldi antenna works as a dipole in lower frequency where the slot can not radiate to extend low frequency limit. However, the bandwidth of the antenna is limited by the transition from the feed line to the slot line of the antenna.

In 1999, the Foursquare antenna was invented and patented by Virginia Tech Antenna Group (VTAG). Even though this antenna does not offer as much bandwidth as other elements, it has its unique characteristics such as unidirectional pattern, dual polarization, low profile and compact geometry [91]-[92]. The compact geometry of the Foursquare antenna is one of a desirable feature for wide scan, phased array antenna.

In 2003, the trend in UWB antenna was to design notched band antennas [25]. This antenna made insensitive to particular frequencies. This technique is useful for creating UWB antennas with narrow frequency notches, or for creating multi-band antenna. Since then, many researchers extended their research to investigate the possibility interference between UWB system and existing wireless communication systems such as HIPERLAN/WLAN systems. The commonly technique used is adding a half wavelength slot to the patch antenna. The slot is intended to reject the required frequencies [24]-[34].

In 2004, a new UWB antenna consisting of a rectangular patch with two steps, a single slot on the patch and a partial ground plane has been proposed in [12]. This design provides a quasi-omnidirectional UWB antenna with group delay ripple less than 0.5 ns. The techniques used in this paper are applied as a guideline in the design of proposed UWB antenna in this thesis. The extensive investigation on the effect of slot to the impedance bandwidth has been done since this issue did not

discussed in detail. Other research projects on UWB antenna have been reported in [6][71][8][15][5].

In 2007, evaluation of interference between DS-UWB and WLAN using a GTEM cell has been proposed in [22]. In 2008, the researchers extend their research to evaluate the interference between MB-OFDM UWB and WLAN. As a result, even if the UWB signal smaller than the receiver noise of WLAN the interference still exist. Until 2008, hundreds of paper presenting UWB antenna design and development are available in many international journals and conferences and some of them as listed in this thesis' references.

2.4 Application of UWB Technology

UWB is the leading technology for freeing people from wires, enabling wireless connection of multiple devices for transmission of video, audio and other high bandwidth data. Designed for short range, WPAN, it is used to relay data from a host device to other devices in the immediate area (up to 10 m or 30 feet).

Recent years, rapid developments have been experimented on the technology using UWB signals. UWB technology offer major enhancements in three wireless application areas: communications, radar and positioning or ranging. UWB technology can be delivered also over wire lines and cables such as cable television (CATV) application. Each of these applications illustrates the unique value of UWB [1].

2.4.1 Communication Systems

Using UWB techniques and the available large RF bandwidths, UWB communication links has become feasible. The exceptionally large available bandwidth is used as the basis for a short-range wireless local area network with data

rates approaching gigabits per second. This bandwidth is available at relatively low frequencies thus the attenuation due to building materials is significantly lower for UWB transmissions than for millimeter wave high bandwidth solutions. By operating at lower frequencies, path losses are minimized and the required emitted power is also reduced to achieve better performance.

UWB radios operate in the presence of high levels of interference by trading data rate for processing gain. The attributes of low emitted power and wide signal bandwidth result in a very low spectral power density of the UWB signal. This means that UWB radios operate in the same spectrum space as narrowband radios on a non-interfering basis. Computer peripherals offer another fitting use of UWB, especially when mobility is important and numerous wireless devices are utilized in a shared space. A mouse, keyboard, printer, monitor, audio speakers, microphone, joystick, and PDA are in wireless, all sending messages to the same computer from anywhere in the given range [55].

UWB also is used as the communication link in a sensor network. A UWB sensor network frees the patient from the tangle of wired sensors. Sensors are being used in medical situation to determine pulse rate, temperature, and other critical life signs. UWB is used to transport the sensor information without wires, but also function as a sensor of respiration, heart beat, and in some instance for medical imaging.

UWB pulses are used to provide extremely high data rate performance in multi-user network applications. These short duration waveforms are relatively immune to multipath cancellation effects as observed in mobile and in-building environments. Multipath cancellation occurs when a strong reflected wave arrives partially or totally out of phase with the direct path signal, causing a reduced amplitude response in the receiver. With very short pulses, the direct path has come and gone before the reflected path arrives and no cancellation occurs. As a consequence, UWB systems are particularly well suited for high-speed multimedia, mobile wireless applications. In addition, because of the extremely short duration waveforms, packet burst and time division multiple access (TDMA) protocols for multi-user communications are readily implemented [38].

2.4.2 Radar Systems

For radar applications, these short pulses provide very fine range resolution and precision distance and positioning measurement capabilities. The very large bandwidth translates into superb radar resolution, which has the ability to differentiate between closely spaced targets. This high resolution is obtained even through lossy media such as foliage, soil and wall and floor of the buildings. Other advantages of UWB short pulses are immunity to passive interference (rain, fog, clutter, aerosols, etc) and ability to detect very slowly moving or stationary targets [37]. UWB antennas arrays are especially important, to have both fine range and angular resolution in radars.

In radar cross-section (RCS) range, a single UWB antenna replaces a large set of narrow band antennas that are normally used to cover the whole frequency band of interest. UWB signals enable inexpensive high definition radar. Radar will be used in areas currently unthinkable such as; automotive sensors, smart airbags, intelligent highway initiatives, personal security sensors, precision surveying, and through-the wall public safety application [55].

Operation of vehicular radar in the 22 to 29 GHz band is permitted under the UWB rules using directional antennas on automobiles. These devices are able to detect the location and movement of the objects near a vehicle, enabling features such as near collision avoidance, improved air bag activation, and suspension systems that better respond to road conditions [55].

2.4.3 Positioning Systems

For Global Positioning System (GPS), location and positioning require the use of time to resolve signals that allow position determination to within ten of meters. Greater accuracy is enhanced with special techniques used. Since there is a direct relationship between bandwidth and precision, therefore increasing bandwidth will also increase positional measurement precision, with UWB techniques

extremely fine positioning becomes feasible, e.g., sub -centimeter and even sub-millimeter [38]. In satellite communications where wide band feeds save space and weight by supporting many communication channels with just one antenna.

The architectures for UWB position-determination systems would resemble traditional systems, e.g. multi-alterations like GPS or radio ranging like the military's Enhanced Position Location and Reporting System (EPLRS). Having relatively low frequency of operation, this type of system has the potential to work within buildings with minimal attenuation of the signal.

With UWB techniques, it becomes feasible to fuse these unique capabilities into a single system. Thus, it is possible to create communications systems in which position is determined to within less than a centimeter. Moreover, it is possible to build radars (proximity sensors) that communicate simultaneously. Since UWB exhibits all of these characteristics while allowing spectrum bandwidths to be re-use and maintain that little or no interference to be generated between other communication systems. Therefore, the emission of UWB will greatly boost the performance of intrusion detection radar precision geo-location systems, proximity fuses and secure ground communications for troops which far outweigh the impact of UWB may have on other systems.

2.4.4 UWB over Wires

UWB technology is also delivered over wire lines and cables. This could effectively double the bandwidth available to CATV systems without modification to the existing infrastructure. Over wire technology for coaxial cable provide up to 1.2 Gbps down-stream and up to 480 Mbps upstream of additional bandwidth, at low cost, on differing CATV architectures. The wire-line UWB technology does not interfere with or degrade television, high speed internet, voice or other services already provided by the CATV infrastructure [55].

2.5 Short-Pulse Generation

UWB technology involves the radiation, reception and processing of very wide bandwidth radio frequency emissions. The main reason for such high bandwidths is that UWB devices send out tiny bursts of radio signals over many frequencies. Data goes out in millions of pulses per second and is re-assembled by a receiving UWB device. These bursts represent from one to only a few cycles of an RF carrier wave. The resultant waveforms are extremely broadband, it is often difficult to determine an actual RF center frequency thus, the term "carrier-free". Most other wireless technologies use a single radio frequency carrier.

In general, UWB radio systems transmit and receive single band (SB) or multi-band (MB) pulses. SB based, employing one single transmission frequency band, and MB based, employing two or more frequency bands, each with at least 500 MHz bandwidth.

In the SB solution, the UWB signal is generated using very short, low duty-cycle, baseband electrical pulses with appropriate shape and duration. Due to the carrier-less characteristics, no sinusoidal carrier to raise the signal to a certain frequency band, these UWB systems are also referred to as carrier-free or impulse radio (IR-UWB) communication systems [93]. Such systems are capable of providing low system complexity and low cots because of their direct transmission and reception of pulsed signals and the least RF devices in their front-ends as against conventional narrow-band radio systems [5].

The MB UWB systems is implemented carrier less (different pulse shapes/lengths are used according to the frequency band) [36] or carrier based (multi-carrier like) [94] known as UWB-OFDM. In UWB-OFDM bandwidth is split into many sub-bands applying communication techniques well-known from narrowband systems.

The requirements for UWB antennas can vary for different schemes. In the multiband scheme, the consistent or flat gain response of the UWB antennas is more important than a constant group delay or a linear phase response, which is conversely more important in the single band scheme. Therefore, the performance of UWB

antennas can be assessed in terms of the system transfer function and group delay together with conventional frequency-domain parameters such as return loss, gain, radiation patterns, and polarization matching path loss as well as the time-domain parameters such as pulse waveforms, and fidelity [16].

In the IR UWB solutions, typically the radiated pulse signals are generated without the use of local oscillators or mixers, thus potentially a simpler and cheaper construction of the transmitter (TX) and receiver (RX) is possible, as compared to the conventional narrow-band systems. The characteristics of the pulse used (shape, duration), determine the bandwidth and spectral shape of the UWB signals. The most common pulse shapes used in IR-UWB are: Gaussian monocycle (and its derivatives) and Hermitian pulses [95].

The impulse radio technology has been widely used in radar applications due to its spatial resolution, detectable material penetration, easy target detection and feature extraction and low probability of intercept signals [96]-[98]. Military and government multi-user networking and high precision localization applications rely on the UWB communication systems [99].

The basic properties of the impulse radio systems make the UWB technology ideal candidate also for commercial, short-range, low power, low cost indoor communication systems such as WLAN and WPAN [100]-[102].

2.6 UWB Link Performance

As with narrowband antennas, the link behavior of UWB antennas in free space is governed by Friis's Law [79]:

$$P_{RX} = P_{TX} \frac{G_{TX} G_{RX} \lambda^2}{(4\pi r)^2} = P_{TX} \frac{G_{TX} G_{RX} c^2}{(4\pi r)^2 f^2} \tag{2.3}$$

where P_{RX} is the received power, P_{TX} is the transmitted power, G_{TX} is the transmit antenna gain, G_{RX} is the receive antenna gain, λ is the wavelength, f is the frequency, c is the speed of light, and r is the range between the antennas. Friis's Law depends on frequency, power and gain will be functions of frequency. Thus, in the UWB case, Friis's Law must be interpreted in terms of spectral power density:

$$dP_{RX}(f) = \frac{c^2}{(4\pi r)^2} P_{TX}(f) \frac{G_{TX}(f) G_{RX}(f)}{f^2} \tag{2.4}$$

The total received power and EIRP:

$$P_{RX} = \int_0^\infty dP_{RX}(f) df \tag{2.5}$$

$$EIRP(f) = P_{TX}(f) G_{TX}(f) \tag{2.6}$$

where $G_{TX}(f)$ must be the peak gain of the antenna in any orientation. Since regulatory limits are defined in terms of EIRP, $P_{TX}(f)\, G_{TX}(f)$ to be constant and as close to the regulatory limit as a reasonable margin of safety (Typically 3 dB) will allow [103]. Similarly, this power gain product must roll-off so as to fall within the skirts of the allowed spectral mask.

Note the dependence of the received power on the inverse frequency squared. Colloquially, this $(\lambda/4\pi r)^2$ or $(c/4\pi r f)^2$ variation of the signal power is referred to as path loss. The greater the range r, the larger the $(4\pi r)^2$ surface area over which a signal is spread and thus the weaker the captured signal. This is more a diffusion of the signal energy than a loss.

Antenna gain G is defined in terms of antenna aperture A as:

$$G(f) = \frac{4\pi A(f)}{\lambda^2} = \frac{4\pi A(f) f^2}{c^2} \tag{2.7}$$

This antenna aperture is the effective area of the antenna, a measure of how big a piece of an incoming wave front an antenna can intercept. For directive, electrically large antennas, antenna aperture tends to be comparable to the physical area. For omni directional small element antennas, the antenna aperture may actually be significantly larger than the antennas's physical area. This follow from the ability of electromagnetic waves to couple to objects within about $\lambda/2\pi$.

2.7 Summary

In this chapter, a brief history of UWB antenna technology has been reviewed. From the literature reviews, the UWB antenna concept has been investigated since many decades. The FCC released the regulations of UWB technology for commercial purposed since 2002. The standardizations or regulation applied for this technology in Europe and Asia with their specific requirements is also presented in detail. These regulations are used as guidelines for research work. The frequency bands were allocated based on certain applications. Some applications with their signal characteristics and performance link are discussed. Overview of UWB short pulse and link performance are also given. The contents of this chapter have been published as a full paper in the fifth international conference on wireless and optical communication networks (WOCN 2008).

CHAPTER 3

ULTRA WIDEBAND ANTENNA DESIGN METHODOLOGY

3.1 Introduction

For many years, the idea of an UWB antenna that would allow stable pattern control over many frequency decades seemed elusive at the best. UWB antennas require the phase center and voltage standing wave ratio (VSWR) to be constant across the whole bandwidth of operation. A change in phase center may cause distortion on the transmitted pulse and worse performance at the receiver. The antennas are significant pulse-shaping filters. Any distortion of the signal in the frequency domain (filtering) causes distortion of the transmitted pulse shape, thereby increasing the complexity of the detection mechanism at the receiver [104]. As discussed in Chapter 1, monopole antennas match most these characteristics representing the starting point of the modern research on broadband antenna [14]. Accordingly, many techniques to broaden the impedance bandwidth of small antennas and to optimize the characteristics of broadband antennas have been widely investigated. Detail discussion on various bandwidth enhancement techniques will further examined in section 3.3.

The reduction in antenna size presents various problems due to the performance penalties in antenna characteristics, such as impedance, efficiency, and bandwidth. Small antennas are defined as those which have smallness in terms of size, wavelength, and function, and they are divided into four categories [105]. The first is electrically small antennas, which have a very small size compared to the

wave length (λ). The second is physically constrained small antennas, which are not necessary electrically small, but are shaped in such a way that considerable size reduction is achieved in one plane. The third is physically small antennas, which have dimensions regarded as small in a relative sense. The last is functionally small antennas, which are antenna systems that achieved additional functions without increasing size [105].

In this thesis, the proposed slotted UWB antennas meet those four categories as a small antenna. Their sizes are less than a wavelength, compact size in one plane, considerable smaller size compared to the antennas sizes in the references listed [12][16][106][107]-[108][109]-[111][112], and suitable for many UWB applications. Comparison in terms of antenna sizes between the proposed antennas and several UWB antennas listed in the references has been done. Those proposed antennas originate from conventional rectangular monopole and are realized by adding slots for both patch and feeding strip.

In order to understand the challenges that UWB provides to antenna's designer, a comprehensive background outlining several characterizing antenna parameters will be presented. Next, a clear description of various bandwidth enhancement techniques that required in the design of UWB antennas is presented. Some related research works are reviewed as well. Several techniques that employed in the design reconfigurable UWB antenna with band notched characteristic will be further discussed. Fundamental antenna parameters must be fully defined and explained before a thorough understanding of antenna requirements for a particular application can be achieved.

3.2 Fundamental Antenna Parameter

An antenna is a transducer that converts guided electromagnetic energy in a transmission line to radiate electromagnetic energy in free space. The fundamental principles of an antenna design are based on electromagnetic field theory. An antenna working condition depends on the antenna parameters. These factors will

affect the selection of an antenna. Among the most fundamental antenna parameters are radiation pattern, impedance bandwidth, directivity, efficiency and gain. Other characterizing parameters that will be discussed are field region, polarization and dispersion. All of the aforementioned antenna parameters are necessary to fully characterize an antenna and determine whether an antenna is optimized for a certain application.

3.2.1 Radiation Pattern

One of the most common descriptors of an antenna is its radiation pattern. Radiation pattern can easily indicate an application for which an antenna will be used. Cell phone use would necessitate a nearly omnidirectional antenna, as the user's location is not known. Therefore, radiation power should be spread out uniformly around the user for optimal reception. However, for satellite applications, a highly directive antenna would be desired such that the majority of radiated power is directed to a specific, known location.

A radiation pattern or antenna pattern is a graphical representation of the radiation (far field) properties of an antenna. Two most important measurements are the E-plane and H-plane patterns. Three dimensional radiation patterns are measured on a spherical coordinate system; the x-z plane ($\theta = 0°$) usually indicates the elevation plane, while the x-y plane ($\theta = 90°$) indicates the azimuth plane. Typically, the elevation plane will contain the electric-field vector (E-plane) and the direction of maximum radiation, and the azimuth plane will contain the magnetic-field vector (H-Plane) and the direction of maximum radiation shown in Figure 3.1 [71].

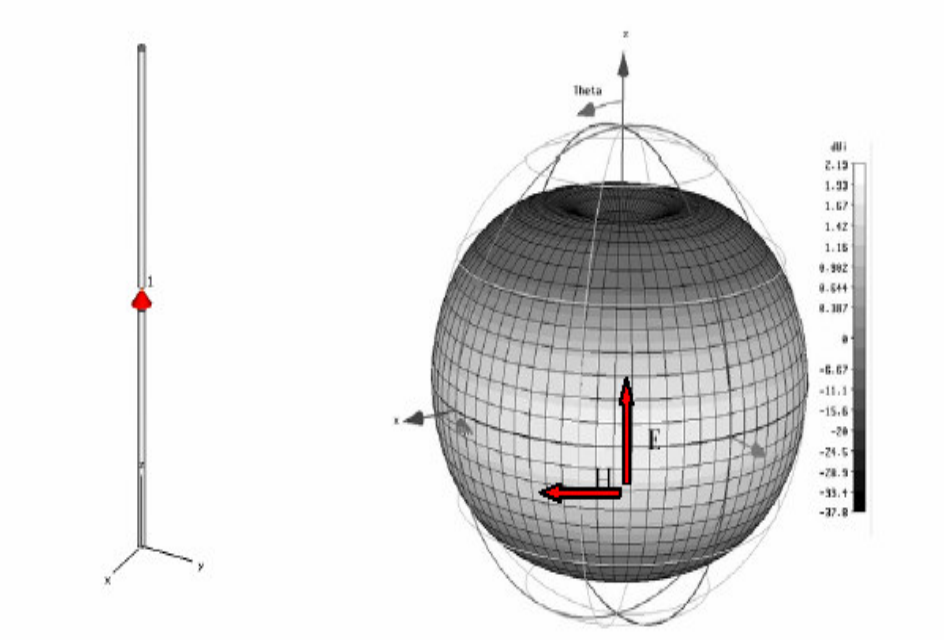

Figure 3.1: Dipole model for simulation and simulated 3D radiation pattern [71]

Figure 3.1 illustrates a half-wave dipole and its three dimensional radiation pattern. The gain is expressed in dBi, which means that the gain is referred to an isotropic radiator. It can be seen quite clearly in Figure 3.1 that the maximum radiation power occurs along the $\theta = 90°$ plane, or for any varying in the azimuth plane. The nulls in the radiation pattern occur at the ends of the dipole along the z-axis (or at $\theta = 0°$ and 180°).

The power received at a point by a receiving antenna is a function of the position of the receiving antenna with respect to the transmitting antenna. The graph of the received power is at a constant radius from the transmitting antenna is called the power pattern of the antenna, which is the spatial pattern. The spatial pattern of the electric (or magnetic field) is called the field pattern. A cross section of this field pattern in any particular plane is called the radiation pattern in that plane [113]. A typical antenna power plot is shown in Figure 3.2 as a polar diagram and a rectangular plot. It consists of several lobes such as main lobe, major lobe or main beam. This lobe contains the direction of maximum radiation [114].

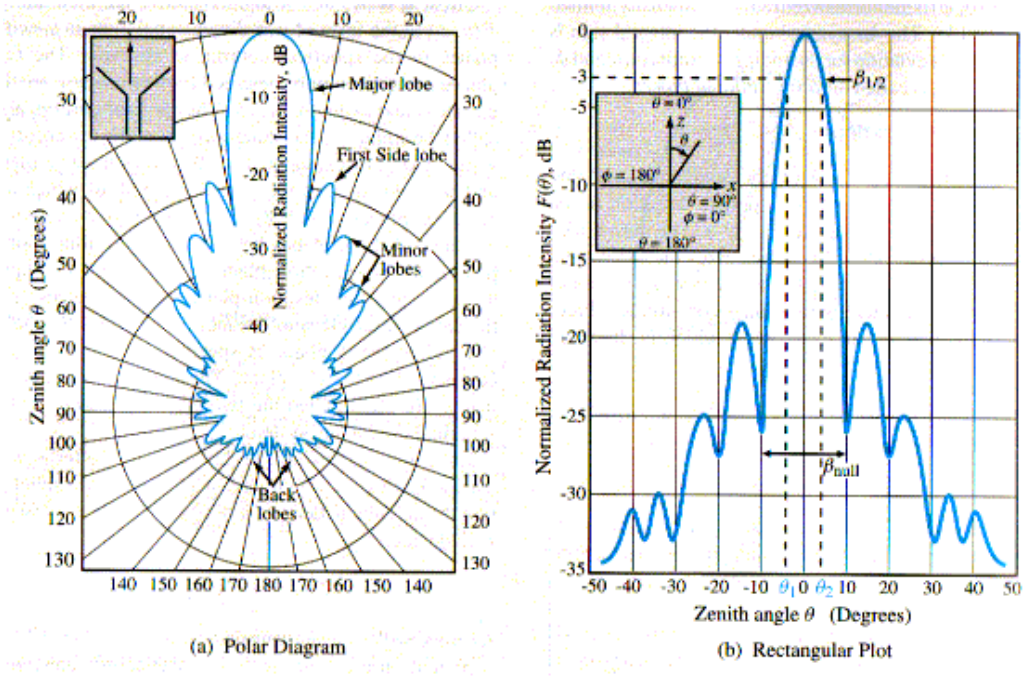

Figure 3.2: Representation plots of the normalized radiation pattern of a microwave antenna in (a) polar form and (b) rectangular form [71]

3.2.2 Field Region

The space surrounding an antenna is subdivided into three regions (or zones). They are respectively termed as reactive near-field region, radiating near-field (Fresnel) region and far-field (Fraunhofer) region as shown in Figure 3.3. The general characteristics of the field distributions in each region can be established, although the boundaries of the regions are not defined precisely.

Reactive near-field region: the region immediately surrounding the antenna where the field patterns change rapidly with distance and radiate both energy and reactive energy, which oscillates towards and away from the antenna.

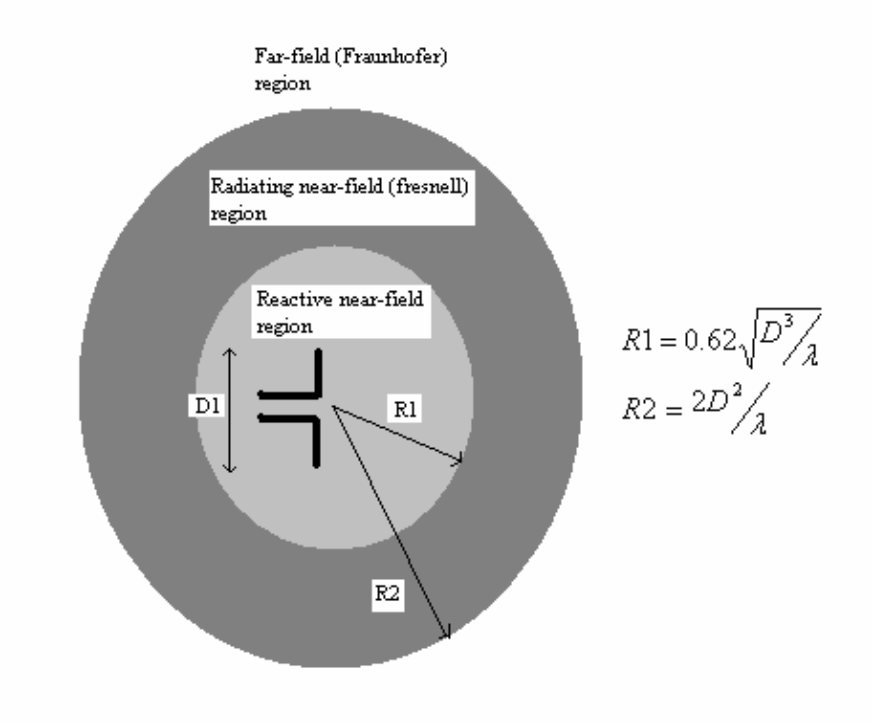

Figure 3.3: Field regions of antenna

Near- field (Fresnel) region: the region further away from the reactive near field region where only the radiating energy is present, resulting in a variation of power with direction which is dependent of distance. These regions are conventionally divided at a radius R, within this radius the zone is known as the near-field or Fresnel region [115].

Far-Field (Fraunhofer) region: this region lies beyond the near field region where waterfronts resemble very much like spherical waves, so that only the power radiated in a particular direction is of importance. In most applications, the power radiated from an antenna is measured from this region [115].

3.2.3 Directivity, Efficiency and Gain

Directivity is how much an antenna concentrates energy in one direction in preference to radiation in other directions. It is equal to its power gain if the antenna is 100% efficient, which means that it is a perfect antenna that radiates equally in all directions. This antenna is called an isotropic radiator. Power gain is expressed relative to a reference such as isotropic radiator or half-wavelength dipole. Since all real antennas will radiate more in some directions than in others, therefore the gain is the amount of power that can achieve in one direction at the expense of the power lost in the others [63]. Gain is always related to the main lobe and is expressed in dBi or dBd.

The antenna efficiency takes into consideration the ohmic losses of the antenna through the dielectric material and the reflective losses at the input terminals. Reflection efficiency and radiation efficiency are both taken into account to define total antenna efficiency. Reflection efficiency, or impedance mismatch efficiency, is directly related to the S_{11} parameter (Γ). Reflection efficiency is indicated by e_r, and is defined mathematically as follows:

$$e_r = \left(1 - [\Gamma]^2\right) \tag{3.1}$$

The radiation efficiency takes into account the conduction efficiency and dielectric efficiency, and is usually determined experimentally with several measurements in an anechoic chamber. Radiation efficiency (e_{rad}) is determined by the ratio of the radiated power, P_{rad} to the input power at the terminals of the antenna, P_{in}:

$$e_{rad} = \frac{P_{rad}}{P_{in}} \tag{3.2}$$

Total efficiency is simply the product of the radiation efficiency and the reflection efficiency. Reasonable values for total antenna efficiency are within the

range of 60% - 90%, although several commercial antennas achieve only about 50% - 60% due to inexpensive, lossy dielectric materials such as FR4.

The antenna gain measurement is linearly related to the directivity measurement through the antenna radiation efficiency. Gain measurement is typically misunderstood in terms of determining the quality of an antenna. A common misconception is that the higher the gain, the better the antenna. This is only true if the application requires a highly directive antenna. Since gain is linearly proportional to directivity, the gain measurement is a direct indication of how directive the antenna is (provided the antenna has adequate radiation efficiency).

3.2.4 Impedance Bandwidth

The Institute of Electrical and Electronic Engineers (IEEE) standard [116] defines the bandwidth of an antenna as "the range of frequencies within which the performance of the antenna, with respect to some characteristics, conforms to a specific standard." Usually the bandwidth is characterized by impedance bandwidth.

The impedance bandwidth indicates the bandwidth for which the antenna is sufficiently matched to its input transmission line such that 10% or less of the incident signal is lost due to reflections. Impedance bandwidth measurements include the characterization of the VSWR and return loss throughout the band of interest.

The impedance of an antenna is the impedance at the antenna terminals with no load attached, impedance may be defined as the ratio of the voltage to current at the antenna terminals or the ratio of the appropriate components of electric and magnetic fields at a point. Maximum power transfer can only be achieved when the impedance of the antenna is matched to those of the load, which involve complex conjugate of the load impedance. Power reflected at the terminals of the antenna is the main concern related to impedance matching.

Impedance matching has been particularly difficult to achieve in UWB antennas, since its impedance has to remain constant over a wide spectrum of frequencies. A good match can be achieved with careful design and employing appropriate mechanisms, such as resistive loading [115]. A good impedance match is indicated by a return loss greater than 10 dB.

VSWR is a measure of impedance mismatch between the transmission line and its load. The higher the VSWR, the greater is the mismatch. The minimum VSWR that corresponds to a perfect impedance match is unity [115]. The typically desired value of VSWR to indicate a good impedance match is 2.0 or less. Most radio equipment is built for an impedance of 50-ohm.

3.2.5 Polarization

Antenna polarization indicates the polarization of the radiated wave of the antenna in the far-field region as shown in Figure 3.4. The position and direction of the electric field with reference to the earth's surface or ground determines wave polarization. In general, the electric field is the same plane as the antenna's radiator. Horizontal polarization is the electric field parallel to the ground. Vertical polarization is the electric field perpendicular to the ground. There is one special polarization known as Circular polarization. As the wave travels it spins to cover every possible angle. It can either be right-handed or left-handed circular polarization depending on which way it is spinning. Another common type of polarization is elliptical, which is a cross between linear (horizontal or vertical) and circular polarization.

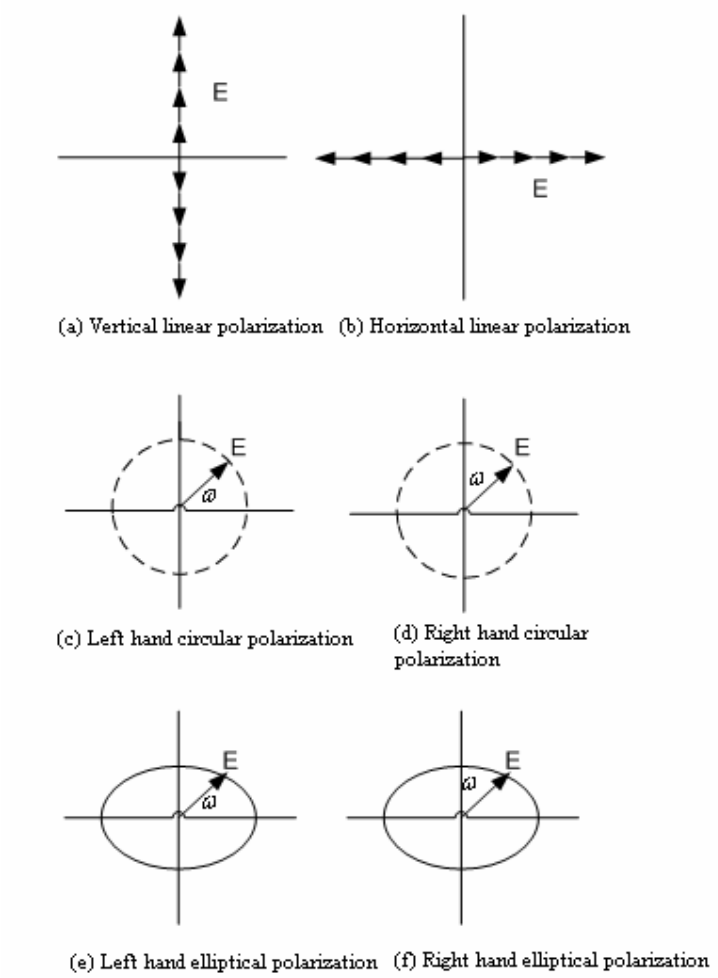

Figure3.4: Some wave polarization states where the wave is approaching

3.2.6 Dispersion and Non-Dispersion

Traditionally, antennas are evaluated according to a few basic parameters such as gain and return loss (matching). For typical narrowband antennas, these parameters are very little across the operational band [117]. The extension to UWB antennas, gain and return loss generally vary with frequency, these parameters may be treated as functions of frequency [117]. Even though an antenna's gain may appear well behaved, if the phase center of an antenna moves as a function of frequency, or as a function of look angle, then an antenna will radiate a mangled and

dispersed waveform. Then UWB system must compensate for these differences. This compensation may be difficult and resources intensive.

The half-wave dipole is a commonly used antenna in carrier based systems. However, when a half-wave dipole pair is used for transmitting and receiving UWB signals, it is very avoid the severe ringing and dispersion problems. These are typical problems using narrow-band antenna to transmit and receive UWB pulses [118].

A log periodic antenna is an example of a dispersive antenna [103]. The log periodical antenna is actually a combination of dipole antennas with different lengths [118]. A smaller scale portion radiates high frequency components and a larger scale portion radiates lower frequency components of a signal. Because the phase center moves as a function of a frequency, frequency independent antennas radiate dispersed signals. The dispersion is a problem for multi-band systems as well as those where a radiated signal occupies the entire band [117]. This phase variation may have a serious impact on UWB antenna performance. The best way to obtain quick qualitative assessment of dispersion is to look at the time domain electromagnetic field signal emitted by an antenna. In addition, a UWB antenna is preferentially non-dispersive, having a fixed phase center.

All of the fundamental parameters described must be considered in designing antennas for any radio application, including UWB. However, there are additional challenges for UWB.

3.3 UWB Antenna Design Methodology

In order to fulfill the UWB antenna requirements, various bandwidth enhancement techniques for planar monopole antennas have been developed during last two decades. The recent trends in improving the impedance bandwidth of small antennas can be broadly divided into the following categories [119], [16], [6], the first category is the leading of all categories in numbers and varieties. By varying the

physical dimensions of the antenna, the frequency and bandwidth characteristics of the resulting UWB pulse could be adjusted [37].

3.3.1 Various Geometries and Perturbations

Planar monopoles with a huge number of different geometries have been numerically characterized [16]. Many techniques to broaden the impedance bandwidth of planar monopole antennas and to optimize the characteristics of these antennas have been widely investigated. Among all these techniques, the beveling technique was reported to yield maximum bandwidth. Various geometries and perturbations are used to introduce multiple resonances as well as input impedance matching. The input impedance is also extremely dependent on the feeding gap configuration [120].

Beveling the bottom edge of the radiating element has been demonstrated to shift upward significantly the upper edge frequency when properly designed [106][35][121][123]. The optimization of the shape of the planar antenna especially the shape of the bottom portion of the antenna, improve the impedance bandwidth by achieving smooth impedance transition [16]. In fact, this part of the radiator results to be very critical for governing the capacitive coupling with the ground plane. Any reshaping of this area strongly affects the current path [106]. A modal study of four common planar monopole geometries has been performed in [120]. The election and beveling angle is critical, as it determines the matching of the mode.

The patch radiator may be slotted to improve the impedance matching, especially at higher frequency. The slots cut from the radiators change the current distribution at the radiators so that the impedance at the input point and current path change [16]. A notch is cut from radiator to reduce the size of the planar antenna [35].

Adding a strip asymmetrically at the top of the radiator can also reduce the height of the antenna and improve impedance matching [124].

An offset feeding point has been used in order to excite more modes and consequently improving the impedance bandwidth [122]. By optimizing the location of the feed point, the impedance bandwidth of the antenna will be further widened because the input impedance is varied with the location of the feed point [122].

Moreover, other strategies to improve the impedance bandwidth which do not involve a modification of the geometry of the planar antenna have been investigated. Basically, these strategies consist of adding a shorting post to the structure or using two feeding points to excite the antenna [120]. A shorting pin is also used to reduce the height of the antenna [125]. In [106], the shorting pin inserted to the antenna that provides a broad bandwidth has been investigated. A dual feed structure greatly enhanced the bandwidth particularly at higher frequencies [126]. By means of electromagnetic coupling (EMC) between the radiator and feeding strip, good impedance matching can be achieved over a broad bandwidth [127].

The use of double feeding configuration to the antenna structure is to enforce the vertical current mode, whereas it prevents other modes such as horizontal and asymmetrical current modes from being excited, which degrade the polarization properties and the impedance bandwidth performance of the antenna [107[128]-[130]. The double feeding gives a significant improvement of the vertical current distribution resulting in better matching notably over the upper-band part [108]. The matching of this upper frequency band is mainly governed by two parameters: the distance between the two monopole ports and the height between the monopole and the ground plane [107]. In [129] a square monopole antenna with a double feed has been proposed. This feed configuration has shown the improvement on radiation pattern and impedance bandwidth. This is due to a pure and intense vertical current distribution generated in the whole structure.

The hidden feed-line technique on printed circular dipole antenna has been investigated in [131]. The specific feeding has shown remove any radiation pattern disturbance generally met with this kind of antenna when fed with a coaxial or a microstrip line. It was also shown a wide frequency bandwidth.

Due to the radiation from planar antenna may not be omni directional at all operating frequencies because they are not structurally rotationally symmetrical. Roll monopoles is a choice to feature broad impedance bandwidth with omni directional characteristics [132]. With the roll structure, the antenna becomes more compact and rotationally symmetrical in the horizontal plane. However, the roll monopoles are not easy to fabricate with high accuracy [16]. The folded antenna was also presented in [133] in order to improve radiation pattern maintaining the broadband behavior. In [133], the antenna was analyzed employing transmission line model (TLM).

In [112], various combinations of bandwidth enhancement techniques was successfully applied in UWB antenna design such as adding slit in one side of the monopole, tapered transition between the monopole and the feed line, and adding notched ground plane.

From various bandwidth enhancement techniques, there are four techniques adopted for this proposed UWB antennas design. The four techniques are the use of slots for both patch and feeding strip, truncation ground plane, bevels or notches at the bottom, and notched ground plane which can lead to a good impedance bandwidth. The original contribution focused on the various slots types design. The proposed slotted UWB antennas are designed by adding asymmetry couple slots without degrading their performance. The performance optimization is done by studying their current distribution.

3.3.2 Genetic Algorithm (GA)

Optimization of patch geometry is an ideal technique to have single or more optimized figures of merit like, impedance bandwidth. The GA has been successfully applied by a number of researchers to improve the impedance bandwidth [5], [134]-[138]. The optimized shape however is too much irregular and unconventional and this can only be fabricated using the pattern produced in true scale by the GA code.

Electromagnetic optimization problems generally involve a large number of parameters. The parameters can be either continuous, discrete, or both, and often include constraints in allowable values. The goal of the optimization is to find a solution that represents a global maximum or minimum. For example, the application of GA optimization is used to solve the problem of design a broadband patch antenna [5]. Parameters that are usually included in this type of optimization problem include the location of the feed probe, the width and length of the patch, and the height of the patch above the ground plane. In addition, it may be desirable to include constraints on the available dielectric materials, both in terms of thickness and dielectric constants; tolerance limits on the patch size and probe location; constraints on the weight of the final design; and possibly even cost constraints for the final production model. Given the large number of parameters, and the unavoidable mixture of discrete and continuous parameters involved in this problem, it is virtually impossible to use traditional optimization methods. GA optimizers, on the other hand, can readily handle such a disparate set of optimization parameters [5].

The use of the GA approach in the design of UWB antennas has been proposed in [134]-[135]. The planar fully-metal monopole (PFMM) of bow tie (BT) and reverse bow tie (RBT) have been demonstrated in [134], [136] have an ultra-wide bandwidth. The element height, the feed height, and the element flare angle were the parameters that used in optimization. The height essentially determines the operating mode and the lower frequency limit of the antenna, while the flare angle and the feed height control the variation of the input impedance over frequency, the high frequency impedance value, as well as the resonance bandwidth [134]. In this paper, the GA was used to determine the optimal dimensions of the selected element shape in order to fulfill the given bandwidth requirement. As a result, the RBT antenna can achieve a much wider impedance bandwidth than the BT with significantly reduced sizes.

In [135], the semi-conical UWB antenna was optimized by using the Green's Function Method (GFM) Absorbing Boundary Condition (ABC) with GA. The goal of this optimization is to have significant reduction in the size of the white space, due to the unique capability of the GFM to model arbitrarily shaped boundaries in close

proximity to the antenna. The white space is defined as the region between the antenna and the absorbing boundary.

The GA optimizer is also used to reconfigure the radiation characteristics of antenna over an extremely wide-band [137]. The design results indicate that the antenna can obtain the required goals over an ultra-wide band through reconfiguring the states of the switch array installed in shared aperture when it operates with the higher order modes [137]. Optimization of broadband and dual-band microstrip antennas on a high-dielectric substrate by using GA was also proposed in [138].

3.3.3 Resonance Overlapping

Normally, the bandwidth of a resonant antenna is not very broad because it has only one resonance. But if there are two or more resonant parts available with each one operating at its own resonance, the overlapping of these multiple resonances may lead to multi-band or broadband performance.

Theoretically, an ultra wide bandwidth can be obtained if there are a sufficient number of resonant parts and their resonances can overlap each other well. However, in practice, it is more difficult to achieve impedance matching over the entire frequency range when there are more resonant parts. Also, it will make the antenna structure more complicated and more expensive to fabricate. Besides, it is more difficult to achieve constant radiation properties since there are more different radiating elements.

3.4 Reconfigurable UWB Antenna

This section presents the concept of reconfigurable antennas and the emerging technologies that make reconfigurable antenna possible. There are three parameters that frequently used for designing the reconfigurable antennas such as, frequency, polarization and radiation patterns.

3.4.1 Reconfigurability Antenna Parameters

Ideally, reconfigurable antennas should be able to alter their operating frequencies, impedance bandwidth, polarizations, and radiation patterns independently to accommodate operating requirements. However, the development of these antennas posses significant challenges to both antenna and system designers. These challenges lie not only in obtaining the desired levels of antenna functionality but also in integrating this functionality into complete systems to arrive at efficient and cost effective solutions.

3.4.1.1 Frequency Response Reconfigurability

Frequency reconfigurable antennas are classified into two categories: continuous and switched [78]. Continuous frequency-tunable antennas allow for smooth transitions within or between operating bands without jumps. Switched tunable antennas use some kind of switching mechanism to operate at distinct and separated frequency bands. The main differences are in the extent of the effective length changes that enable operation over different frequency bands and the devices to achieve these changes. There are different kinds of switching technology, such as optical switches, PIN diodes, FETs, and radio frequency microelectromechanical system (RF-MEMS) switches, in frequency tunable monopole antennas for various frequency bands. The effective length of the antenna can be altered by adding or removing these switches, hence altering its operating frequency.

3.4.1.2 Polarization Reconfigurability

Antenna polarization reconfiguration provides immunity to interfering signals in varying environments as well as provides an additional degree of freedom to improve link quality as a form of switched antenna diversity [139]. The direction of current flow on the antenna translates directly into the polarization of the electric field in the far field of the antenna. To achieve polarization reconfigurability, the antenna structure, material properties, feed configuration have to change in ways that alter the way current flows on the antenna. The main difficulty of this kind of reconfigurability is that this must be accomplished without significant changes in impedance or frequency characteristics [78]. The mechanisms to achieve these modifications are the same as those described for frequency reconfigurability earlier.

3.4.1.3 Radiation Pattern Reconfigurability

Reconfigurable radiation patterns can be achieved with slot-based radiators as presented in [140]. Both frequency and pattern reconfigurabilities are due to incorporated the PIN diode switches into the slot radiator. Frequency reconfigurability is supported through PIN diode switches that control input impedance circuitry, whereas the pattern reconfigurability is enabled with diode switches placed at locations around the slot to control the direction of a pattern null that is inherent to basic antenna operation [78], [140]. For UWB antenna, the reconfigurability of radiation pattern is not an important issue since it requires omni directionality pattern over frequency bands. Next section will be further discussed on frequency notch UWB antenna as main focused in this thesis.

3.4.2 Design Methodology

As mentioned previously, one way to implement a frequency notched UWB antenna is to incorporate a half wave resonance structure in an antenna. In [25], there are two varieties of slotted antennas which have a frequency notched reported, a triangular notch and elliptical notch. Both antennas have frequency notch characteristics where the arc length of slots form a half wavelength resonance structure at particular frequency, thus a destructive interference takes place causing the antennas to be non responsive at that frequency [25].

Other types of this kind of antenna was reported in [141], a band notched UWB antenna using a slot-type split ring resonator (SRR) was found very effective in rejecting unwanted frequency, such as that for WLAN service, in terms of its selectivity and small dimension. The SRR is composed of two concentric split ring slots and proposed for band stop application, since it provides high Q characteristic. It is expected that the smaller structure has a relatively smaller effect on the radiation patterns of the antenna. SRR has a favorable aspect in its size, and it can be designed as small as one-tenth of the resonance wavelength [141]. The slotted SRR was positioned near the feeding point to provide more coupling with the field.

A multiple band-notched planar monopole antenna using multiple U-shape slots for multi band wireless system was presented in [142]. The half wavelength U-shape slots were symmetrically inserted in the center of the planar element. Therefore, in order to generate the two band-notched characteristics, three U-shape slots were proposed. The center U-shape slot makes one notch band at 3.03 GHz and the other two symmetric U-shape slots make notch band at 4.78 GHz, with little effect of mutual coupling between notch bands. The wideband characteristic is due to proper design on antenna size, ground plane size, feed gap, and bevel angle. The frequency corresponding to the lower edge of the bandwidth was found to be dependent on the antenna size and ground size, but the upper edge of the bandwidth was found to be dependent on the feeding gap and bevel angle [143].

At the notch frequency, current is concentrated around at the top of the slot and is oppositely directed between the interior and exterior of the slot. This causes the antenna to operate in a transmission line like mode, which transforms the nearly zero impedance at the top of the slot to high impedance at the antenna feeding point. This high impedance at the feeding point leads to the desired high attenuation and impedance mismatching near the notch frequency [142]. However, the use of a slot can cause deterioration of an antenna performance such as gain, efficiency and radiation pattern [144]. An alternative antenna design without using slot to obtain band-notched characteristic was proposed in [144]. The antenna consists of two same size monopoles and a small strip bar at the center showing the band rejection performance in the frequency band of 4.9 to 6 GHz, which satisfies the UWB system requirement. The use of strip bar leads to high impedance at the notch frequency. The total length of strip bar from the ground plane is equal to a quarter-wavelength at the notch frequency. The current is concentrated around the strip bar and near the dual monopole edges and is oppositely directed and cancelled each other at the notch frequency.

In [24], a novel and compact wideband monopole antenna with a narrow slit having band-notch characteristic was presented. Band-notch characteristic is achieved by inserting a modified inverted U-slot on the main patch, which has length of 0.29λ ($< 0.5\lambda$). The narrow slit leads to produce an additional surface current path. The notch frequency is controllable by changing the length of the slot. Paper [26] has also presented the length of slot less than half wavelength (0.25λ) in order to have a frequency band notch function.

A CPW-fed planar UWB antenna with various slot shape having a frequency notch characteristic of WLAN frequency band was reported in [23], [26], [29]. The band-notch frequency due to the additional slot has increased the reactance value, thus less energy is radiated and it is more reactive within the stop band [23].

In this thesis, the proposed reconfigurable UWB antennas are designed by adopting the half wavelength slot structure techniques. This is corresponding to the previous techniques used when designing the proposed UWB slotted antenna. The main goal is how to design the reconfigurable UWB slotted antenna without major

modification from the previous slotted UWB antennas. The unique of this proposed reconfigurable UWB antenna is the antenna has additional capability in rejecting the FWA bands. Several small gaps are added instead of switches in order to perform the reconfigurability characteristics.

3.5 Theory Characteristic Modes for Planar Monopole Antennas

A great variety of experiments related to planar monopole geometries and feeding configurations have been carried out, but very little analysis on the physical understanding of the operating behavior has been considered up to now. Recently, the theory characteristic modes have been shown useful for antenna design. The theory characteristic modes allows to express the total current in the surface of a conducting body as a superposition of an orthogonal set of real current modes, which are termed characteristic modes [130]. These modes are obtained numerically for arbitrarily shaped bodies without any specific source of excitation, and hence they only depend on the shape and size of the body.

To acquire a clear insight into the physical performance of planar monopole antennas, the theory characteristic modes introduced by Harrington and Mautz [145], will be used to determine how the shape of the planar monopoles affects the input bandwidth performance of the antenna. This theory has been satisfactorily applied to the analysis of wire and patch, and to the study of the coupling phenomena between the antenna and the chassis in mobile handset [130].

For electrically small and intermediate size bodies, only a few modes are needed to characterize the electromagnetic behavior of the body [145]. Characteristic modes (J_n) are real current modes that are extracted at every frequency from generalized impedance matrix of the antenna. This matrix is obtained by the direct application of Method of Moments [120], [145]. Characteristics modes correspond with the eigencurrents of the matrix, and therefore depend only on the shape and size of the antenna [120]. A modal solution for the current J on the surface of the antenna as follows:

$$J = \sum_n \frac{V_n^i J_n}{1 + j\chi_n} \tag{3.1}$$

The term χ_n corresponds with the characteristic value or eigenvalue related to the n^{th} characteristic mode. A mode is at resonance when its associated eigenvalue is zero, it is derived that the smaller the magnitude of the eigenvalue is, the better the modes radiates [120]. The behavior of the modes can be obtained by studying eigenvalue variation with frequency. The eigenvalues χ_n, range from -∞ to +∞, with those of smallest magnitude being more important, for radiation and scattering problems [110]. Those modes with positive χ_n have predominantly stored magnetic energy, while those with negative χ_n have predominantly stored electric energy. Those modes with $\chi_n >$ is called as *inductive modes,* and those with $\chi_n < 0$ is called as *capacitive modes.* A mode having $\chi_n = 0$ is called an *externally resonant mode.* The modes corresponding to the internal cavity resonances or the conducting surface has $|\chi| = \infty$, and do not enter into radiation and scattering problems.

$$V_n^i = \left(J_n, E^i\right) = \oiint_S J_n . E^i ds \tag{3.2}$$

V_n^i is known as modal excitation coefficient, and defined as (3.2). The product $V_n^i J_n$ in (3.1) models the coupling between the excitation and the n^{th} mode, and determines which modes will be excited.

3.6 Summary

In this chapter, fundamental antenna parameters as the guidelines in designing UWB antenna have been discussed. UWB antenna design methodologies with various bandwidth enhancement techniques are also reviewed. Four techniques such as the use of slots for both patch and feeding strip, bevels/notches, truncation ground plane and notched ground plane are the techniques employed to the design of proposed UWB antennas. Theory characteristic mode is used in analyzing the monopole performance. Various reconfigurability antenna parameters are discussed

as well. Half wavelength slot structure is the technique used for designing the proposed reconfigurable slotted UWB antenna. This antenna has capability to reject the frequency bands from existing wireless communication systems such as FWA, HIPERLAN and WLAN. The proposed antennas are small UWB antennas with regards to the small antenna definition.

CHAPTER 4

SLOTTED AND RECONFIGURABLE UWB ANTENNA DESIGN

4.1 Introduction

In choosing an antenna topology for UWB design, several factors must be taken into account including physical profile, compatibility, impedance bandwidth, radiation efficiency, directivity and radiation pattern. On the other hand, there are special design considerations for antennas for the UWB systems, especially for microwave wireless communications [16]. Studies have shown that the antenna designs should be considered from a systems point of view, and the system transfer function is a good measure to evaluate the performance of the antennas in terms of system gain (the magnitude of the system transfer function) and group delay (the derivative of phase of the system transfer function), especially for the impulse systems.

In this chapter, the proposed slotted and reconfigurable UWB antennas are presented in detail. The novelty slotted UWB antennas are achieved by evaluating various slots configurations. The effect of slots, bevels and notches to the antenna impedance bandwidth are analyzed by using FDTD Zeland simulation software before the actual prototype is built. The proposed reconfigurable slotted UWB antennas with varying the slot length will investigate how the small gaps incorporated to slots having ability to band-notched frequency at FWA, HIPERLAN and WLAN bands. The controllable slot length by the gaps is intended to reject the required frequencies. Both simulation results of slotted and reconfigurable UWB antennas are presented.

4.2 Slotted UWB Antenna Design Consideration

Antennas play a critical role in the UWB communication systems and the choice of a specific UWB antenna design has to be based on the application main requirements. As mentioned in the previous chapter, the various geometries and perturbation techniques of planar monopole antennas are applied as guidelines in the proposed UWB antenna design. Several planar monopole geometries such as circular, elliptical, square, rectangular, hexagonal and pentagonal, have been proposed in many papers, providing wide impedance bandwidth. In this thesis, the rectangular geometry is taken as initial geometry to form various novelties polygonal. This is due to the flexibility of this geometry to be modified. Some novelty polygonal monopole antennas are proposed and studied in the frequency domain for UWB system in this chapter. The configuration of these antennas will be investigated both numerically and experimentally to obtain some quantitative guidelines for designing this type of antennas. The effect of bevels/notches technique, cutting slots on the patch and slotted ground plane to the impedance bandwidth is discussed with some examples on it. In addition, the UWB antennas printed on PCBs are more practical to implement. The antennas can be easily integrated into other RF circuits as well as embedded into UWB devices.

4.2.1 Various Bevels and Notches

Figure 4.1 and Figure 4.2 depict several typical polygonal planar monopoles, which are vertically installed above a ground plane. The dimension of the ground plane is chosen to be (30 x 11.5) mm^2 in this study. The original design has a rectangular radiator with a width (w) of 15 mm and a length (l) of 12 mm. The main objective in this antenna design is to reduce the size. Thus, the dimension of this rectangular radiator is kept to be constant. Obviously, it is difficult to do this without degrading the antenna performance but the main question is whether this degradation is acceptable or not for a given application.

The radiator may be varied and have a bevel or a smooth bottom or a pair of bevels for good impedance matching. The simulation results have proved that the bevel at the bottom or at upper edge of radiator give a very broadband bandwidth when properly designed. The objective of this study is to develop a design methodology to control the matching bandwidth of antenna

Figure 4.1(a) shows the rectangular monopole antenna with various steps notches cutting at the bottom edge. The feed width (w_f) is set to be 3 mm and the feed length (f_l) is set to be 12.5 mm. The first and third notch dimensions are (1 x 1) mm^2 and the second notch is (1 x 1.5) mm^2.

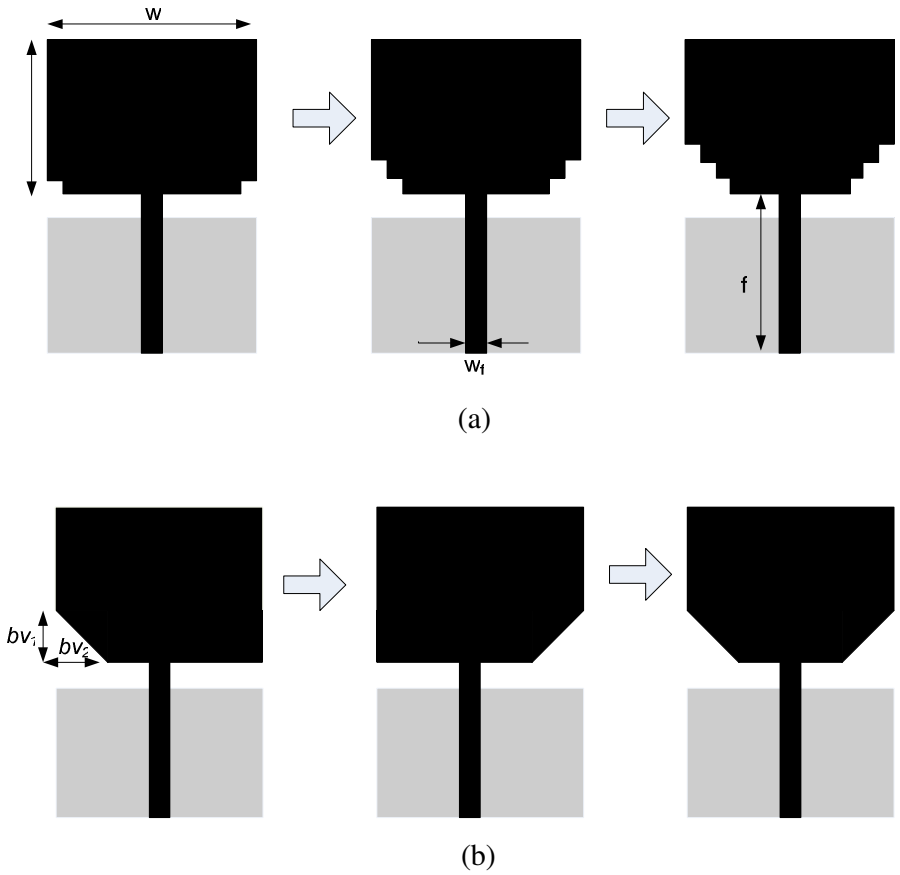

Figure 4.1: Various type of polygonal monopole antennas: (a) various steps notches at the bottom and (b) various bevel at the bottom

Figure 4.1(b) shows various beveling techniques applied to the rectangular monopole antennas. Beveling at the left side, right side and both sides have shown a different simulation results. The optimized dimension of a bevel that found to increase the impedance bandwidth is (bv_1 x $bv_{2)}$ of (3 mm x 2.5 mm), respectively.

The simulated return loss curves and input impedance for antenna shape in Figure 4.1(a) are shown in Figure 4.2. Cutting notches at the bottom techniques are aimed to change the distance between the lower part of the planar monopole antenna and the ground plane in order to tune the capacitive coupling between the antenna and the ground plane, thereby wider impedance bandwidth can be achieved. This technique is confirmed by the simulation result shown in Figure 4.2. As shown in Figure 4.2(a), the return loss of antenna with three steps notches cutting at the bottom edge is the worst curve with respect to -10 dB. This is due to its notch variation is more abrupt, thus the bandwidth is smaller. For the two steps notches, the return loss curve is the best, covering 3.17 GHz to 11.5 GHz of frequency ranges. While one step notch at the bottom provides a good matching bandwidth at below 9 GHz and start degrading at higher frequencies.

The simulated input impedance shows the loops around matching impedance point. It shows that the one step and three steps notches cutting at the bottom give more capacitive to the antenna than the two steps notches especially at higher frequency ranges. The ground plane as an impedance matching circuit and also it tunes the resonant frequencies.

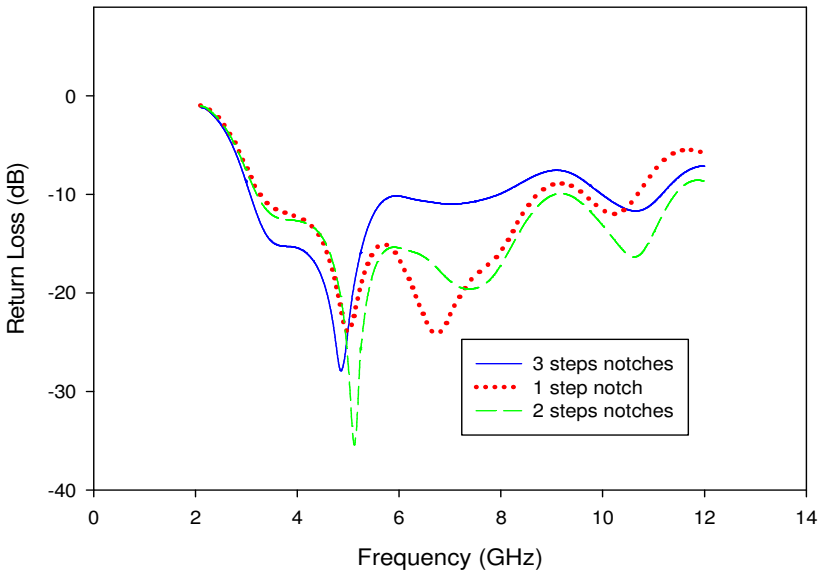

(a)

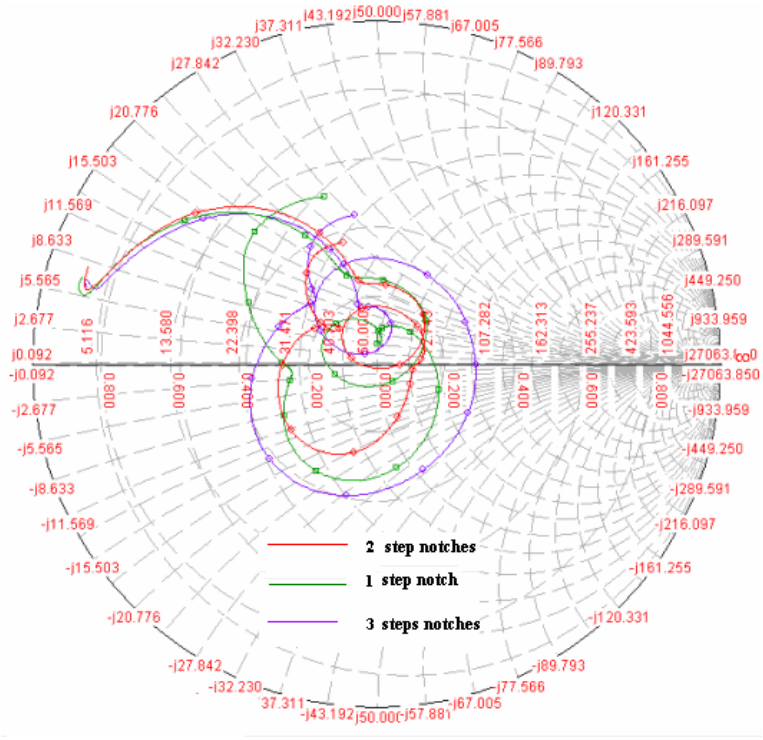

(b)

Figure 4.2: (a) Simulated return loss curves and (b) input impedance for various notches

There is an important phenomenon in Figure 4.2 at the first resonance occurs at 5.2 GHz for the patch with two notches at the bottom. When the antenna has only one and three notches at the bottom, the first resonances are 4.9 GHz and 5.1 GHz, respectively. Both first resonances are shifted slightly, but still not far from 5.2 GHz. In fact, the quarter wavelength at this first resonant frequency (5.2 GHz) just equals to the length of the antenna and optimized by the simulation software.

Table 4.1: The effect of notches to the simulated -10dB bandwidths of the proposed antenna

No. Notch	**f_L (GHz)**	**f_U (GHz)**	**Absolute BW (GHz)**	**Fractional BW (%)**
0	3.56	9.05	5.49	87
1	3.27	8.7	5.43	90
2	3.17	11.5	8.33	113
3	3.07	7.98	4.91	88

Table 4.1 shows the effect of two notches at the bottom of the patch to the antenna bandwidth. The basic rectangular patch antenna with a length of 12 mm and a width of 15 mm only provides the fractional bandwidth of 87%. This fractional bandwidth increases to 90% by cutting one notch at the bottom, while the maximum fractional bandwidth reach to 113% by applying two notches at the bottom of the patch antenna. Then, the fractional bandwidth decreases again by cutting three notches. Hence, the proper selections in the size of notches lead to the UWB characteristic.

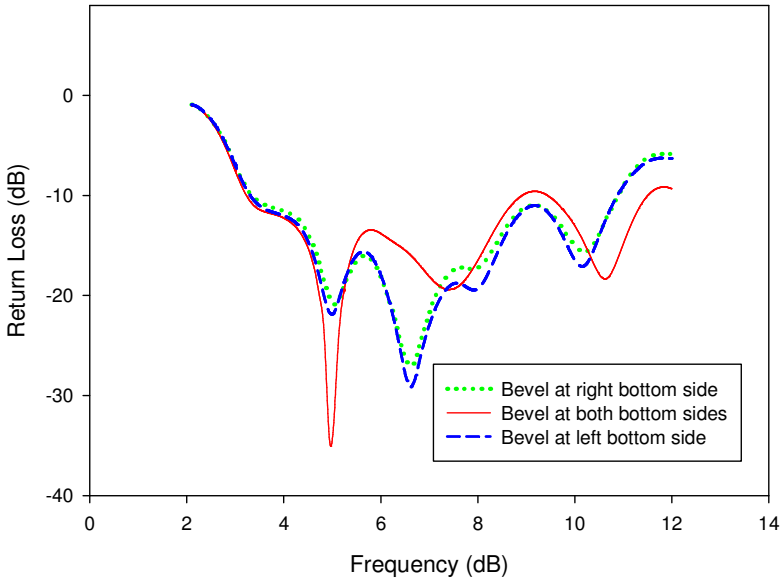

(a)

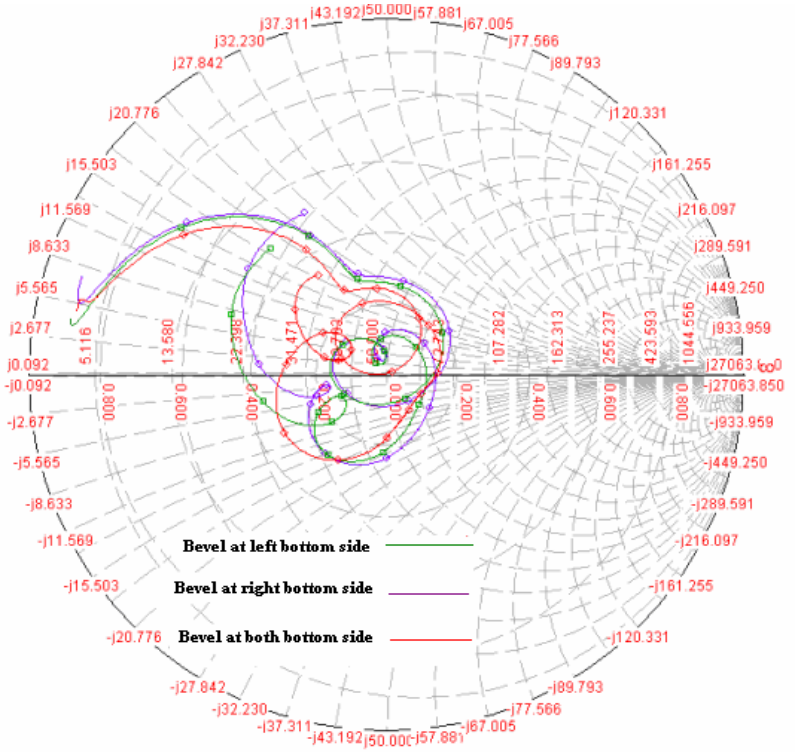

(b)

Figure 4.3: (a) Simulated return loss curves and (b) input impedance for various bevels

Figure 4.3 is simulated return loss curves and input impedance for antenna shape in Figure 4.1(b). The return loss of antenna with bevel at left or right bottom side shows almost identical result, which cover 3.27 to 10.82 GHz. Both bevels at both sides have found to increase the matching impedance bandwidth up to 11.5 GHz. The loops around matching point for all these types of antenna have shown a very broad bandwidth.

Table 4.2: The effect of bevels to the simulated -10dB bandwidths of the proposed antenna

Bevel	**f_L (GHz)**	**f_U (GHz)**	**Absolute BW (GHz)**	**Fractional BW (%)**
Left	3.27	10.82	7.55	107
Right	3.27	10.82	7.55	107
Both	3.27	11.5	8.23	111

Table 4.2 shows the fractional bandwidth of various bevels of proposed antennas. All three antenna designs show the UWB characteristic bandwidth. Bevel both sides has increased the fractional bandwidth to 111%.

In order to vary the geometry of antennas, a combination between pair bevels and notches steps are applied at edges corner as shown in Figure 4.4(a). The radiator is found to be irregular shape. Bevel and notch are kept same dimension with the previous model.

Trapezoidal and pentagonal antennas are also proposed in Figure 4.4(b). Both shapes are as variation of rectangular shape with bevel techniques. The dimension of w_1, bv_3, bv_4, bv_5, bv_6, is 12, 10, 7.5, 6, 6 mm, respectively. By varying the height of bevel at the bottom edge gives significant improvement of impedance bandwidth.

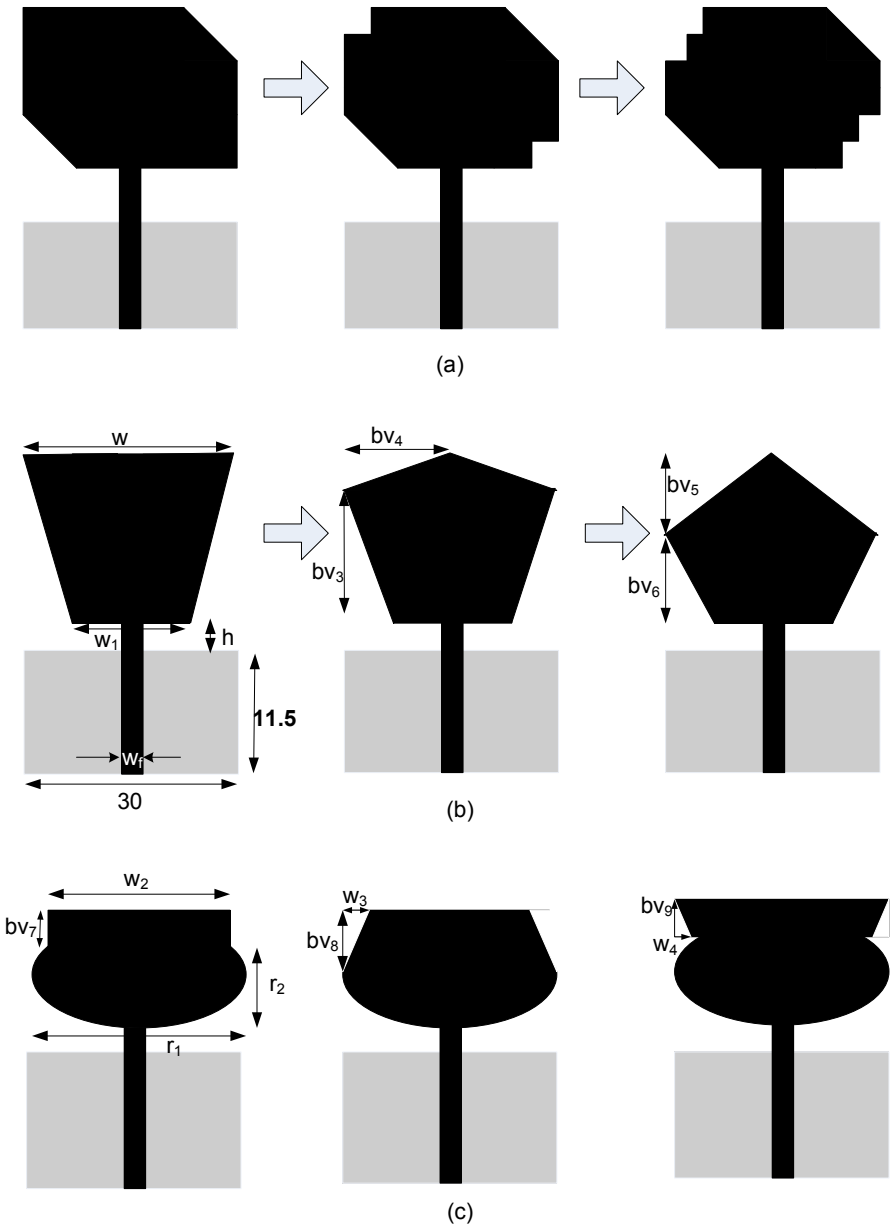

Figure 4.4: Various type polygonal monopole antennas: (a) combination of notch and bevel, (b) trapezoidal and pentagonal bevels, and (c) smooth bevels at the bottom

Figure 4.4(c) presents a smooth bevel at the bottom edge. The smooth bevel is resulted by an ellipsis with r_1 and r_2 of 15 mm and 10 mm, respectively. By optimizing the major and minor axes of the ellipse as well as feed gap between the bottom of the ellipse and ground plane, the antenna features a high-pass impedance response. The broadband characteristics are due to the smooth transition between the radiator and feeding strip. Overlapping an ellipsis and modified rectangular results a new polygonal shape. The dimension of w_2, w_3, w_4, bv_7, bv_8, bv_9 is 12, 1.5, 1, 2, 7, 2.5 mm, respectively.

The simulated return loss curves of antenna shape in Figure 4.4(a) are shown in Figure 4.5. The original goal of additional notches to the patch is to increase the bandwidth. In fact, the simulated return loss curves for both types of antenna, pair bevels with one and two steps notches, do not give any improvement of bandwidth even though coupled with the notches. They degrade the return loss performance especially at 8.7 to 10 GHz. It is clearly shown from this simulated result that the impedance bandwidth is critically determined by proper design and place of notches at antenna edges.

The matching characteristics of these types of antennas are shown in the smith chart Figure 4.5(b). Cutting notches at the antenna edges has moved antenna to be more capacitive at higher frequency ranges. The loops are also found around the impedance matching point.

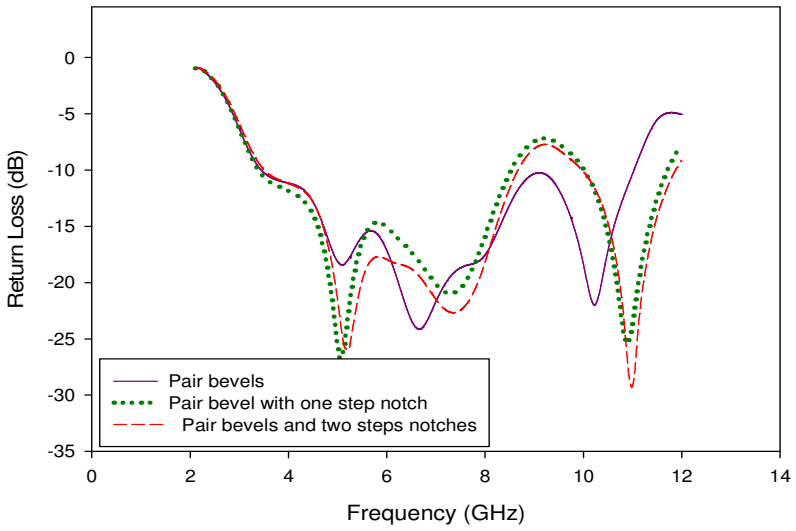

(a)

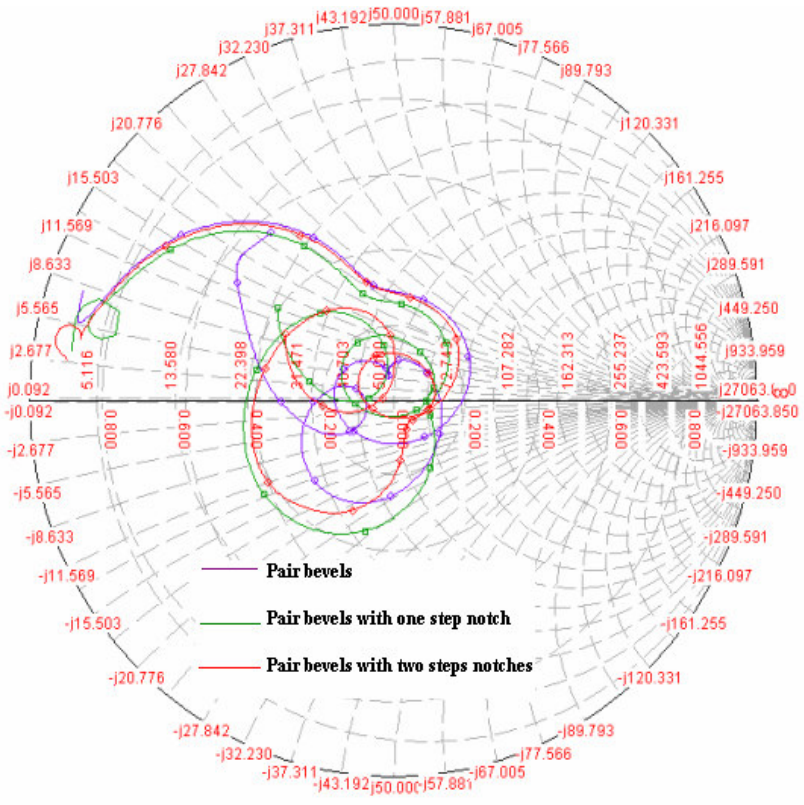

(b)

Figure 4.5: (a) Simulated return loss curves and (b) input impedance for various pair bevel and notches

Table 4.3: The effect of bevels coupling notches to the simulated -10dB bandwidths of the proposed antenna

Bevel & notch	**f_L (GHz)**	**f_U (GHz)**	**Absolute BW (GHz)**	**Fractional BW (%)**
Pair bevels	3.37	11	7.63	106
Pair bevels with 1 notch	3.37	8.56	5.19	87
Pair bevels with 2 notches	3.47	8.66	5.19	85

Table 4.3 lists the fractional bandwidth of antenna with pair bevels and notch. An additional of notch to the antenna edge coupled with the bevels has shown the bandwidth decrement. The maximum fractional bandwidth of 106% is achieved for antenna with bevels at the upper and lower edges.

Trapezoidal and various height pentagonal shapes are proposed. The simulated return loss curves and the input impedance are shown in Figure 4.6(a) and Figure 4.6(b), respectively. The ratio between upper height and lower height are critically determined the input impedance bandwidth. By changing the height will degrade the return loss performance as proved in Figure 4.6(a).

The lower height determines the lower resonance frequency and the upper height determines the upper frequency. This behavior is shown by comparing the return loss curves between pentagonal with lower height of 10 mm and pentagonal with lower height of 6 mm. The first type with 6 mm of height, the lower resonance is 7 GHz while the second type is 5.2 GHz. The difference of height results much shifted to the lower resonance frequency. The smooth beveling transition at upper edges of pentagonal gives a flat return loss curves below -15 dB. The abrupt transition at the upper edges has degraded the antenna performance especially at higher frequency ranges of 8.7 to 9.7 GHz, as shown in Figure 4.6(a).

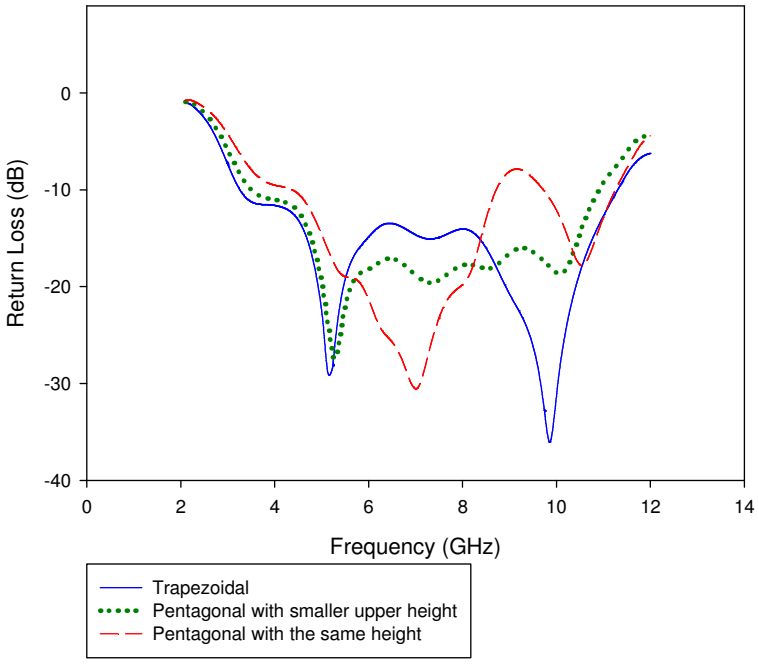

(a)

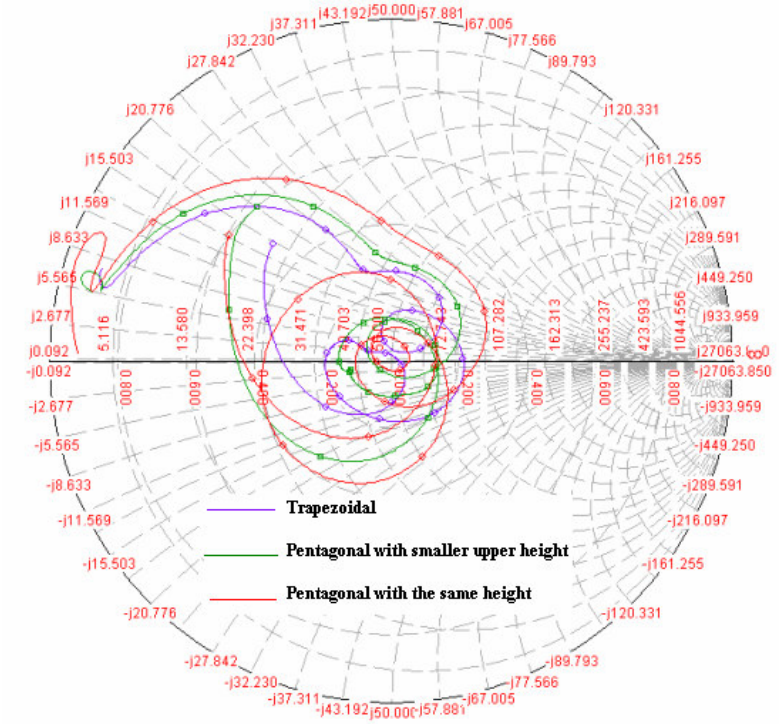

(b)

Figure 4.6: (a) Simulated return loss curves and (b) input impedance for trapezoidal and various pentagonal

The return loss curve of trapezoidal shape shows two resonance frequencies of 5 GHz and 9.8 GHz with covering bandwidth of 3.27 to 11.3 GHz, except the middle frequency ranges which the return loss lower than the pentagonal with 10 mm of height.

Table 4.4 shows the fractional bandwidth of proposed trapezoidal and pentagonal antennas. The maximum fractional bandwidth of 110% is achieved for trapezoidal antenna. Even though the trapezoidal antenna has a maximum fractional bandwidth, the pentagonal antenna with 10 mm lower height has a flat return loss below -15 dB. Decreasing the lower height of pentagonal has decreased the fractional bandwidth, as listed in Table 4.4.

Table 4.4: Trapezoidal and pentagonal fractional bandwidth with respect to the simulated return loss of -10dB

Model	**f_L (GHz)**	**f_U (GHz)**	**Absolute BW (GHz)**	**Fractional BW (%)**
Trapezoidal	3.27	11.3	8.03	110
Pentagonal with 10 mm lower height	3.47	10.9	7.43	103
Pentagonal with 6 mm lower height	4.35	8.7	4.35	67

Figure 4.7 shows the return loss curves and input impedance of various shapes of antenna with smooth bevel at the bottom and various transitions shape at the upper edge. From all simulated return loss curves, the antenna with reverse trapezoidal transition results a nearly flat response curve at higher frequency. The impedance bandwidth covers 3.27 to 12 GHz. All simulated return loss curves are not varying too much. The matching curve lines are shown in Figure 4.7(b).

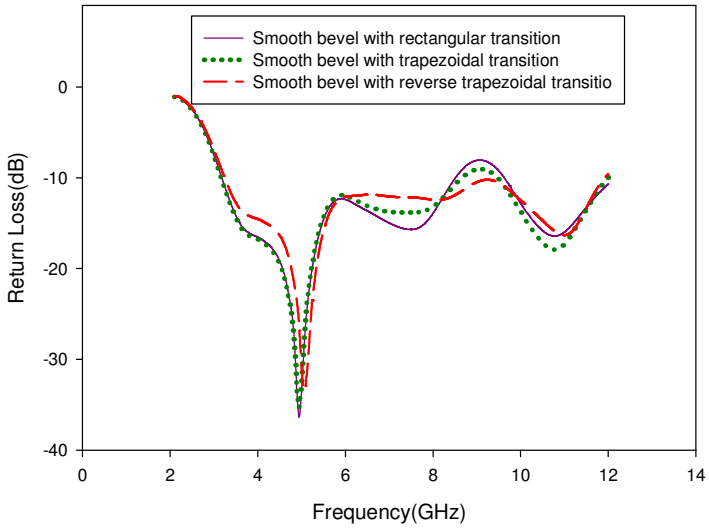

(a)

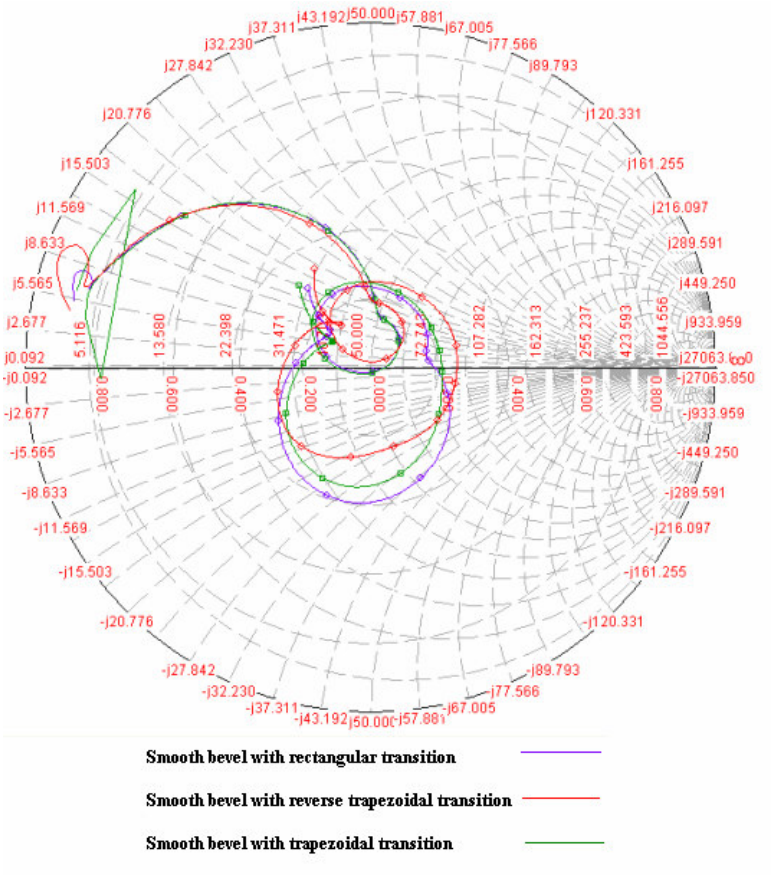

(b)

Figure 4.7: (a) Simulated return loss curves and (b) input impedance for various transitions with smooth bevel

Table 4.5: The effect of smooth bevels and upper edge transition to the simulated -10dB bandwidths of the proposed antenna

Model transition	f_L (GHz)	f_U (GHz)	Absolute BW (GHz)	Fractional BW (%)
Rectangular	3.17	8.56	5.39	92
Trapezoidal	3.17	8.66	5.49	93
Reverse trapezoidal	3.27	12	8.73	114

It is shown in Table 4.5, the antenna with smooth bevels and reverse trapezoidal at upper edges has a maximum fractional bandwidth of 114%. The bandwidth start degrading at 8.5 to 9.5 GHz for rectangular and trapezoidal shape transition, this is due to these shape give more capacitive to the antenna.

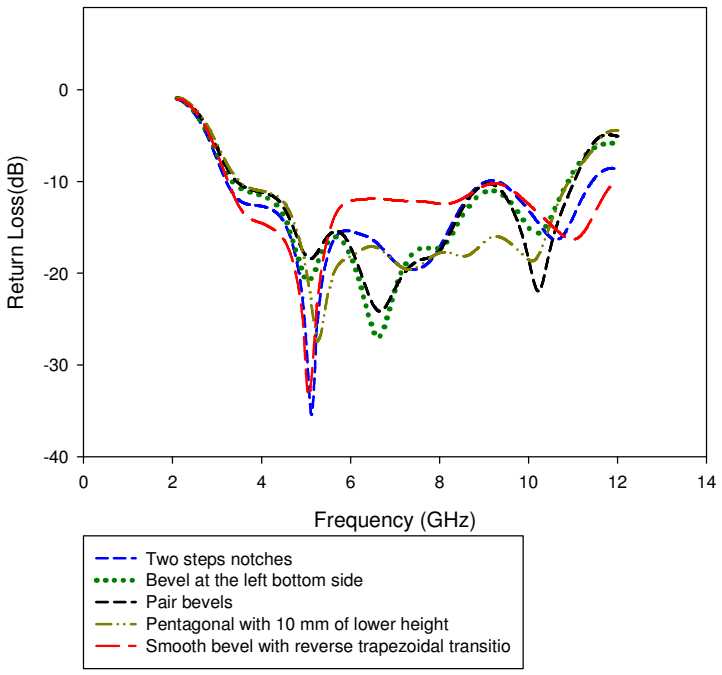

Figure 4.8: Simulated comparison return loss curves for each best type of antenna

Figure 4.8 provides a simulated comparison return loss curves for each group of antenna, as described above, which give the best performance. This comparison is

to investigate which shape of the antenna model gives the best performance in term of return loss. Next, the effect of slots insertion to these models will be discussed in the next section. To simplify the next step, two model antennas chosen are two steps notches, and pentagonal with 10 mm of lower height.

It is also clearly shown from the graph that the lower resonance frequency for all antenna models is around 5.2 GHz. It is correspondence to the dimension of antenna where kept to be constant for all models. The only variation of return loss curves occur at higher frequency range and this is determined by how properly notch and bevel designed.

4.2.2 Current Distribution Behavior

Antennas are divided in two zones; active and neutral zones. They can be identified with the study of the currents. The geometry of the antenna implies the current courses and makes it possible to identify active and neutral zones in the antenna, thus it will be possible to fix which elements will act on each characteristic. The active zone is the matching and radiator zone. Acting on matching and radiating areas allows controlling the bandwidth [146]. Zone closed to feeding point is the active zone. The neutral zones where geometry modifications are useless because neither the radiation pattern nor the matching bandwidth is much influenced. Study on current distribution of planar monopole antenna by transmission line modeling (TLM) was performed in [147].

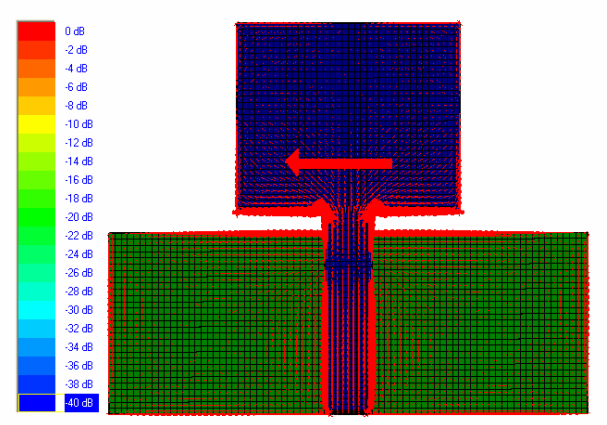

(a)

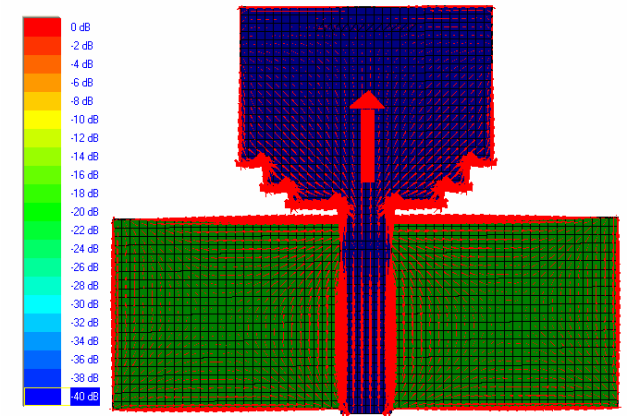

(b)

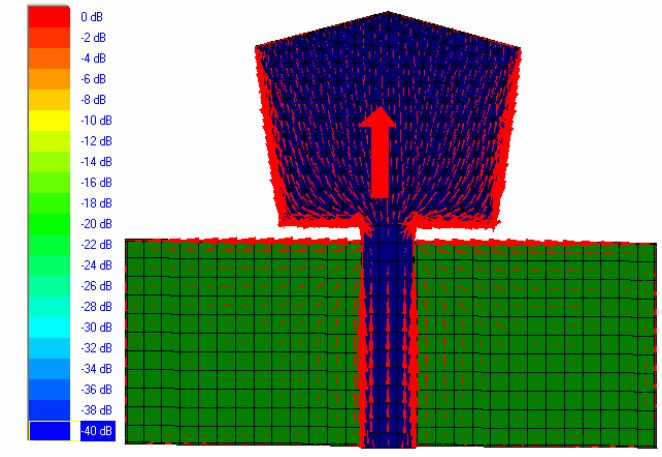

(c)

Figure 4.9: Simulated current distribution for three model antennas with affect to the impedance bandwidth: (a) rectangular, (b) rectangular with two notches, and (c) pentagonal

Matching bandwidth is due to the shape of the antenna closed to the feeding point, where currents are the strongest. It is possible to enlarge or reduce it in accordance with the application to implement by modifying its geometry close to this one as shown in Figure 4.9. Figure shows the current distribution for three model antennas at 7.5 GHz, such as rectangular, pentagonal with 10 mm of lower height and rectangular with two notches. As mentioned in Chapter 3, when properly designed, the bevels and notches improve significantly the impedance bandwidth at upper frequency.

The study of the current flow on a planar monopole antenna reveals that it is mostly concentrated in the vertical and horizontal edges, as shown in Figure 4.9. It is observed that the horizontal currents distributions are focused on the bottom edge of rectangular patch. Besides, the horizontal component is also greater than the vertical on this part of the antenna. The field supported by these currents would be mainly confined between the bottom part of the rectangular antenna and the ground plane; this is due to the small distance, a small fraction of wavelength, of this edge to the ground plane [147]. Thereby, this part acts as a matching element.

Figure 4.10 shows the return loss performance of this rectangular antenna. The return loss starts degrading its performance at 7.5 GHz, this is due to more horizontal current mode occurs in the whole structure which degrade the polarization properties and the impedance bandwidth performance of the antenna [129]. In order to modify the equivalent characteristic impedance on the antenna, the distance of the bottom edge to the ground plane and the bottom profile of the monopole should be varied. By varying the edges closed to the feeding point means modifying the current path on the antenna.

The discontinuity occurred from cutting notch or beveling at the bottom side of a rectangular antenna has enforced the excitation of a particular characteristic mode (the vertical current mode) in the structure, which presents a very wide bandwidth. Much current density occurs closed to the feeding edge, while at the top of antenna; the current levels are not too strong as shown by simulated result in Figure 4.9(b) and Figure 4.9(c). From the simulated return loss, the rectangular shape has the smallest impedance bandwidth. In addition, the double notches at the base of

the antenna have demonstrated to shift upward the upper edge frequency of the bandwidth.

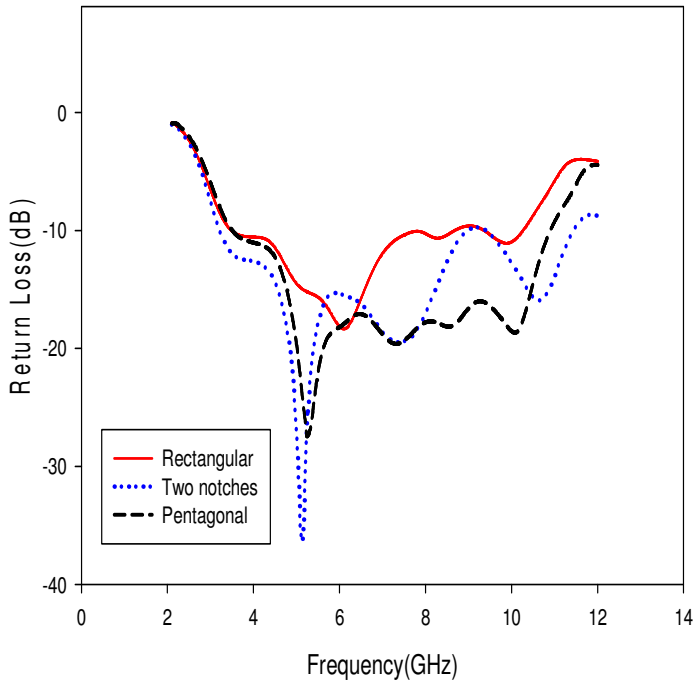

Figure 4.10: Simulated return loss for three model antennas with affect to the impedance bandwidth

To better control an antenna behavior, it is necessary to identify neutral zones. The neutral zone can be used to simplify the antenna structure and integrate other function of the systems such as antenna circuits. This investigation has been proposed in [146], but not much explanation given. How to determine the neutral zone is not explained in detail.

Thorough literature reviews [146]-[147] and simulation experiences, there are four types of current distribution modes in the antenna surface; vertical current mode, horizontal current mode, diagonal current mode and asymmetry current mode. By observing the current distribution flow, the pentagonal has a diamond neutral zone and both rectangular and two steps notches have a rectangular neutral zone. In this zone, the current level is not too strong but it is not zero level. Normally, this zone

occurs at the middle of the antenna structure. The neutral zone for each frequency appears at different position. This is due to the difference current mode behavior at every frequency. From simulation experiences, as long as the size and the position of the neutral zone are precisely determined, this zone can be removed with no much influence on the radiation pattern and the matching bandwidth as shown in Figure 4.11 to Figure 4.14, respectively.

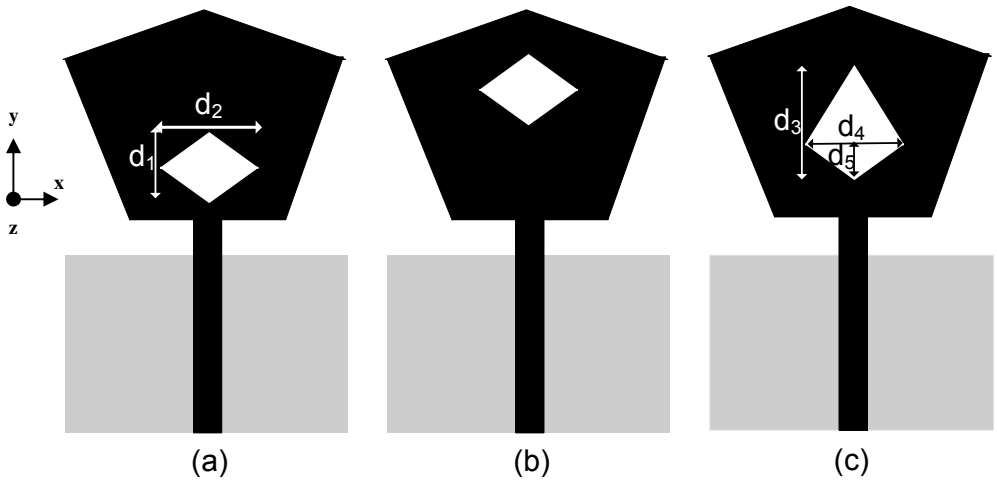

Figure 4.11: Neutral zones for various frequencies of pentagonal antenna: (a) 5 GHz, (b) 8GHz, and (c) 10.5 GHz

Figure 4.11 presents the neutral zones for 5, 8, and 10.5 GHz of pentagonal antenna. From observation, each frequency has a different neutral zone size and position. The neutral zones of 5 GHz and 8 GHz have the same size. This neutral zone size is determined by observing the current distribution mode in the antenna surface. The slot size is precisely measured in order not to degrade the antenna performance. This size is obtained and optimized by Zeland simulation software. The optimum size of diamond slot at 5 and 8 GHz is d_1 x d_2 of 4 x 4 mm, while d_3 x d_4 x d_5 of 6 x 4 x 2 mm at 10.5 GHz. The effect of this diamond slot to the return loss and radiation pattern of proposed antenna are described in Figure 4.12.

Figure 4.12 shows the simulated radiation pattern and return loss for both pentagonal antennas with and without diamond neutral slot. The simulated return

loss for all types of diamond slots does not influence the impedance bandwidth with respect to -10 dB. The Radiation patterns of these antennas are computed at 5.25 GHz using the Zeland FDTD. The radiation patterns displayed have been normalized to the 0 dB of gain and a 10 dB/division scale is adopted for all the figures. In this software, the radiation patterns are simulated into elevation and azimuth directions. For elevation direction, E-theta and E-phi are plotted with varying the phi angle. While the azimuth direction, the E-theta and E-phi are plotted with varying theta angle.

For Zeland FDTD and IE3D software, the terminologies used are Total Field (E-total), Theta Field (E-theta), and Phi Field (E-phi). The E-total is the properties of the antenna with all the field considered, the E-theta and E-phi are considered only E-theta field and E-phi field, respectively. For linear polarized antenna, the E-total or E-theta is primary radiation pattern, while the E-phi pattern as the cross polarization [148].

The elevation patterns for antennas simulated at E-theta, phi = 90^0 is shown in Figure 4.12. It is observed that the patterns behaviors for all neutral zones do not much vary with respect to the patterns that obtained without the slot. This leads to be ideal for ultra wideband antenna characteristic.

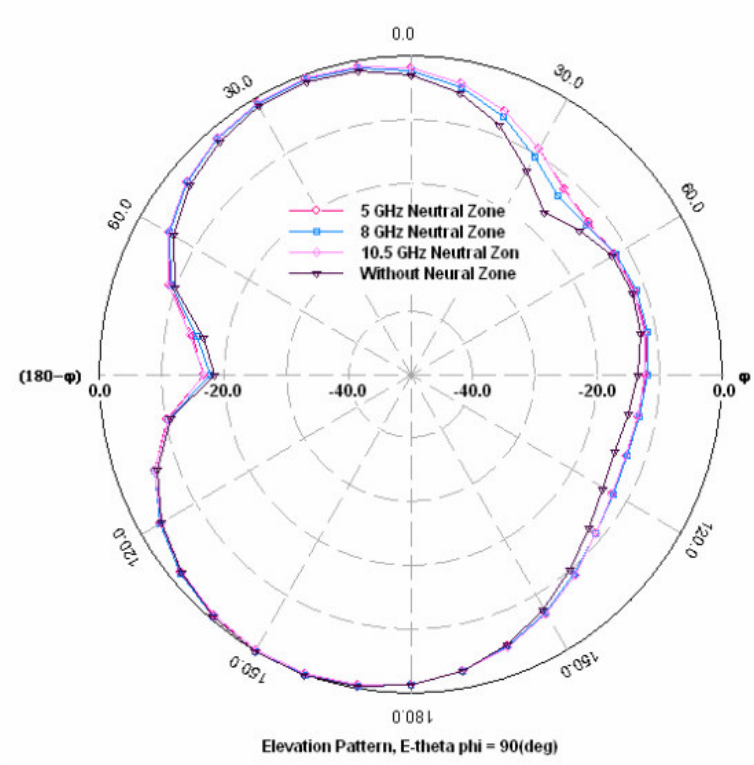

(a)

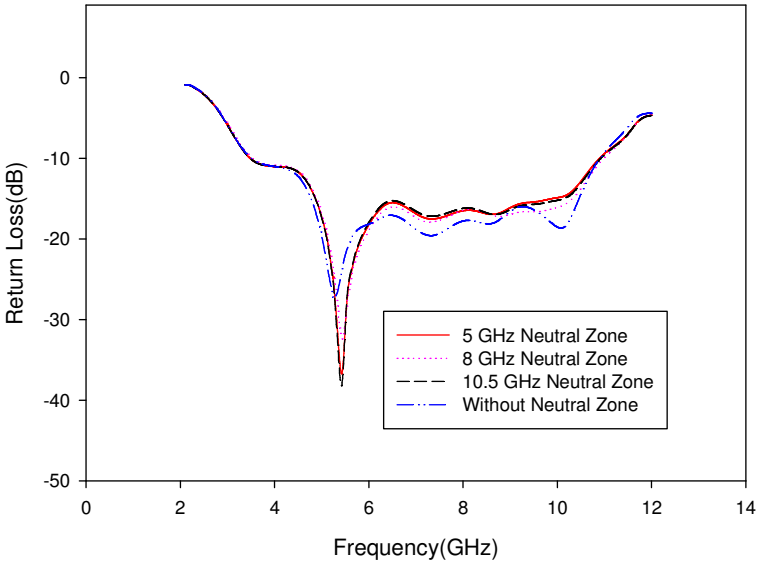

(b)

Figure 4.12: (a) The simulated radiation pattern for various diamond slots of pentagonal antenna at 5.25 GHz and (b) the simulated return loss for various diamond slots

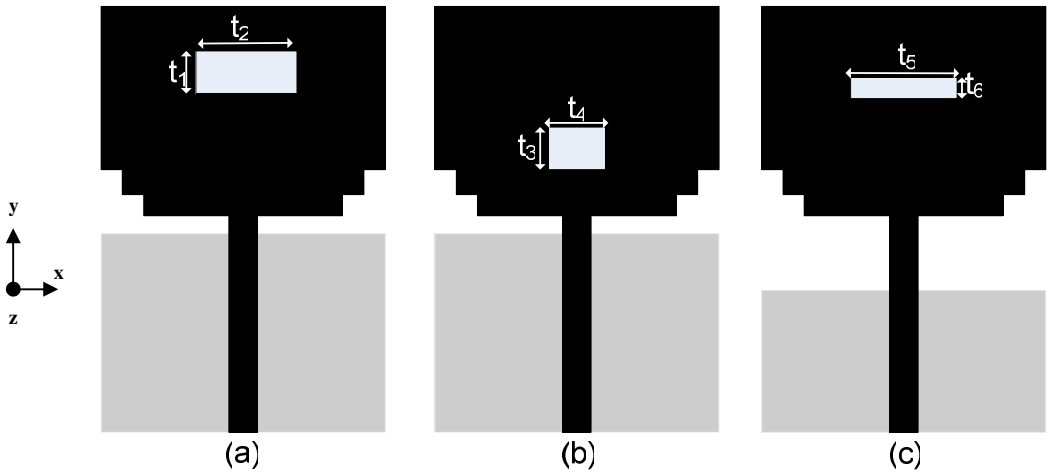

Figure 4.13: Neutral zones for various frequencies of rectangular with two notches antenna: (a) 4.5 GHz, (b) 5 GHz, and (c) 8 GHz

Figure 4.13 shows the rectangular neutral zones at 4.5, 5, 8 GHz of rectangular with two notches antenna, respectively. The sizes of t_1, t_2, t_3, t_4, t_5, t_6 are 3, 6, 3, 3, 5, 1.5 mm. The simulated radiation pattern and return loss for these antennas are shown in Figure 4.14.

It is shown from simulation results that rectangular slots cut in the neutral zone not give significant affect to the impedance bandwidth. The radiation pattern is simulated at 5.25 GHz for various rectangular slots. Thus, by identifying the neutral zone and active zones on an antenna, the size of antenna can be reduced and its characteristic can be controlled.

It can be concluded, from simulation experience, that this theory of slot cut on the neutral zone is only valid for a single slot. If there are some slots cut on the same patch, the mutual coupling effect between slots will influence the antenna performance as discussed in the next section.

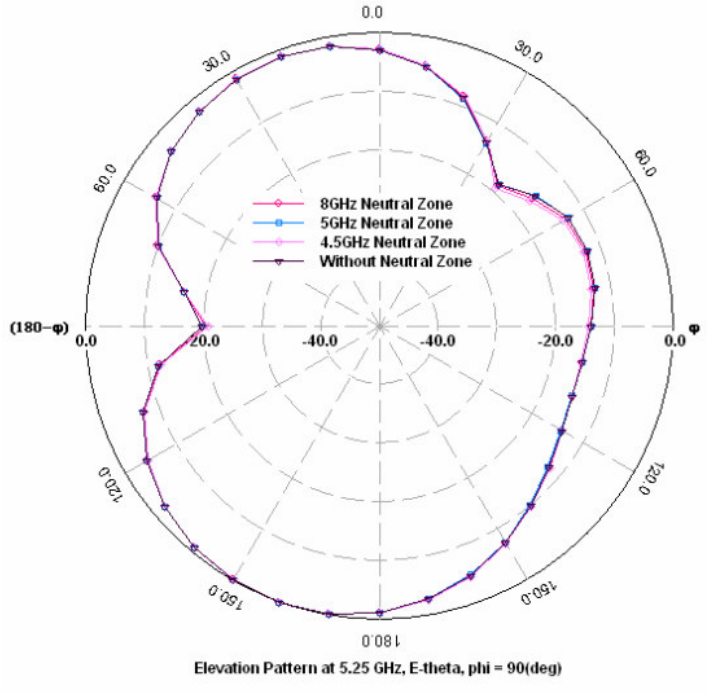

(a)

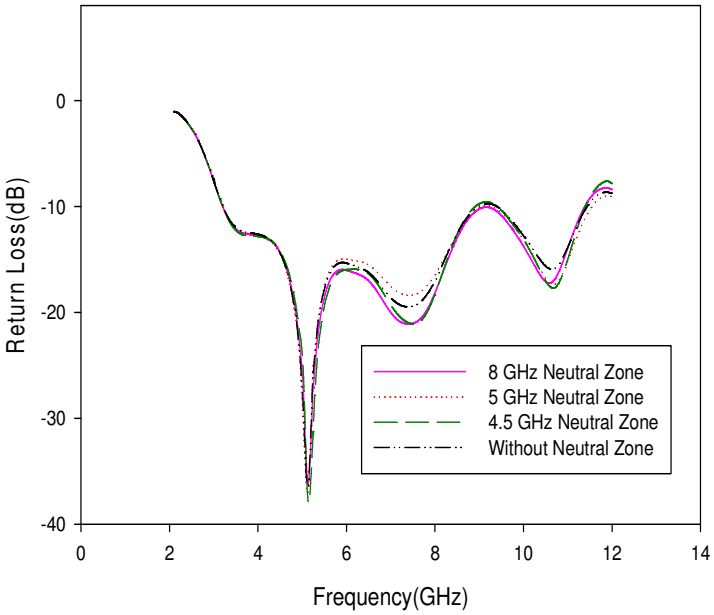

(b)

Figure 4.14: (a) The simulated radiation pattern for various rectangular slots of rectangular antenna with two notches at 5.25 GHz (b) The simulated return loss for various rectangular slots

4.2.3 Various Slots

As mentioned in Chapter 3 that slots on patch antenna have resulted improvement of the impedance bandwidth especially at higher frequency ranges [16]. Slots are also used to control simultaneously the radiation pattern shape [146]. These behaviors can be identified with the study of the current distribution as discussed in previous section.

In [146], by modifying the current paths on the monopole antenna, it is possible to have a radiation pattern without any zero of radiation while keeping the bandwidth. The monopole radiation pattern presents a zero of radiation in the axis of the antenna that comes from a destructive recombination of the currents at this point. The analysis in [146] has shown that slots must be placed on the top of the antenna, where current levels are not to strong, even though the matching bandwidth may be reduced. Typically, slots are placed on the half top of the antenna. The current path is modified on one side of the antenna. The dissymmetry created by the slots removes the zero current point.

Figure 4.15 and Figure 4.16 depict both proposed antennas with various slots design. The slots shape is designed very carefully by studying the current flow distribution which will give input impedance improvement. Each antenna has three different slots shapes in order to determine which shape of slot produced the best performance. This study will investigate the effect of vertical slot, horizontal slot and circular slot cut on the patch to the current distribution flow and impedance bandwidth. The rectangular antenna with two notches at the bottom side is inserted by T slots for feeding strip and patch radiator, a ring and L slots, and dual asymmetry L slots. The slot sizes of these rectangular antennas are listed in Table 4.6. The T slot and dual L slot are as combination between vertical and horizontal slot, a ring and L slots are designed as combination of circular, horizontal and vertical slots. The pentagonal radiator is added by dual L and U asymmetry slots, an arrow slot and an epsilon (ε) slot. The slot sizes of these pentagonal antennas are listed in Table 4.7. Analysis has proved the theory of slots in [16]. Various slot designs on these proposed antennas result novelty structure of slotted UWB antenna, this is as one of contribution in this thesis.

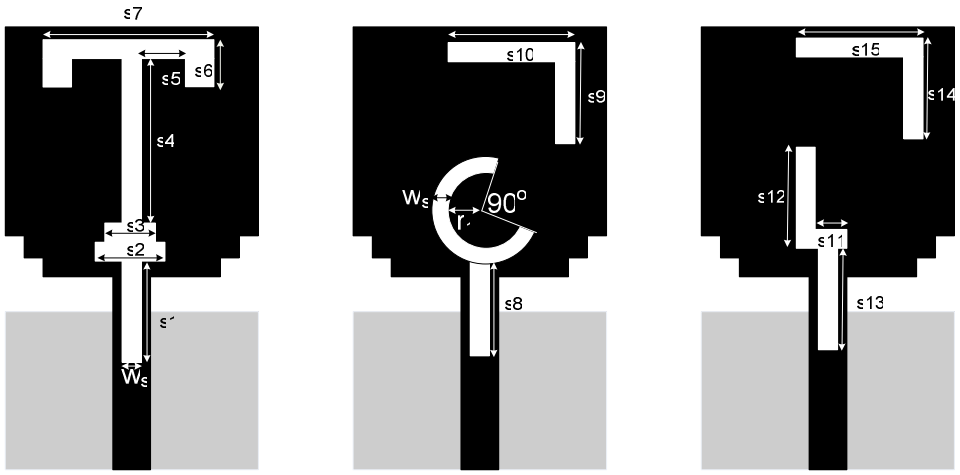

(a) (b) (c)

Figure 4.15: Various slots design for rectangular with two notches antennas: (a) T slots for patch and feeding, (b) a ring and L slot, and (c) dual asymmetry L slots

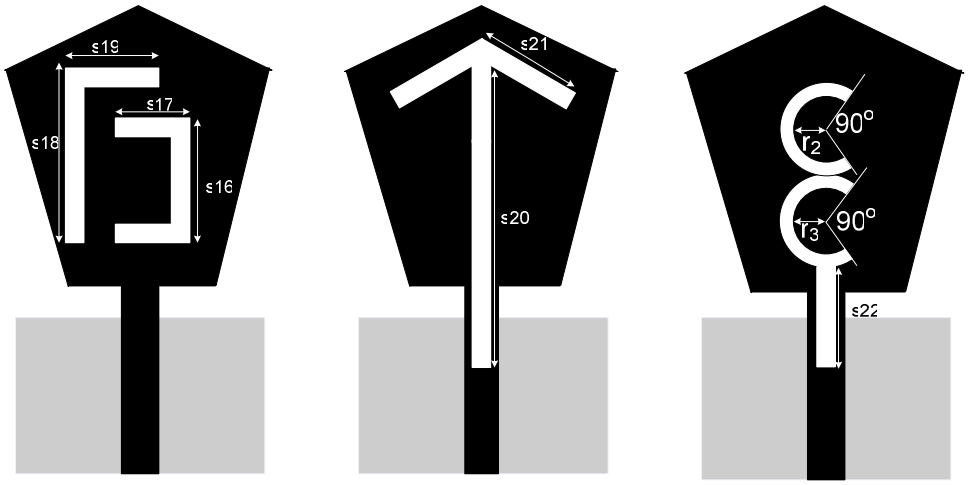

(a) (b) (c)

Figure 4.16: Various slots design for pentagonal antennas: (a) dual L and U asymmetry slots, (b) arrow slot, and (c) epsilon slot

Table 4.6: Slot size for slotted rectangular antenna in Figure 4.3

Model	Description	Symbol	Size (mm)
(a)	slot width	w_s	1
	slot length	l_{s1}	11
		l_{s2}	5
		l_{s3}	3
		l_{s4}	7
		l_{s5}	1.5
		l_{s6}	2
		l_{s7}	6
(b)	slot width	w_s	1
	slot length	l_{s8}	11
		l_{s9}	6
		l_{s10}	6
	radius	r_1	3
(c)	slot length	l_{s11}	3
		l_{s12}	6
		l_{s13}	11
		l_{s14}	6
		l_{s15}	6

Table 4.6 presents the slot size of three types slot design for rectangular antennas. The w_s is kept constant of 1 mm for whole antenna design. The original idea cutting a slot at feeding strip for most slots design is to increase the vertical current distribution to antenna radiator. Table 4.7 lists the slot size of three types slot design for pentagonal antennas. Figure 4.16(a), the slot width is decreased to 0.5 mm in order to improve the bandwidth above 10 GHz. Other types have the same slot width of 1 mm. The length and width of slots for proposed antennas are optimized by Zeland simulation software.

Table 4.7: Slot size of slotted pentagonal antenna in Figure 4.4

Model	Description	Symbol	Size (mm)
(a)	slot length	l_{s16}	6.5
		l_{s17}	3
		l_{s18}	9
		l_{s19}	6
(b)	slot length	l_{s20}	20
		l_{s21}	9
(c)	slot length	l_{s22}	6
	radius	r_2	1
		r_3	1

The simulated return loss for various slot designs of proposed slotted pentagonal antennas as shown in Figure 4.17. It is shown from the graphs that the first resonance frequency is not much shifted for all slot designs. The length and shape of slots are only affecting to the mid and higher frequency ranges. Here, the resonance frequencies are defined where the dips on the return loss curve are located. The L and U slot design has shown improvement bandwidth at frequency above 10 GHz. The slot width for this slot design is set to 0.5 mm; this is due to the fact that slot width of 1 mm does not provide improvement at the upper frequency. From simulation, the U slot improves the upper dip resonance of 10.3 GHz and the L slot improves the lower dip resonance of 5.3 GHz. The coupling both slots has shown a very good return loss below -15 dB. The length of L slot is 14.5 mm approximately equal to 0.25λ at 5.3 GHz, and the length of U slot is 11.5 mm approximately equal to 0.4λ at 10.3 GHz.

Arrow slot on pentagonal patch produces an additional dip resonance frequency at 8.3 GHz, which are overlap with the main resonance of the patch antenna, but degrade the bandwidth at around 9 GHz. The degradation is due to the head arrow slot placed at the top of antenna. The slot length of the head arrow is 17 mm approximately equal to 0.5λ at 9 GHz. The dip resonance at 8.3 GHz is caused

by the long vertical slot coupled with the head arrow. The total length slot of these couple slots is 37 mm approximately 1λ at 8.3 GHz. It is noticed from the simulation result that any slot placed at the top of pentagonal antenna critically determine the impedance bandwidth.

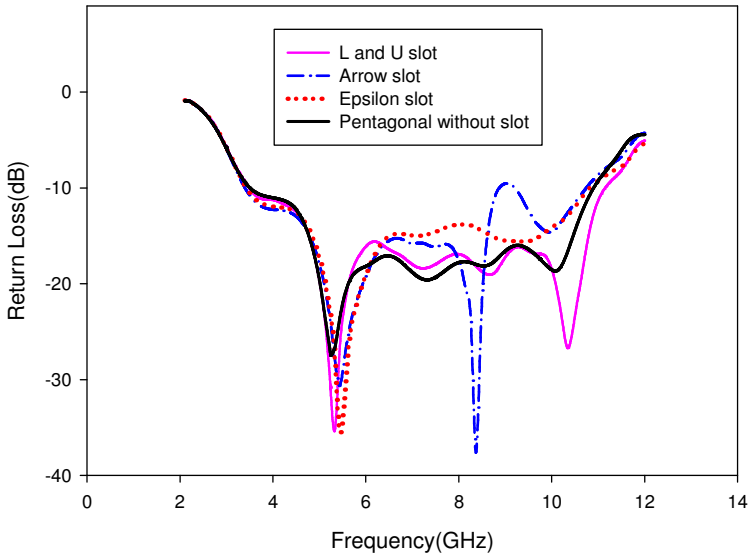

Figure 4.17: The simulated return loss of various slot designs for pentagonal antennas

The epsilon slot has shown a very flat return loss at mid range of frequencies. The width slot is 1 mm with the radius (r_3) of 1 mm. Two coupled ring slots are designed to form an epsilon slot. The total arc length of both epsilon slots is 19 mm. The total vertical and epsilon length slots are approximately equal to 0.5λ at 5.4 GHz. Even though the epsilon slot improves the return loss of lower resonance at 5.4 GHz but degrade the return loss of frequency range above 6 GHz if compared with antenna without slot.

Figure 4.18 shows the simulated return loss of slotted rectangular antennas. Two slots design such as ring and L slot and dual asymmetry L slot has shown multiple resonances. In [12], a new UWB antenna which consists of a rectangular

patch with two steps, a single slot on the patch, and a partial ground plane is reported. However, the performance and characteristic of this antenna is not analyzed in detail. How exactly this antenna operates across the entire bandwidth, remains a question. With this proposed various slot on rectangular antenna with two steps, the effect of slot to the antenna performances are investigated in detail.

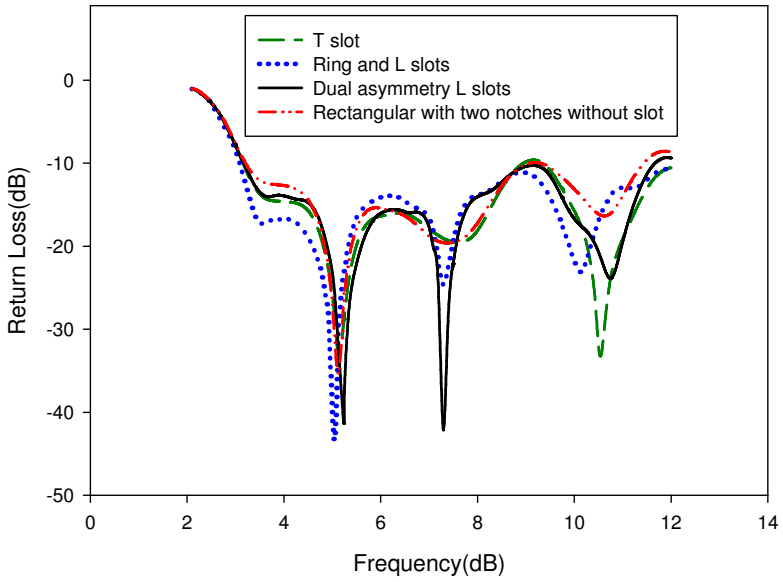

Figure 4.18: The simulated return loss of various slot designs for rectangular with two notches antennas

The T slot on the feeding strip produces more vertical current thus improve the matching impedance performance at higher frequencies. The length of the T slot on the feeding strip is designed approximately equal to $\lambda/2$ at 10.5 GHz. From the graph in Figure 4.18, at upper frequency of 10.5 GHz of T slotted antenna, the $|S_{11}|$ reaches -30 dB. The bandwidth enhancement is due to much more vertical electrical current achieved in the patch through the T slots resulting in much regular distribution of the magnetic current in the slots. While the T slot cut on the patch shows the return loss improvement at the first resonant point of 5.2 GHz. By cutting the slots on the patch disturb the current distribution flow. Thus, the slot wideband

behavior is due to the fact that the currents along the edges of the slot introduce the same resonance frequencies, which, in conjunction with the resonance of the main patch, produce an overall broadband frequency response characteristic. The slot also appears to introduce a capacitive reactance which counteracts the inductive reactance of the feed [109]-[110]. Thus, the bandwidth broadening comes from the patch and T-slot, coupled together to form UWB characteristic [111]. The use of slot embedded on the microstrip patch has been investigated extensively in [109], [111][149]-[151]. This most successful technique utilizes a coupled resonator approach, in which the microstrip patch acts as one of the resonator and slot as the second resonator near its resonance [149].

The ring slot with the open angle of 90^{o} and radius (r_1) of 3 mm has shown an improvement to the return loss at the lower resonance of 5 GHz and the upper resonance of 10 GHz. The arc length of ring slot is 19 mm. The total length of vertical slot and ring slot is approximately equal to 1λ at 10 GHz. The vertical slot cutting at the feeding strip has guided the vertical electrical current flowing through the antenna radiator and most concentrated near to the ring edge. The L slot at the right upper corner of the patch shows the second dip resonance at 7.3 GHz. The length of L slot is 11 mm and optimized by the Zeland simulation software. This coupled slot has presented multiple resonances which cover 3 to 12 GHz frequency range.

The dual asymmetry L slot on rectangular patch has shown multiple resonances. The second dip resonance of 7.1 GHz is due to the right upper corner L slot length, while the dip resonance of 10.7 GHz is caused by the lower L slot. The lengths of right upper L slot and the lower L slot are 11 mm and 9 mm and approximately equal to 0.25λ at 7.1 GHz and 0.3λ at 10.7 GHz, respectively. Both coupled asymmetry L slots has provided the UWB characteristic which cover 3.1 to 11.7 GHz.

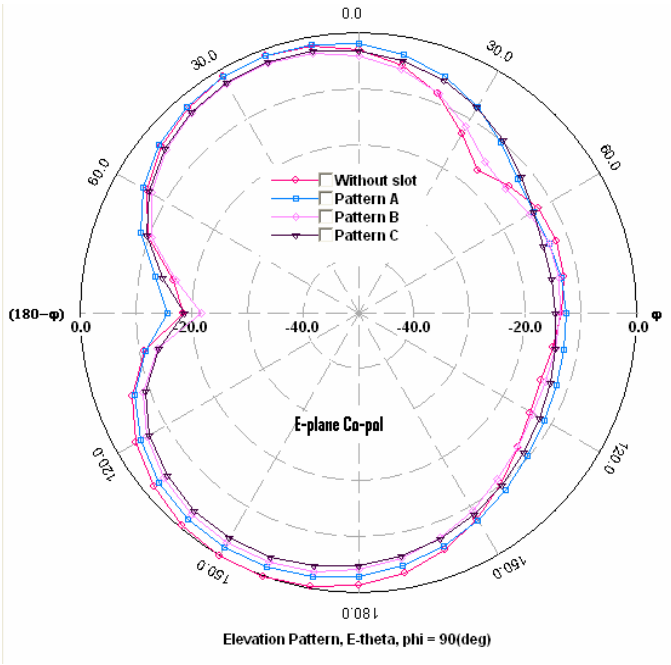

(a)

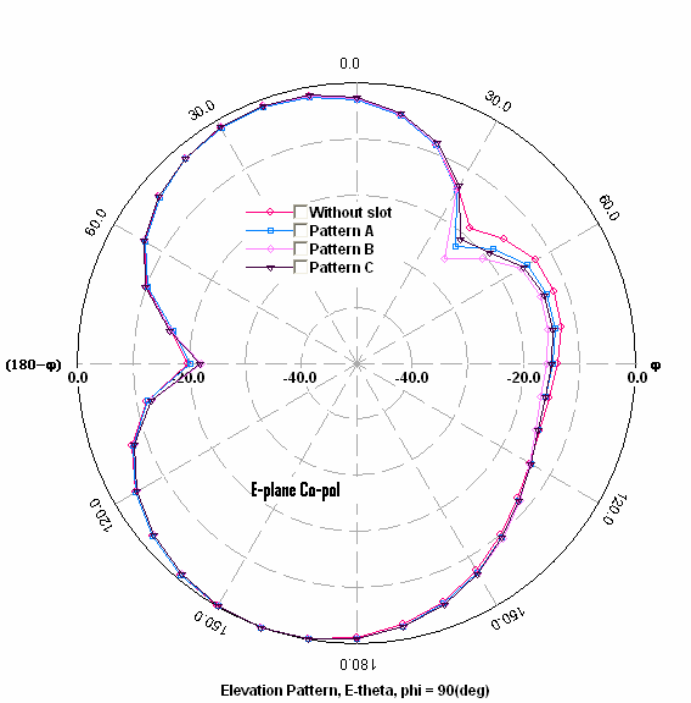

(b)

Figure 4.19: The simulated radiation pattern of various slot designs: (a) rectangular with two notches and (b) pentagonal

Figure 4.19 is the simulated E-theta radiation patterns for both slotted UWB antennas at 5.25 GHz. These radiation patterns are computed using FDTD Zeland software. From the simulation results, both slotted UWB antennas have shown omni directional patterns with remove the null radiation pattern. From the results, The T slotted antenna has shown very good omni directional pattern by removing the null pattern at 45^{o} besides provides a broad bandwidth.

4.2.4 Feed Gap and Slotted Ground Plane

The feed gap between ground plane to the bottom of patch is known given crucial effect to the impedance bandwidth. The modified truncated ground plane acts as an impedance matching element to control the impedance bandwidth of a rectangular patch. This is because the truncation creates a capacitive load that neutralizes the inductive nature of the patch to produce nearly-pure resistive input impedance [42].

Slotted or notched ground plane is also taken into consideration. The size of notches should be properly designed while still maintaining the antenna's performance. The efficient technique to determine the size of notches in the ground plane is by calculating the optimum feed gap between the ground plane and the bottom patch required without adding the notches. Then, the size of notches can be adjusted with respect to the optimum distance.

To investigate the effect of feed gap and slotted ground plane to the antenna performance, two antenna models are chosen, pentagonal with L and U slots and rectangular with T slot. Both antenna models are selected based on the best antenna performance given.

Figure 4.20 illustrates the simulated return loss curves for different feed gaps to the ground plane of T slotted antenna, their corresponding input impedance curves are plotted in Figure 4.21. It is shown in Figure 4.20 and Table 4.8 that the -10 dB operating bandwidth of the antenna varies with the variation of the feed gap (h) and

the dimension of the ground plane. The optimal feed gap is found to be 1 mm with the fractional bandwidth of 116%.

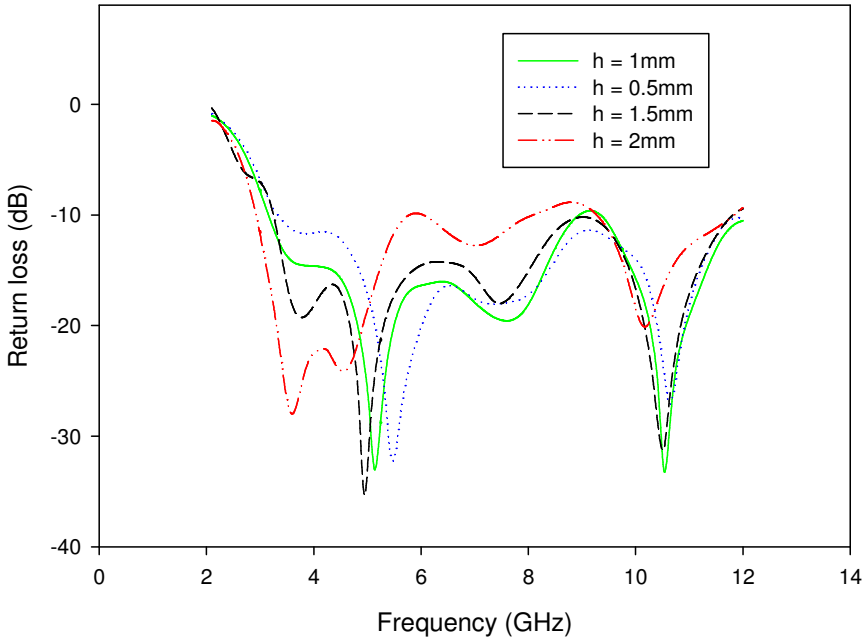

Figure 4.20: Simulated return loss curves of T slotted antenna for different feed gaps

Table 4.8: Simulated -10dB bandwidths of the T slotted antenna for different feed gaps of the ground plane

h (mm)	**f_L (GHz)**	**f_U (GHz)**	**Absolute BW (GHz)**	**Fractional BW (%)**
0.5	3.27	12	8.73	114
1.0	3.17	12	8.83	116
1.5	3.27	11.8	8.53	113
2.0	2.98	8.17	5.19	93

It can be seen in Table 4.8 that the -10 dB bandwidth of T slotted antenna does not change much with the variation of the feed gap of the ground plane below 1.5 mm. But beyond this ranges, it will degrade the impedance bandwidth performance. These simulated results indicate that the antenna bandwidth is dependent on the feed gap of the ground plane, since the ground plane serves as an impedance matching circuit.

As shown in Figure 4.21(a), the return loss < -10 dB always occurs over the frequency range when the input impedance is matched to 50 ohm. The real part (Re) is close to 50 Ω while the imaginary part (Im), as shown in Figure 4.21(b), is not far from zero for the four different feed gaps. When h is 1mm and 1.5 mm, Re varies tardily at the level of 50 Ω whilst Im remains small across wide frequency range, leading to a UWB characteristic. However, when h rises to 2 mm, Re varies more widely and Im also fluctuates significantly across the frequency range, thus resulting in impedance mismatch at the antenna and hence the decrease of the operating bandwidth. The peak value of resistance is as high as 100 ohms, while the maximum reactance is around 35 ohms.

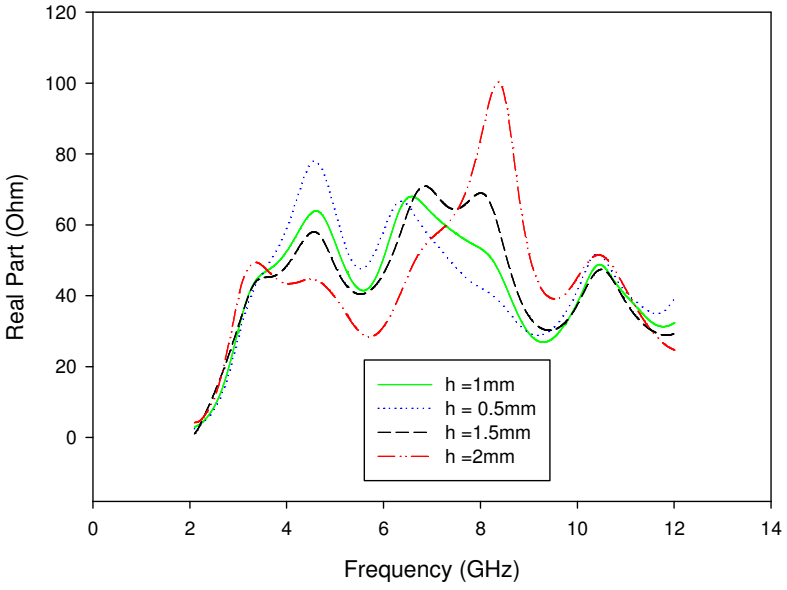

(a)

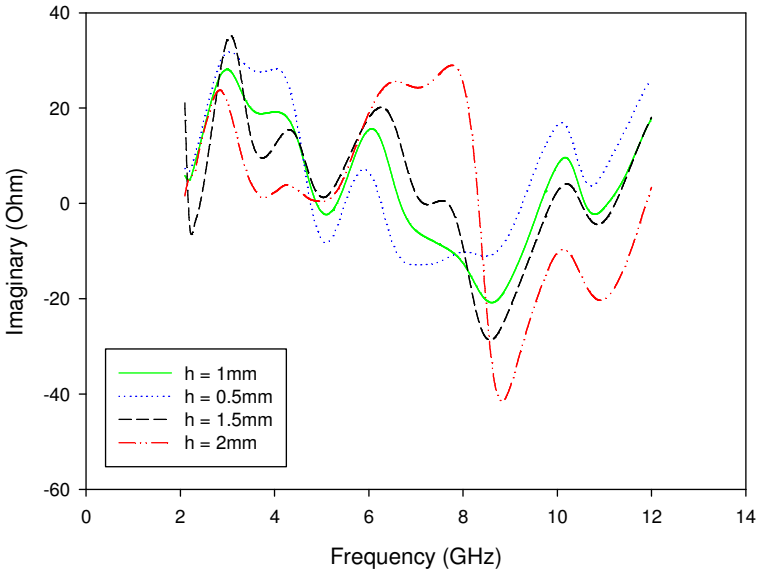

(b)

Figure 4.21: Simulated input impedance curves of T slotted antenna for different feed gaps: (a) real part and (b) imaginary part

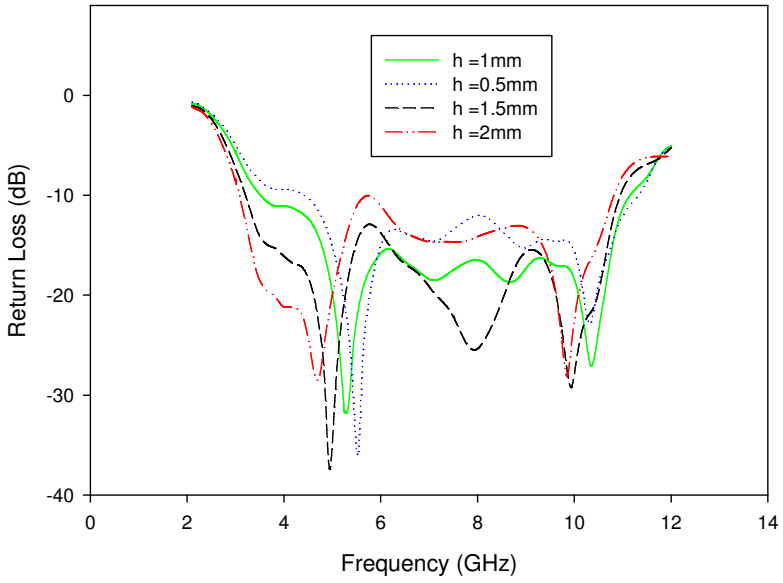

Figure 4.22: Simulated return loss curves of L and U slotted antenna for different feed gaps

Table 4.9: Simulated -10dB bandwidths of the L and U slotted antenna for different feed gaps of the ground plane

h (mm)	**f_L (GHz)**	**f_U (GHz)**	**Absolute BW (GHz)**	**Fractional BW (%)**
0.5	4.35	11.3	6.95	89
1.0	3.47	11.2	7.73	105
1.5	3.27	10.9	7.63	107
2.0	3.07	10.8	7.73	111

Figure 4.22 presents the simulated return loss of the L and U slotted antenna for different feed gap. From the Table 4.9 shows that by increasing the feed gap from 0.5 mm to 2 mm to the ground plane, shifted the return loss curve to the left side and caused decreasing the lower resonance frequency but increasing the fractional

bandwidth. The optimum feed gap is found to be 1.5 mm with fractional bandwidth of 107 %. Even though the lower resonance is shifted to 3.27 GHz. The maximum fractional bandwidth is achieved for feed gap of 2 mm to the ground plane, but the return loss at mid range frequency is not as good as others curves.

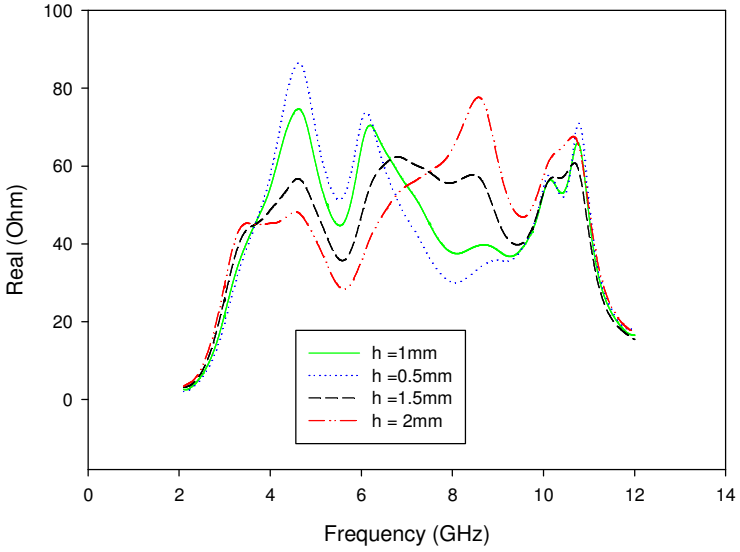

(a)

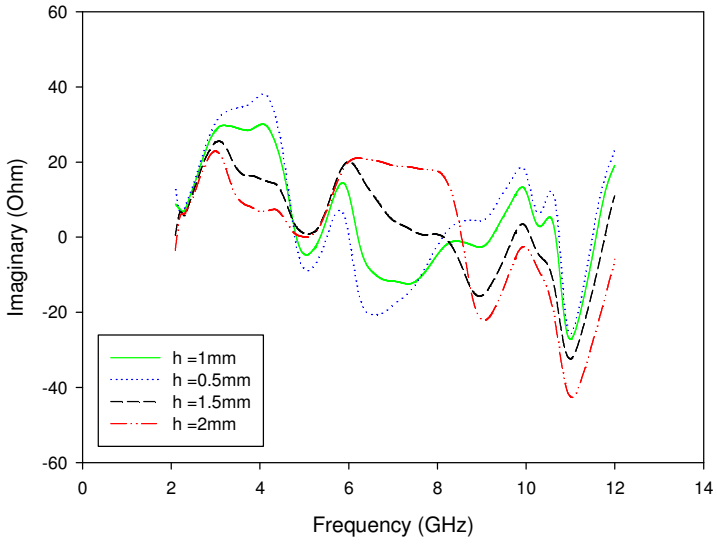

(b)

Figure 4.23: Simulated input impedance curves of L and U slotted antenna for different feed gaps: (a) real part and (b) imaginary part

Figure 4.23 is simulated input impedance of L and U slotted antenna for different feed gap. It is shown that the real part varies closed to 50 ohm for 1.5 mm of feed gap and the imaginary part fluctuates closed to 0 ohm. The peak value of resistance is as high as 85 ohms, while the maximum reactance is around 38 ohms.

As mentioned previously, the ground plane acts as impedance matching of the antenna. Modify the partial ground plane to staircase slotted ground plane has improved the return loss of antenna, especially at higher frequency. The geometry of staircase slotted ground plane is shown in Figure 4.24.

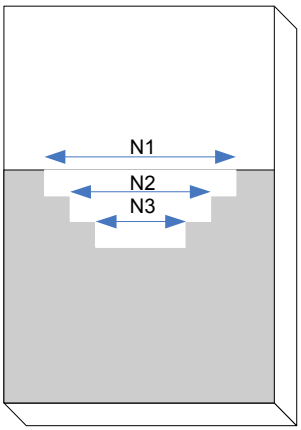

Figure 4.24: Geometry of staircase slotted ground plane

Figure 4.24 shows the geometry of staircase slotted ground plane. By varying the lengths and the widths of slots of ground plane, it is possible to tune the impedance matching as shown in Figure 4.25. The simulated return loss as shown in Figure 4.25 presents the results of various length of slotted ground plane for both slotted antenna. The width of this slotted ground plane is set to 0.5 mm. The optimum feed gap for T slotted antenna is found to be 0.5 mm above the slotted ground plane. The optimum feed gap for L and U slotted antenna is 1 mm above ground plane. The gap of patch radiator to ground plane is critically effect to the input impedance of antenna. From the simulation, the lengths of slots of N_1, N_2, N_3 of 10, 7, 3 mm give the best return loss for both slotted antennas. It is shown that by

increasing the length of slotted ground plane caused degrading the impedance bandwidth of antenna performance.

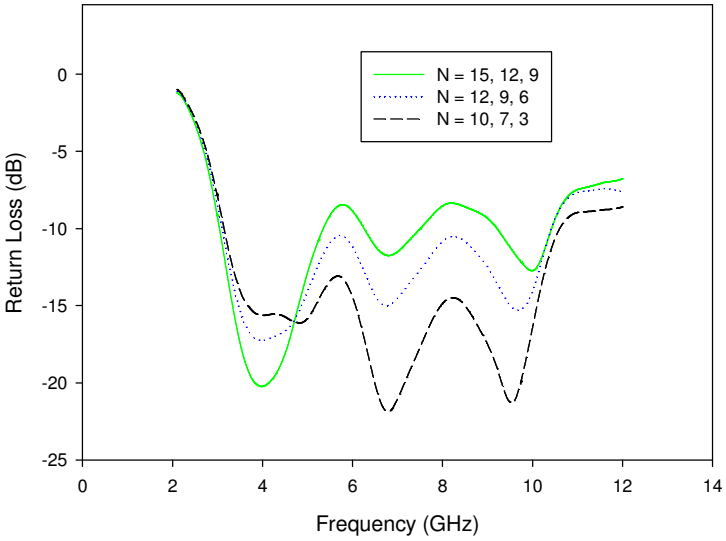

(a)

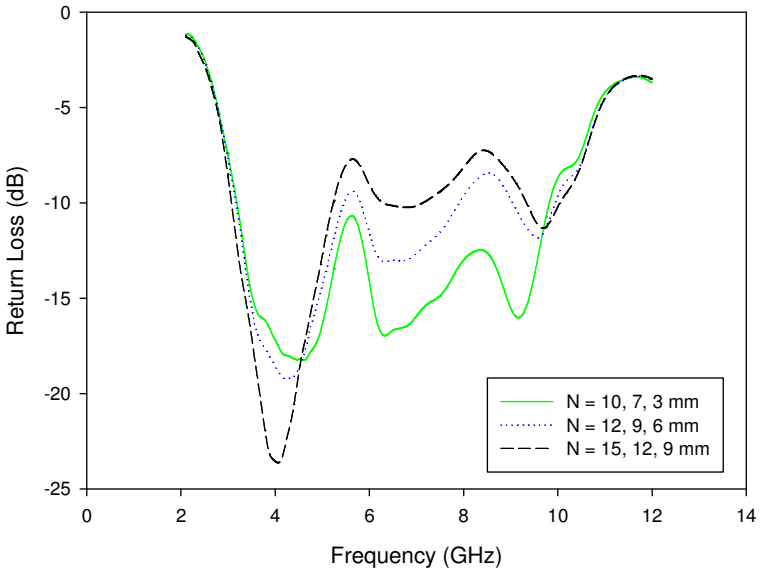

(b)

Figure 4.25: The effect of various length slotted ground plane to the antenna performance: (a) T slotted antenna and (b) L and U slotted antenna

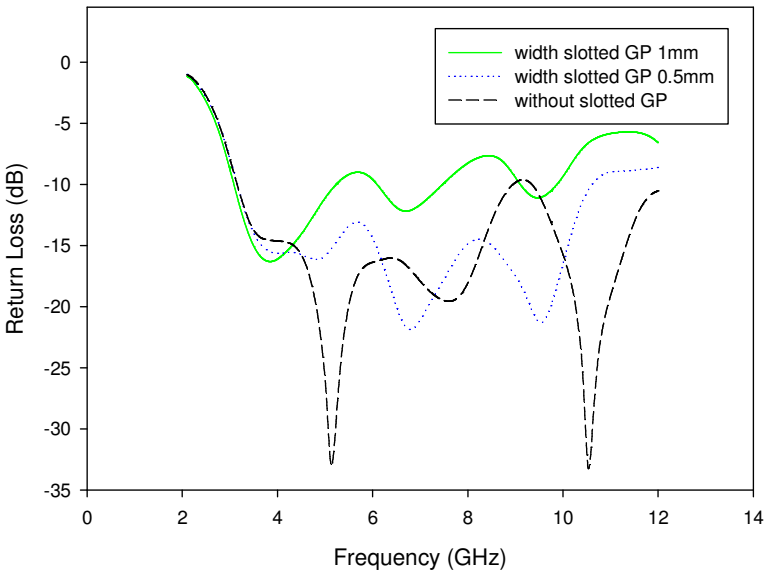

(a)

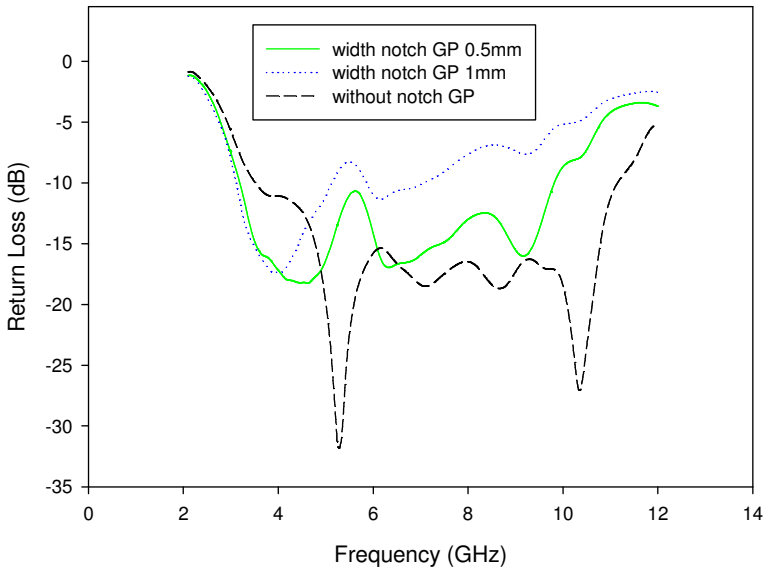

(b)

Figure 4.26: The effect of various width slotted ground plane to the antenna performance: (a) T slotted antenna and (b) L and U slotted antenna

Figure 4.26 presents the effect of various width slotted ground plane to the antenna performance. The width slotted ground plane of 1 mm has degraded the antenna return loss above -10 dB. This is due to the width slot has brought the antenna to much more capacitive and far away from the resonance point. The staircase slotted ground plane has improved the return loss around at 9 GHz for T slotted antenna with the width slot of 0.5 mm, but this degrade the return loss for L and U slotted antenna at above 4 GHz. It is also shown that the staircase slotted ground plane has removed the lower and upper dip resonances for both slotted antenna. The return loss curves fluctuate around -15 dB. The T slotted with slotted ground plane antenna cover frequency range of 3.17 GHz to 10.6 GHz with fractional bandwidth of 108%. The L and U slotted with slotted ground plane antenna cover 3.17 GHz to 9.8 GHz with fractional bandwidth of 102%.

The simulated return loss curves for various number of slotted ground plane for both antennas are depicted in Figure 4.27. It is clearly shown that by increasing the number of slotted ground plane has degraded the antenna performance and led the antenna to much more capacitive especially at higher frequency range.

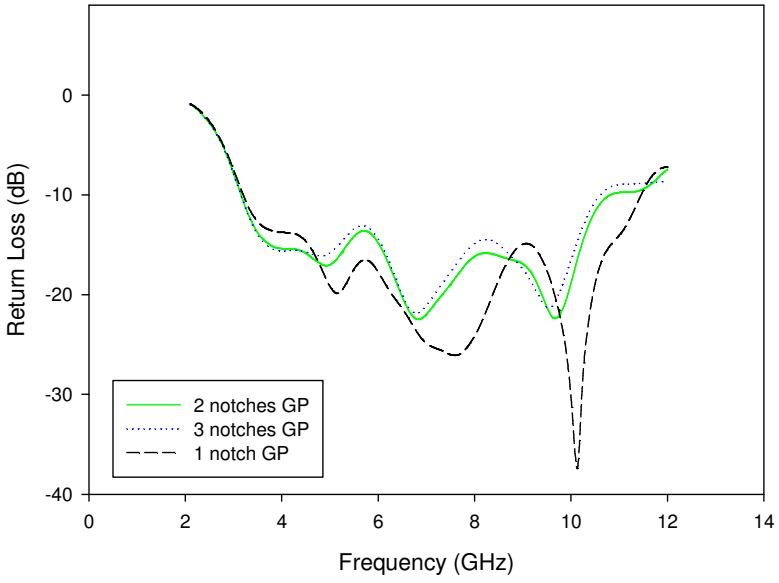

(a)

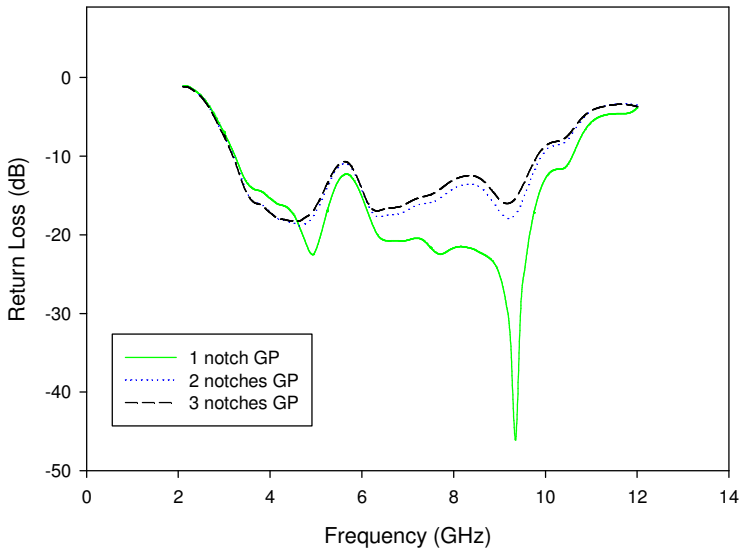

(b)

Figure 4.27: The effect of various number slotted ground plane to the antenna performance: (a) T slotted antenna and (b) L and U slotted antenna

4.2.5 Substrate Permittivity and Thickness

The relative permittivity of the substrate materials is a very important parameter and it must be shown very precisely because of its effect on various quantities such as resonance frequency, characteristic impedance**,** and phase velocity. A number of methods have been reported for measurement of dielectric constant of the planar substrate materials in [152]-[154]. The proposed method in [152]-[154] for determination of dielectric constant is as a function of patch dimension and measured frequency for different low and high permittivity.

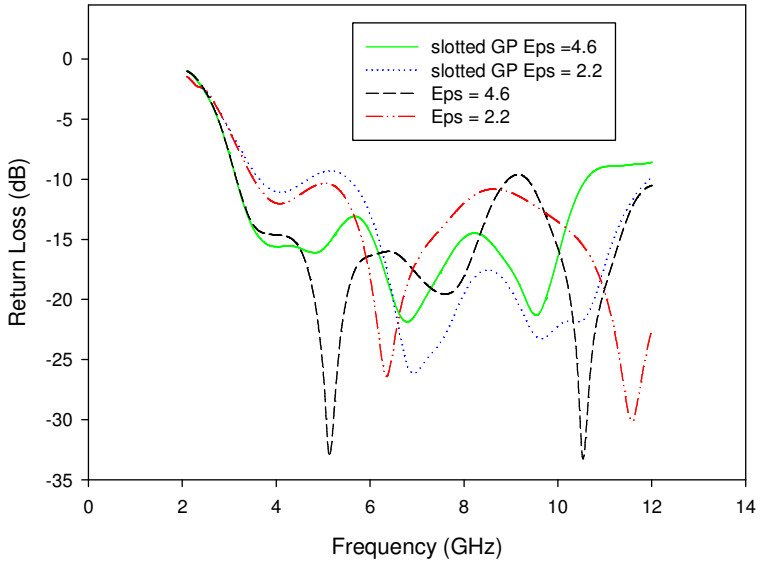

Figure 4.28: Simulated return loss curves of T slotted antenna for different substrate permittivity

Figure 4.28 depicts the return loss of T slotted antennas for ε_r 4.6 and ε_r 2.2, respectively. In this study, the thickness substrate for both dielectrics is 1.6 mm. For both T slotted with slotted ground plane antennas, the lower dielectric has shifted the lower edge frequency to 3.6 GHz and improved the impedance matching at frequency above 5.5 GHz with respect to -10 dB. The return loss of 4.7 GHz to 5.4

GHz has degraded due to this lower dielectric substrate. Meanwhile, the T slotted antenna without slotted ground plane with dielectric substrate of 2.2 has fractional bandwidth of 108% covering 3.56 GHz to 12 GHz. It is concluded that the lower dielectric substrate has improved the upper frequency but shifted the lower edge resonance.

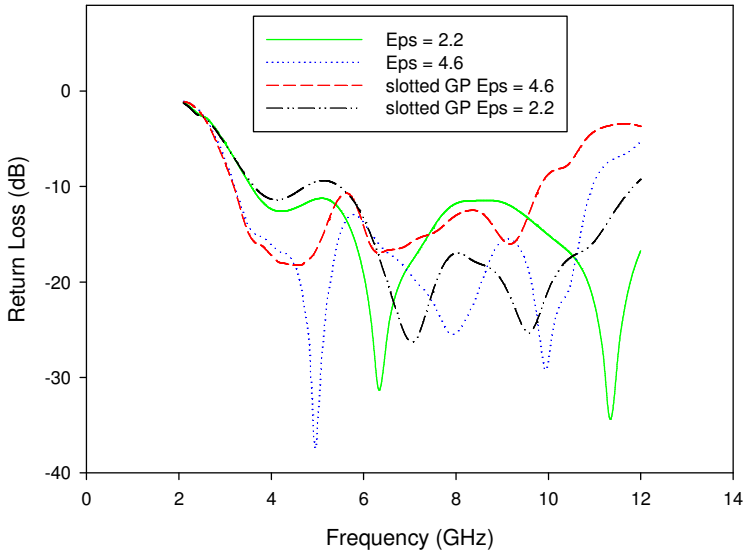

Figure 4.29: Simulated return loss curves of L and U slotted antenna for different substrate permittivity and thickness

The simulated return loss curves for different permittivity of L and U slotted antenna is shown in Figure 4.29. The return loss curve with dielectric permittivity of 2.2 of slotted ground plane above 5.5 GHz shows much lower than the antenna with dielectric permittivity of 4.6. The lower dielectric permittivity also has shifted the lower edge resonance to 3.6 GHz and degraded the performance at 4.7 GHz to 5.4 GHz. This is due to the dielectric constant as a function of patch dimension as shown in Figure 4.30. The L and U slotted antenna without slotted ground plane has presented fractional bandwidth of 108% covering 3.56 GHz to 12 GHz.

Figure 4.30 shows the return loss of T slotted antenna with the length of patch antenna of 14 mm. It is shown that by increasing the length of patch to 14 mm giving a very significant improvement for whole frequencies ranges, especially at the lower edge resonance.

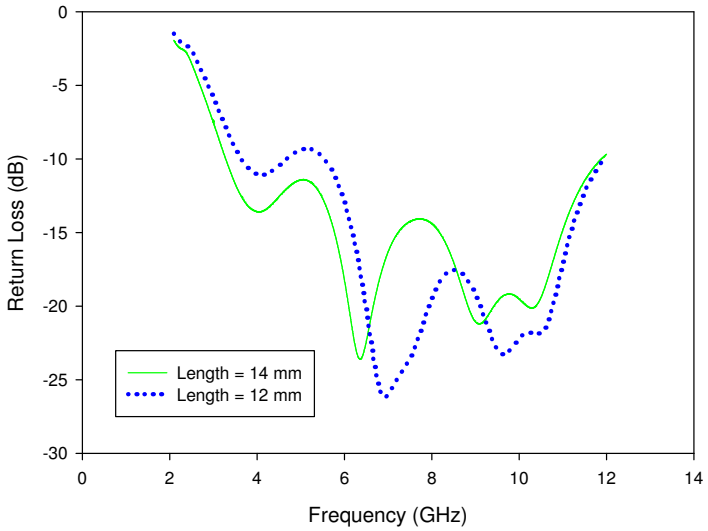

Figure 4.30: The simulated return loss of T slotted antenna with different length of patch radiator

4.3 Reconfigurable Slotted UWB Antenna Design Consideration

In these sections two basics models of new reconfigurable UWB slotted antennas having band notched frequency at FWA, HIPERLAN and WLAN bands are presented. Band-notched operation is achieved by incorporating some small gaps instead of PIN diodes into the slot antenna. The term of small gap in this thesis will refer to the switch for next explanation. The switches are used to short the slot in pre-selected positions along the circumference. It is found that by adjusting the total length of slot antenna to be about a half-wavelength or less at the desired notched frequency, a destructive interference can take a place, thus causing the antenna to be non-responsive at that frequency.

In this thesis, the switches are used to reconfigure slot element of UWB antenna for frequency notch tuning. The length of the slot antenna can be lengthened or shorted by closing or opening the switch allowing for a change in the notched frequency. For the simulation proposed, the PIN diodes as switches are considered to be ideal switch. The switches are modeled as small patches that connect or disconnect the adjacent slot changing the antenna's slot length. For implementation, the gaps are created in the UWB antenna pattern, which are represented as switches. The selections of PIN diodes as switch are based on its low cost, higher speed and it has better insertion losses at higher frequency than FET switches.

4.3.1 Reconfigurable Modified T Slotted Antenna

In this section, the modified T slotted antenna from the previous model is used with some switches incorporated into the slot antenna. In order to modify the previous model to become a reconfigurable notched frequency, the length of inverted U upper slot is varied and keeps other parameters to be constant. The switches are modeled as a very small patch with dimension of 0.7 x 1 mm. Thus, this proposed antenna has double functions as an UWB antenna as well as a frequency notched antenna without major modification applied.

Figure 4.31 shows the proposed antenna model. The dimension and type of substrate used is same with the previous model as well as the antenna dimension, except the dimension for inverted U upper slot. The inverted U slot consists of one horizontal slot and two verticals slots. To accommodate the proposed notched frequencies, the length of inverted U upper slot is lengthened than the previous model. The maximum length of horizontal slot of inverted U upper slot is 11 mm (TL1), with varying the length of vertical slot based on the proposed notched frequency. It is investigated that the notched frequency response given only by the inverted U upper slot rather than other slots. Thus, this simulation is focused on how the vertical slot affects to the notched frequencies.

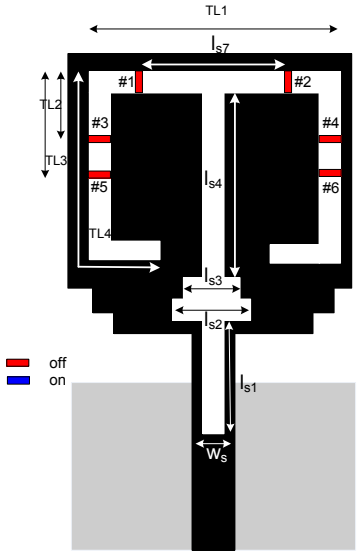

Figure 4.31: The reconfigurable modified T slotted antenna

Figure 4.31 shows the reconfigurable modified T slotted antenna with 6 switches attached into the slot. The antenna examined has vertical arms length of 29 mm, 17 mm and 16 mm which correspond to frequency notched of 3.5 GHz, 5.25 GHz and 5.8 GHz. The ideal switches model in this figure use removable metal patches to simulate the PIN diodes switches. To place a switch in the off state, the patch is deleted from the geometry, leaving a gap of 0.7 mm along the length of the vertical arms.

When the antenna is operating in the UWB band without frequency notch function, the switch #1 and #2 are in the off state and the rest of switches are in the on state as shown in Figure 4.32(b). The simulation also shows that to obtain the notched frequency at 3.4 to 3.7 GHz, the total length of inverted U upper slot should be equal to 29 mm (TL4). This length is approximately equal to $\frac{\lambda}{3}$ at 3.5 GHz, which is the center frequency of FWA frequency band. For this notched frequency, all switches are in the on state position as shown in Figure 4.32(a).

In order to reject the HIPERLAN band, the total length of inverted U slot is designed to be equal to 17 mm or approximately equal to $\frac{\lambda}{3}$ at 5.25 GHz (TL3). Most of switches are in the on state (#1, #2, #3, #4) and two of them are in the off state (#5, #6). This configuration is illustrated in Figure 4.32(c).

For notched frequency at WLAN band, the total length of inverted U upper slot is equal to 16 mm or approximately equal to $\frac{\lambda}{3}$ at 5.8 GHz. Only switches of #3 and #4 are in the off state, others are in the on state. The configurations of switches into slot antenna for WLAN notched band mentioned are illustrated in Figure 4.32(d). The numbers of switches used are set as minimal as possible in order to avoid the complexity.

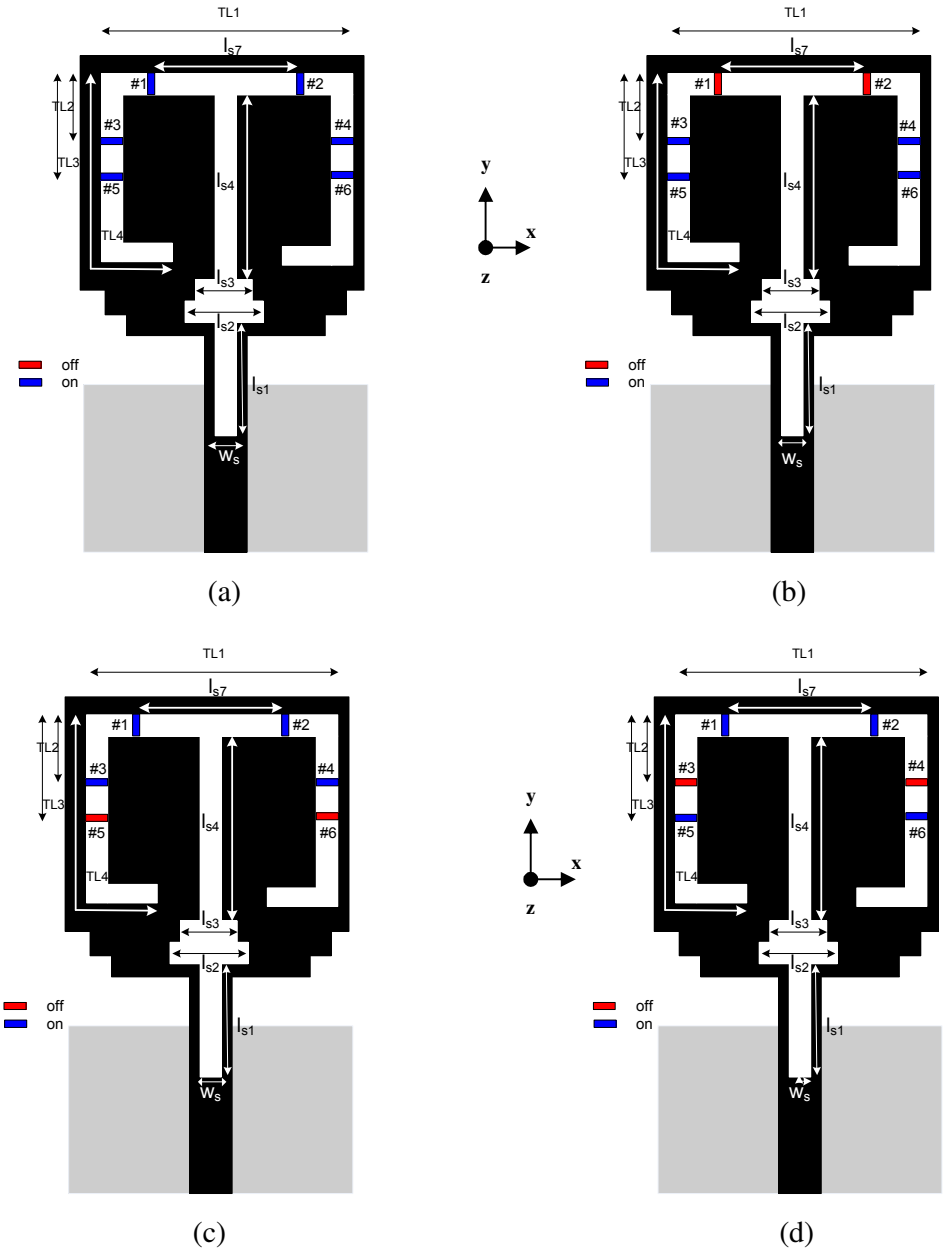

Figure 4.32: Switching configuration for T slotted antenna: (a) notched at FWA, (b) UWB bandwidth (w/o notched), (c) notched at HIPERLAN, and (d) notched at WLAN

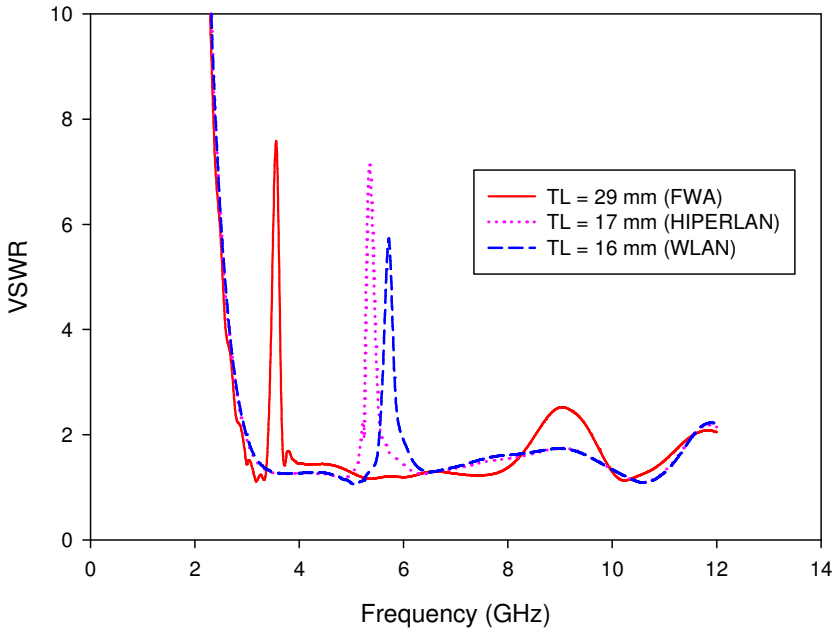

Figure 4.33: The simulated VSWR for reconfigurable modified T slotted antenna

The simulated VSWR for the proposed frequency notched antennas are illustrated in Figure 4.33. It is shown that by varying the length of vertical slot of inverted U upper slot, the desired frequency notched is achieved. Notice that the VSWR is less than 2 over the most frequency band in the case of without frequency notch function. After extending the total length of 29 mm for inverted U upper slot, a frequency notched at 3.47 – 3.66 GHz has resulted with VSWR changed to more than 6, but it has degraded the frequency band of 8.5 – 9.5 GHz. At that frequency notched band, the slot can be considered as a secondary antenna. The degradation result is maximum VSWR of 2.5, this result is considered acceptable.

The total lengths of inverted U upper slot of 17 mm and 16 mm have resulted frequency notched bands at HIPERLAN and WLAN, respectively. The frequency notched bands of 5.23 GHz – 5.53 GHz is obtained for HIPERLAN and 5.62 GHz – 5.92 GHz for WLAN. At these frequency-notched bands, the VSWR is changed to more than 5 without degrading the VSWR for the most frequency bands which are

less than 2. Thus, this antenna is very compromise to be used for UWB application without having interference to HIPERLAN and WLAN systems. Other feature for this antenna is this antenna non responsive to FWA band which was assigned by MCMC. Therefore, it fulfills the local wireless communications needs. This is considered as one of contribution for this thesis.

4.3.2 Reconfigurable Modified L and U Slotted Antenna

Modified L and U slotted antenna for reconfigurable frequency notched at FWA, HIPERLAN and WLAN are shown in Figure 4.34. There are maximum six switches used to provide the reconfigurable function. The dimension of antenna and substrate are kept same with the previous model. The length of L and U slots are same with the previous length, except two additional slot lengths, I_{s20} and I_{s21}. The additional slots are very critically determined the frequency notched band characteristics.

A switch PIN diode is modeled as a small patch with different color for on and off state condition. In order provide the UWB characteristic, the switches are placed as shown in Figure 4.34 (a). Three switches of #2, #3, and #4 are in the off state position. Other switches of #1, #5, and #6 are in the on state condition. When the switches are in the off state condition, the gap between slots occur and the current flowing to the gap. When the switches are in the on state condition, there is no current flowing to the slots. Thus it forms continuous slots. The switches of #2 and #3 are incorporated to the first additional slot (I_{s20}) which is 3.5 mm of slot length. The switch of #4 is attached to the second additional slot (I_{s21}) which is 2.5 mm of slot length.

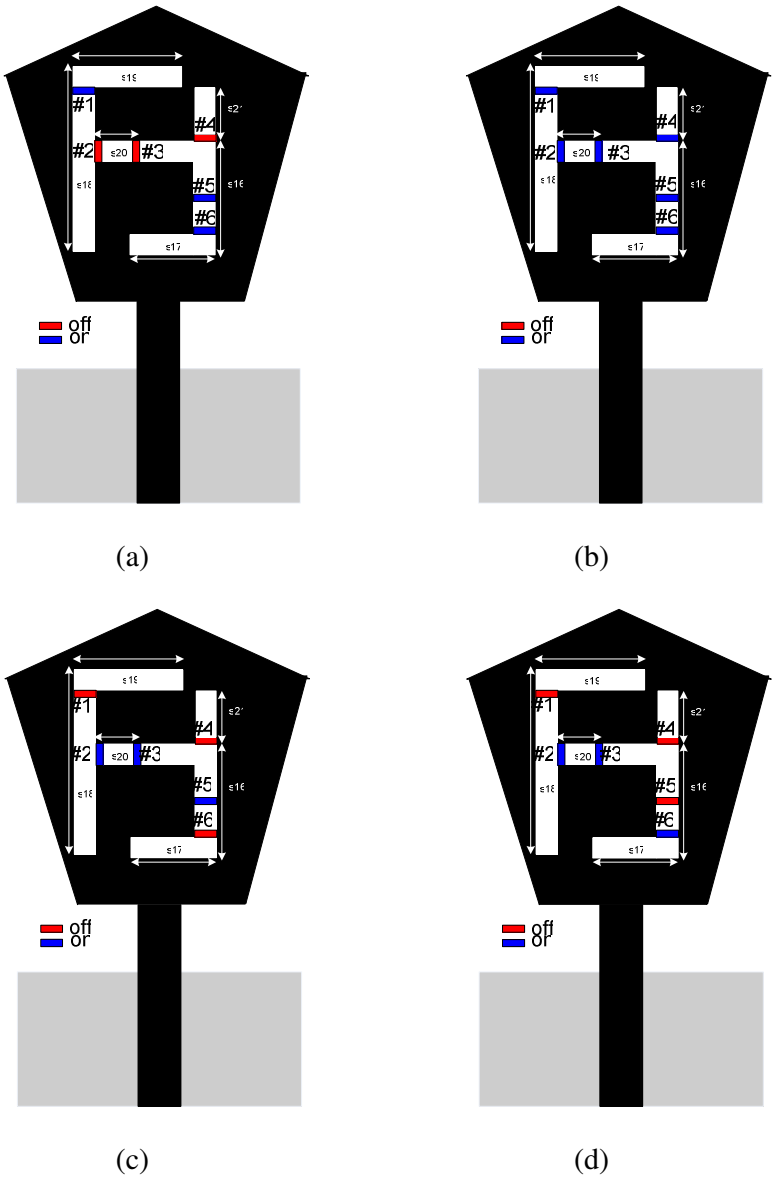

Figure 4.34: Switching configuration for L and U slotted antenna: (a) UWB bandwidth (w/o notched), (b) notched at FWA, (c) notched at HIPERLAN, and (d) notched at WLAN

The frequency notched characteristic antenna at FWA is shown in Figure 4.34 (b). All switches are in the on state or continuous slot. Total slot lengths are 32 mm or approximately equal to 0.4λ at 3.7 GHz. The total slot length means the sum

of slot lengths of L, U and additional slots. Figure 4.34 (c) and Figure 4.34 (d) present the frequency notched characteristic antenna at HIPERLAN and WLAN, respectively. To reject interference from HIPERLAN, the switches of #1, #4, and #6 are in the off state while switches of #2, #3, and #5 are in the on state. It is investigated that by inserting those switches in the off state condition broke the connection between slots. This break connection has reduced the slot length to be 20.75 mm or approximately equal to 0.33λ at 5.2 GHz. Thus, the antenna has frequency notched at HIPERLAN band. The total slot length is measured from the connecting slots.

The configuration of switches in Figure 4.34(d) have resulted an antenna with frequency notched at WLAN. It is shown that the switch of #5 set in the off state in order to reduce the slot length, while the switch of #6 is in the on state. This is the only different while compared to the HIPERLAN configuration. Total slot lengths are 18 mm or approximately equal to 0.33λ at 5.75 GHz measured from the connecting slots.

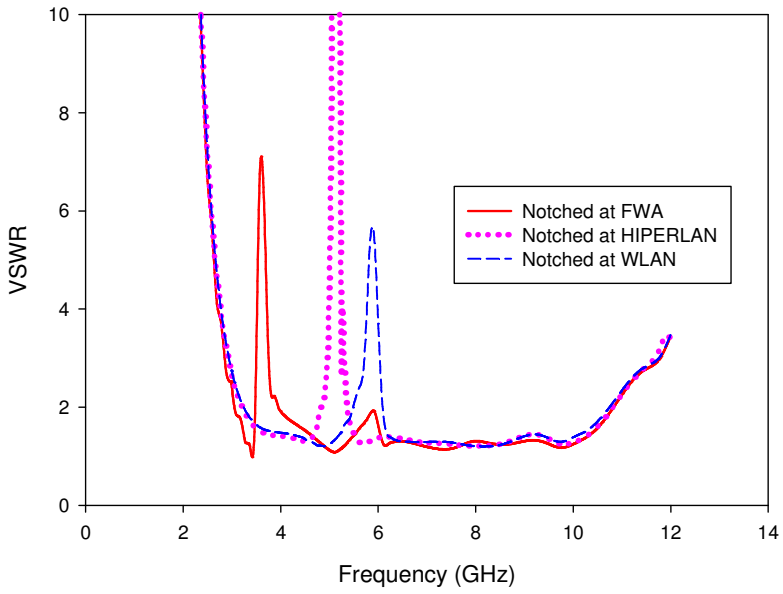

Figure 4.35: The simulated VSWR for reconfigurable modified L and U slotted antenna

Figure 4.35 shows the simulated VSWR for reconfigurable modified L and U slotted antenna. By varying the slot lengths and break the connection between slots using switches, the proposed frequency notched is achieved. The FWA notched bands are obtained from 3.57 GHz – 3.86 GHz with the total slot length of 32 mm at 3.7 GHz, which is the centre frequency. While the HIPERLAN and WLAN notched bands are from 4.84 GHz to 5.33 GHz and 5.53 GHz to 6.02 GHz, respectively. It is noted that beyond the frequency notched bands, the VSWR is kept to be less than 2.

4.4 Summary

In this chapter, various polygonal UWB antennas have been presented with some parameters design taken into consideration. There are two models UWB slotted antennas resulted in this study, such as T slotted antenna with slotted ground plane and L and U slotted antenna. Both antennas show a very broad bandwidth and nearly omni directional pattern. Both antennas show a very good radiation and antenna efficiency within UWB frequency range which exceed 75% except at 12 GHz. This chapter also investigates the reconfigurable characteristic for proposed UWB antennas by inserting the half-wavelength slot to the patch. These proposed types of antennas are variation from the previous models. The reconfigurability behaviors are achieved by shortened or widened the slot. The switching is model as a small patch of 0.7 mm x 1 mm instead of PIN diodes.

CHAPTER 5

FINAL RESULTS AND DISCUSSIONS

5.1 Introduction

After intensive investigation for various polygonal monopole antennas as discussed in Chapter 4, and observing their performance with regard to the UWB antenna requirements, there are two model slotted UWB antennas resulted from this study, the T slotted antenna with slotted ground plane and L and U slotted antenna. Both types of antennas have been developed and tested. This selection is based on the best performance given in terms of resonance frequency, impedance bandwidth, current distribution, slots effect, permittivity and radiation pattern. For reconfigurable slotted UWB antennas, it is shown from the simulation results that by modifying the length slots of slotted UWB antenna, it provides the band notched characteristics without major modification by using one antenna. In this chapter, the simulation results of both proposed antennas will be further discussed and compared to the experimental works.

5.2 Final Design of Slotted UWB Antenna and Experimental Verification

Figure 5.1 shows the geometry and prototypes of slotted UWB antennas. The size of slotted ground plane has described previously. The slot dimensions for both models have been given in Table 4.6 and Table 4.7, respectively. . The optimum feed

gap for T slotted with slotted ground plane and L and U slotted antennas are 0.5 mm and 1.5 mm, respectively.

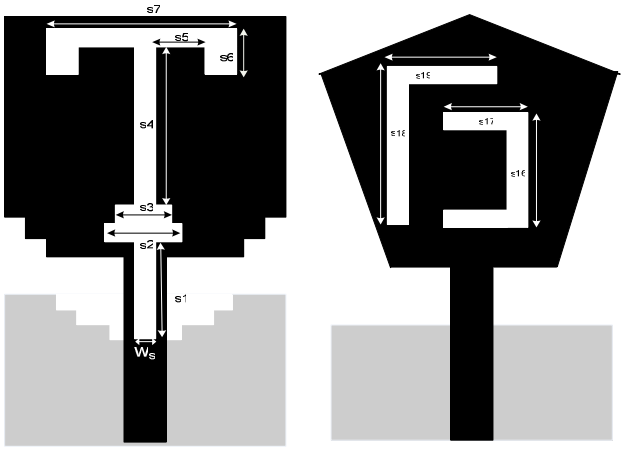

(a)

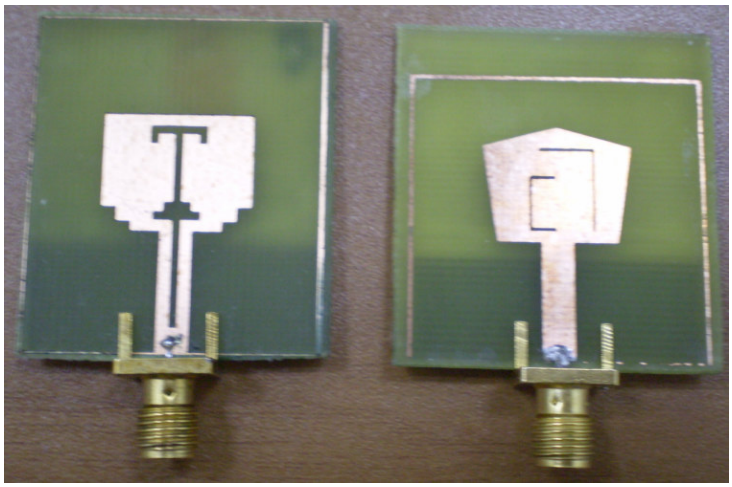

(b)

Figure 5.1: The geometry and prototypes of final design for slotted UWB antennas: (a) geometry, (b) prototypes

As shown in Figure 5.1, both prototypes are printed in the front of substrate FR4 of thickness 1.6 mm and relative permittivity (ε_r) 4.6. The return losses were measured by using Agilent 8722 ES network analyzer. The measured of both prototypes and simulated return loss curves are plotted in Figure 5.2 and Figure 5.3, respectively. The return loss predicted by the FDTD solutions is reasonably close to the measured values.

5.2.1 Simulated and Measured Return Loss

As shown in Figure 5.2, the measured return loss curves for both T slotted antennas with and without slotted ground plane are reasonably close to the simulated results. It is shown that both results have produced multiple resonances frequencies, which shifted from the simulated resonances, but they are still covering the UWB bandwidth requirement. For T slotted antenna with slotted ground plane as shown in Figure 5.2(a), the frequency ranges cover 3 GHz to 10.23 GHz with respect to -10 dB of return loss. While the second antenna without slotted ground plane as shown in Figure 5.2(b), the return loss covers 2.3 GHz to 10.4 GHz. From this measured results, the antenna without slotted ground plane is better than the antenna with slotted ground plane in terms of the impedance bandwidth. This is due to the antenna with slotted ground plane need very accuracy in alignment between the slotted ground plane and patch on both sided of substrate during fabrication. The distance of patch to the ground plane is also very small of 0.5 mm. The misalignment occurred affects the impedance bandwidth. The measurements confirm the UWB characteristic of the proposed slotted UWB antennas, as predicted in the simulations.

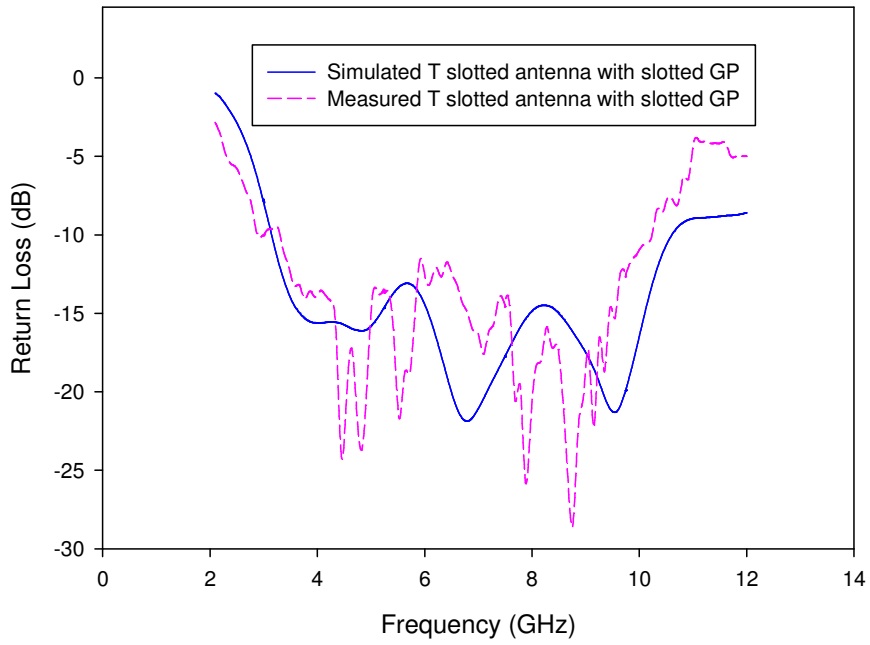

(a)

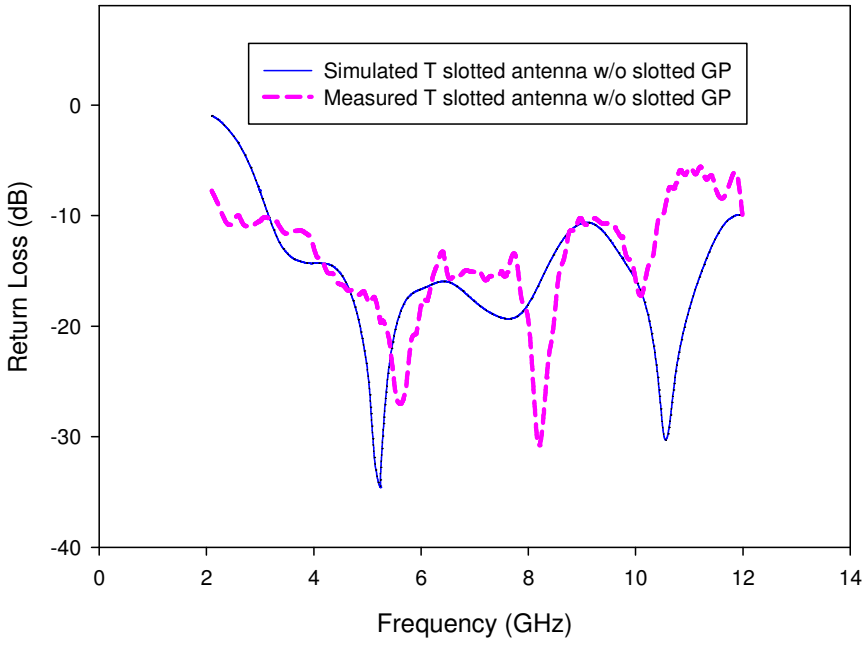

(b)

Figure 5.2: The measured and simulated return loss for T slotted antenna: (a) with slotted ground plane and (b) without slotted ground plane

For L and U slotted antenna, as shown in Figure 5.3, the measured return loss is very close to the simulated result which covers frequency band of 2.5 GHz to 10.1 GHz. In both prototypes, measurements are done by using a 50-Ω SMA connecter which is soldered at the bottom edge of microstrip line and connected to network analyzer by an RF cable. The RF cable significantly affects the performance of antenna under test [35]. However, some differences in the simulated and measured results are expected, since in the simulation model the mismatch due to the adapter and connector used are not taken into consideration. In reality the coaxial cable has a considerable effect, especially the length of its inner conductor, which is connected to the input of the antenna, creating an additional inductance. In addition, since the antenna is fed by a microstrip line, misalignment can result because etching is required on both sides of the dielectric substrate. The alignment error results degradation to the antenna performance.

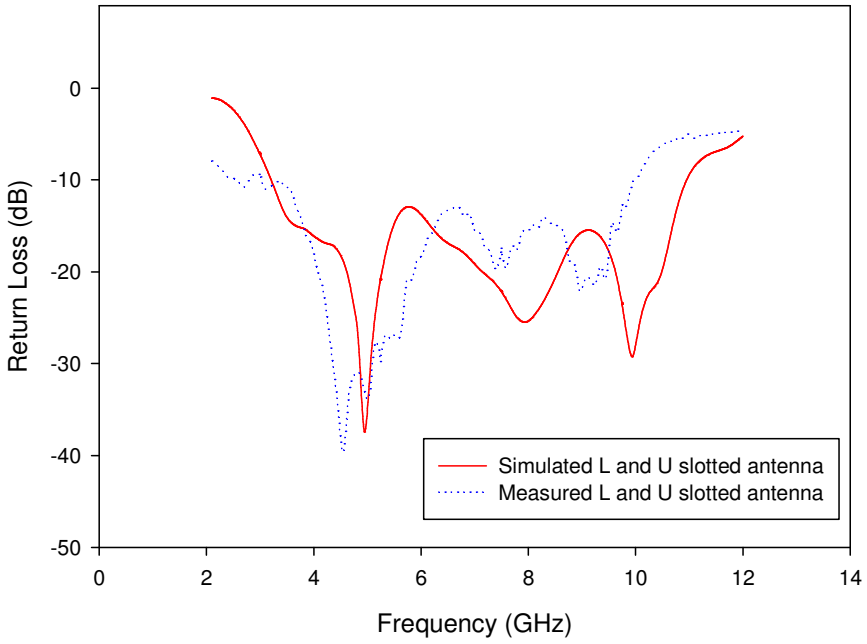

Figure 5.3: The measured and simulated return loss for L and U slotted antenna

From experimental experiences, the multiple resonances of return loss occurred on the proposed antennas are due to these antennas printed in the front of FR4 substrate. It has been investigated during the return loss measurement of many wideband antennas that have been developed. In addition, the FR4 substrate quality needs to be taken into consideration. It should be used within six months after purchased in order to avoid the oxidation process. The poor quality of FR4 substrate used produces a poor measured return loss and need longer time during etching process. Thus, perfect impedance match is not easily obtainable. These fabrication processes are important, because a slight error could result in major degradation in antenna performance.

5.2.2 Simulated and Measured VSWR

The VSWR for both prototypes were computed and measured as well and shown in Figure 5.4. The agreement between measured and calculated results indicates that accurate design studies can be performed by simulation. The VSWR curves are referenced to a 50-Ω input impedance in both simulation and measurement. The VSWRs are well below 2:1 achieved by tapering the bottom of the patch and properly designed on the gap to the ground plane.

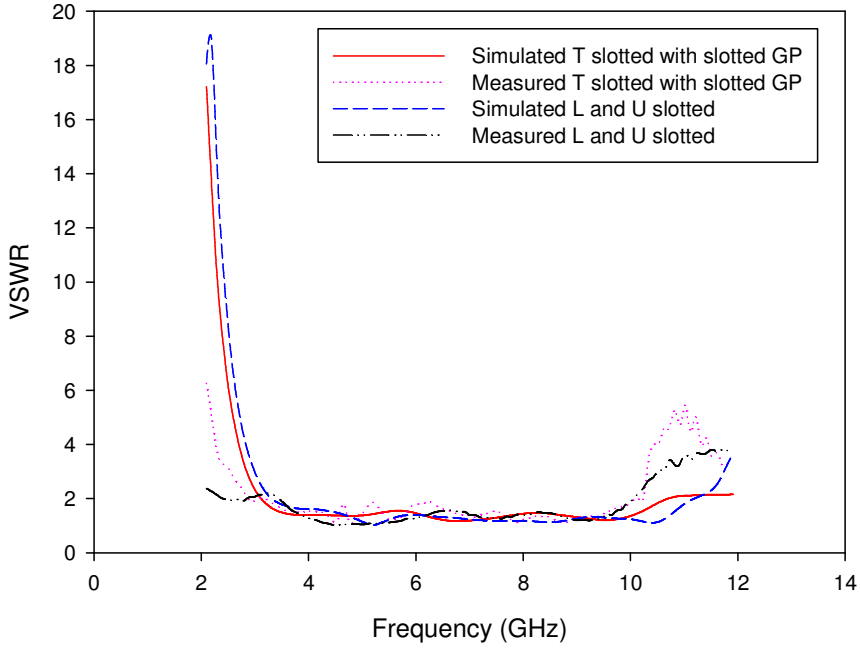

Figure 5.4: The measured and simulated VSWR for both antennas

5.2.3 Simulated and Measured Gain

The simulated maximum gain and maximum directivity of T slotted antenna is shown in Figure 5.5. The gain varies from 1.7 to 5.6 dBi and the directivity varies from 2.6 to 7.3 dBi. The simulated maximum gain and directivity related to the angle is listed in Table 5.1. The lower gain is obtained due to the antennas exhibit omnidirectional radiation pattern. In this thesis, the gain measurements for both proposed antennas are not performed with a standard gain of horn antenna. Variation of gain and directivity for antenna can also be observed from the variation of antenna radiation pattern [154]. Therefore, since these antennas have the omnidirectional behavior, the azimuth plane (H-plane) pattern plots are considered.

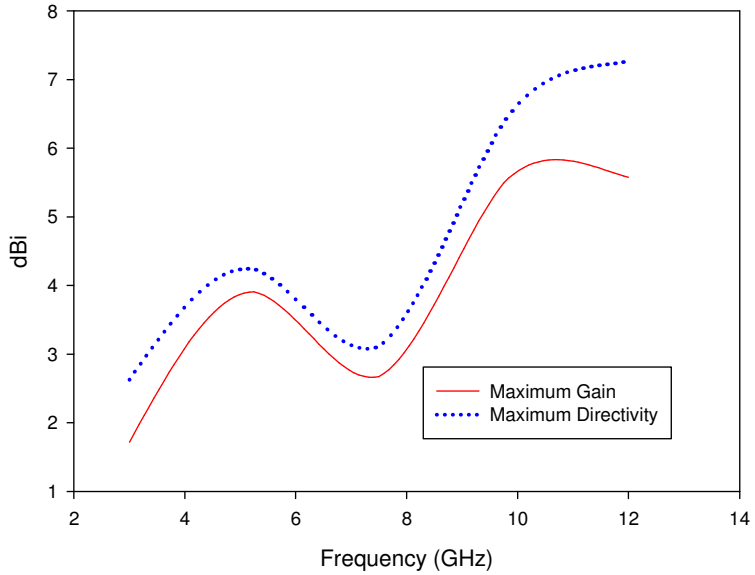

Figure 5.5: The simulated maximum gain and directivity of T slotted antenna with slotted ground plane

Table 5.1: The simulated maximum gain and directivity of T slotted antenna with slotted ground plane

Freq. (GHz)	**Max. Gain (dBi)**	**Max. Directivity**		**3dB beam width (deg)**
		dBi	**(θ, φ) deg**	
3	1.7	2.6	(170, 330)	(85.5, 180)
5.25	3.9	4.2	(160, 260)	(48.9, 192.8)
7.5	2.7	3.1	(80,150)	(68, 244.7)
9.75	5.5	6.4	(80, 120)	(39.5, 85.6)
12	5.6	7.3	(90, 120)	(29.5, 70.4)

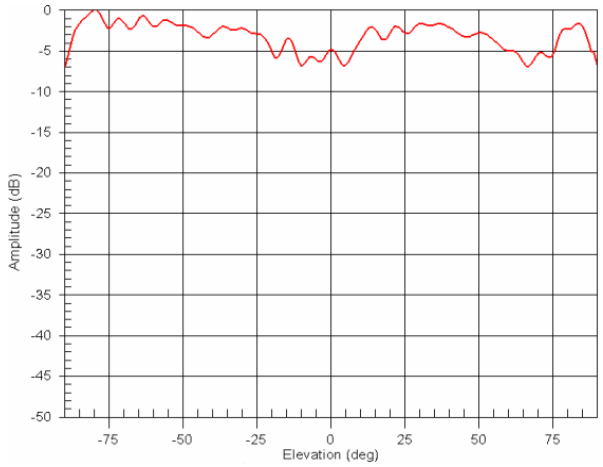

(a)

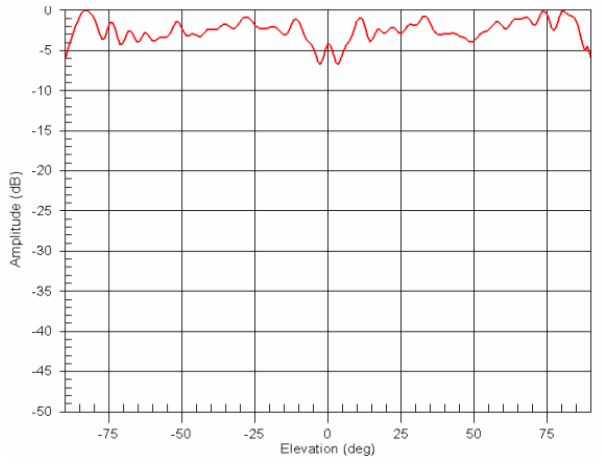

(b)

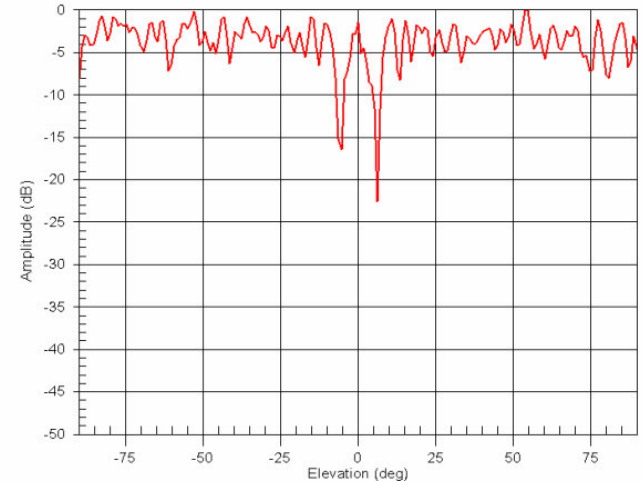

Figure 5.6: The measured relative gain for T slotted antenna with slotted ground plane with respect to the peak plot in the H-plane: (a) 4 GHz, (b) 5.8 GHz, and (c) 10.6 GHz

The measured gain obtained is only relative gain (dB) to the peak measured radiation pattern plot. This gain is normalized to 0 dB. The relative gain of 4 GHz and 5.8 GHz varies around -6 dB for T slotted antenna. The gain varies around -15 dB to -23 dB at elevation ± 5 degrees of 10.6 GHz. The measured relative gain for T slotted antenna is shown in Figure 5.6. For L and U slotted antenna, the gain varies around -7 dB at both frequencies of 4 GHz and 5.8 GHz. Then it decreases to be -20 dB at elevation ± 5 degrees of 10.6 GHz. Figure 5.7 shows the measured relative gain for L and U slotted antenna.

It is observed from the results, at lower frequencies, the radiation patterns are nearly omni directional with small variation; however, as frequency increases the radiation pattern starts degrading. This is caused by the presence of the coaxial cable that feeds the antenna and disturbs the symmetry of the measurement setup [154]. Since the cable is electrically large at higher frequencies, a more pronounce asymmetry on the radiation patterns are observed at higher frequencies.

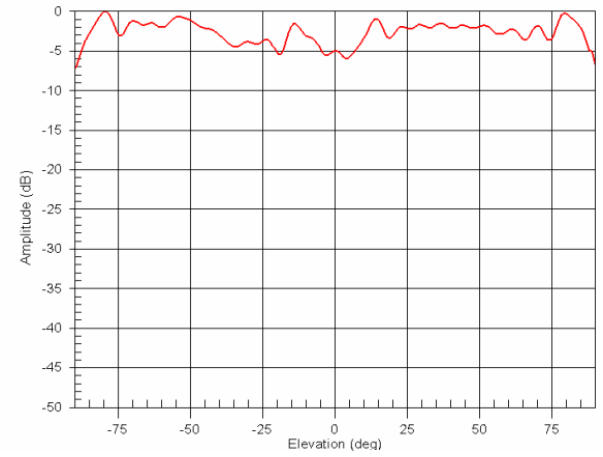

(a)

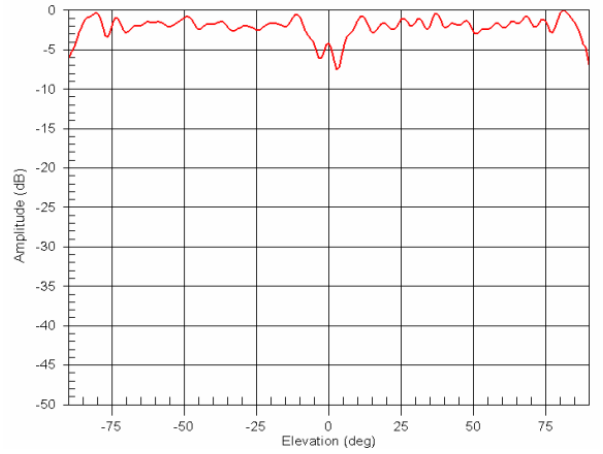

(b)

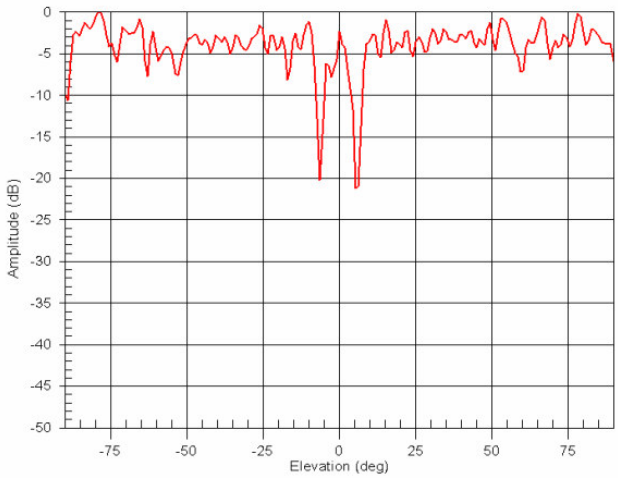

(c)

Figure 5.7: The measured relative gain for L and U slotted antenna with respect to the peak plot in the H-plane: (a) 4 GHz, (b) 5.8 GHz, and (c) 10.6 GHz

The simulated antenna efficiency and radiation efficiency for T slotted antenna with slotted ground plane is also presented in Figure 5.8. The antenna efficiency is defined as the ratio between the radiated power and the incident power. Whereas, the radiated power is defined as the total radiated power into the space by the antenna. Incident power is the power of the incident wave with respect to the normalization impedance Zc [148]. Thus, the radiation efficiency is the ratio between radiated power and input power. The input power is the net power delivered to the antenna or incident power minus reflected power.

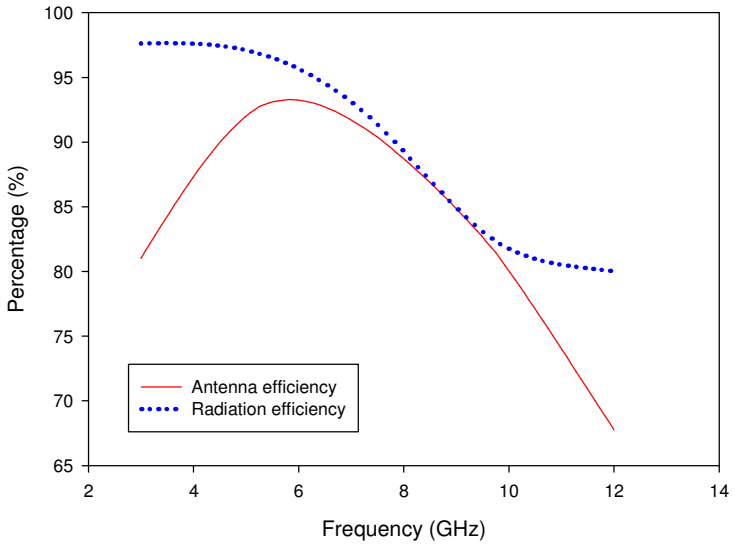

Figure 5.8: The simulated antenna and radiation efficiency of T slotted antenna with slotted ground plane

The antenna efficiency of T slotted antenna reaches a maximum of 92.7% at 5.25 GHz, and start degrading at frequency above 6 GHz, but it is still above 67%. The radiation efficiency varies from 80% to 97% and decreasing with increasing the frequency. Both results show a well match between radiated power and input power. The antenna radiation properties are listed in Table 5.2.

Table 5.2: The simulated radiation properties of T slotted antenna with slotted ground plane

Freq. (GHz)	Incident power (W)	Input power (W)	Radiated power (W)	Radiation eff. (%)	Antenna eff. (%)
3	0.01	0.00829955	0.00810181	97.6174	81.0181
5.25	0.01	0.00957716	0.00927255	96.8194	92.7255
7.5	0.01	0.00989331	0.00903805	91.3552	90.3805
9.75	0.01	0.0098948	0.00814509	82.3169	81.4509
12	0.01	0.00846983	0.0067767	80.0098	67.767

For L and U slotted antenna, the simulated antenna gain is shown in Figure 5.9. From the result, the maximum directivity varies from 2.6 dBi to 6.8 dBi over frequency range with maximum gain of 1.5 to 5.9 dBi. Table 5.3 shows maximum directivity and gain of L and U slotted antenna. The simulated antenna efficiency and radiation efficiency is shown in Figure 5.10. The radiation efficiency varies from 79.5% at 12 GHz to 97.9% at 5.25 GHz. The antenna efficiency at most frequencies are above 75% except at 12 GHz of 57.2%.

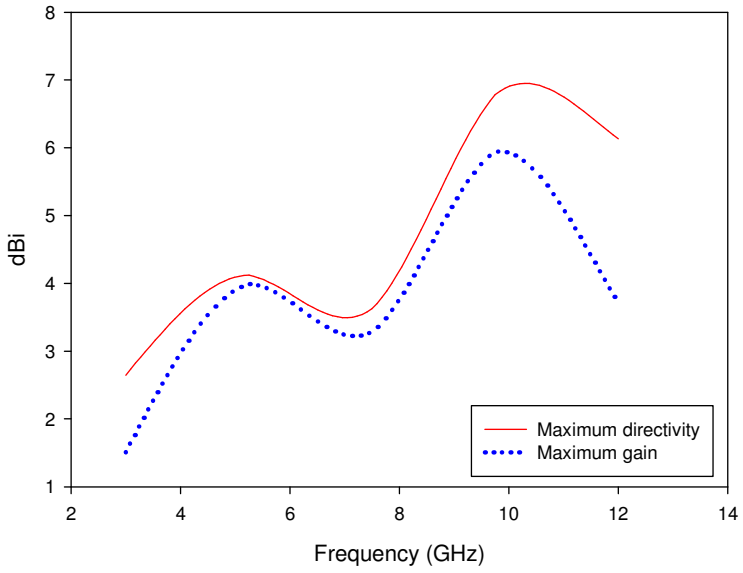

Figure 5.9: The simulated maximum gain and directivity of L and U slotted antenna

Table 5.3: The simulated maximum gain and directivity of L and U slotted antenna

Freq. (GHz)	Max. Gain (dBi)	Max. Directivity		3dB beam width (deg)
		dBi	(θ, φ) deg	
3	1.5	2.6	(170, 330)	(86.3, 180)
5.25	4.0	4.1	(160, 250)	(53.7, 197.8)
7.5	3.3	3.6	(80, 160)	(62, 245)
9.75	5.9	6.8	(80, 120)	(41, 84.2)
12	3.7	6.1	(80, 70)	(32, 66.3)

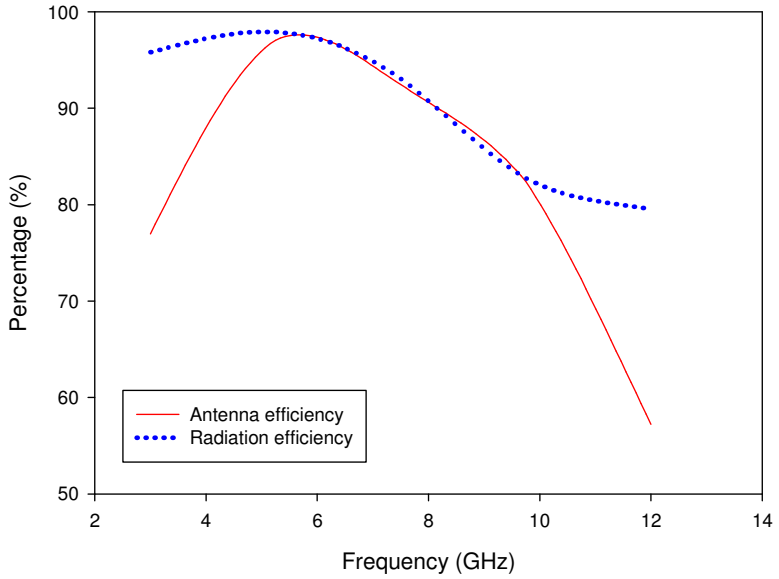

Figure 5.10: The simulated antenna and radiation efficiency of L and U slotted antenna

Table 5.4 shows the simulated radiation properties. The radiation efficiency above 75% is achieved for this type of antenna and meets the UWB antenna requirement. The antenna efficiency decreases at frequency of 12 GHz only.

Table 5.4: The simulated radiation properties of L and U slotted antenna

Freq. (GHz)	Incident power (W)	Input power (W)	Radiated power (W)	Radiation eff. (%)	Antenna eff. (%)
3	0.01	0.00803227	0.00769477	95.7982	76.9477%
5.25	0.01	0.00991543	0.00970641	97.892	97.0641
7.5	0.01	0.00993616	0.00924668	93.0609	92.4668
9.75	0.01	0.00995734	0.00823922	82.7452	82.3922
12	0.01	0.00719585	0.00572247	79.5246	57.2247

5.2.4 Various Slot Design

The effect of various slots design to the antenna performance is discussed in the next section. The observation has been done in terms of the slot length, the current distribution, and the slot width to the impedance bandwidth by simulation.

5.2.4.1 Various T Slot Design

Figure 5.11 shows various modified of T slotted antenna with their current distribution at 3, 5.5 and 9 GHz, respectively. Figure 5.11(a) presents the current distribution of antenna with both T slot on patch and feed, T slot on patch only, and T slot on feed only at 3 GHz. The T slot has resulted much more vertical current through antenna radiator. Most vertical electrical current is distributed near the T slot edges and lead to impedance matching at 3 GHz. The vertical current is most concentrated near the patch edges and slots rather than distributed on the antenna surface at 5.5 GHz and this cause the decrement of the intensity of vertical electrical current on antenna surface. For the antenna's current distribution at 9 GHz, the horizontal current mode occurs on the antenna surface. And it is also shown that some vertical current start flowing down to the base. The simulated return loss for these various T slots antennas is shown in Figure 5.12.

Figure 5.12 shows that the T slots have improved the return loss at mid frequencies range, while slightly shifted the upper edge resonance. The return loss provides a very broad bandwidth below -15 dB.

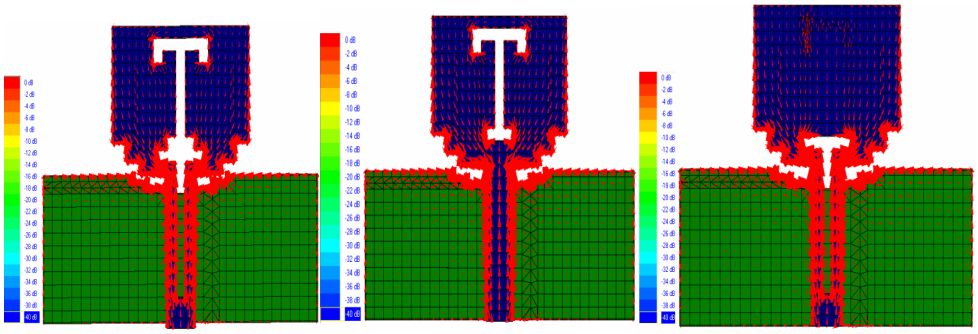

(a)

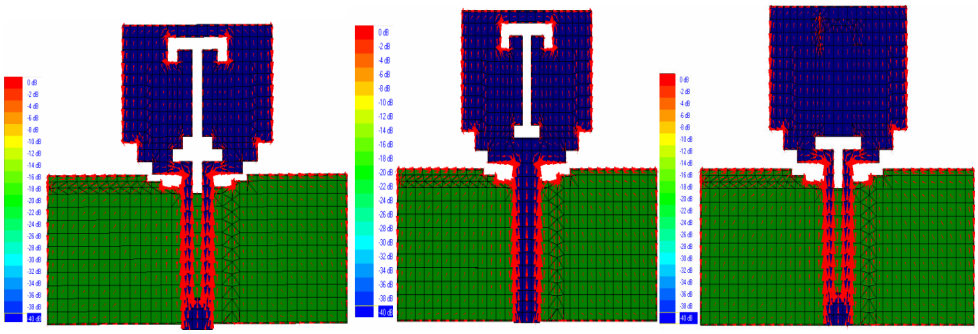

(b)

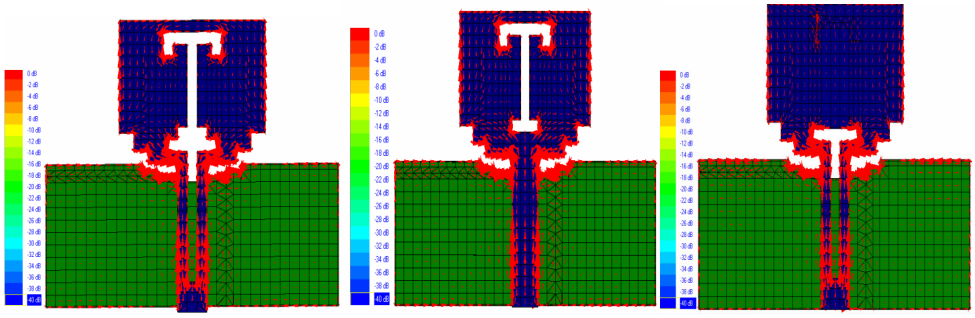

(c)

Figure 5.11: The simulated current distribution for T slotted with slotted ground plane antenna: (a) 3 GHz, (b) 5.5 GHz, and (c) 9 GHz

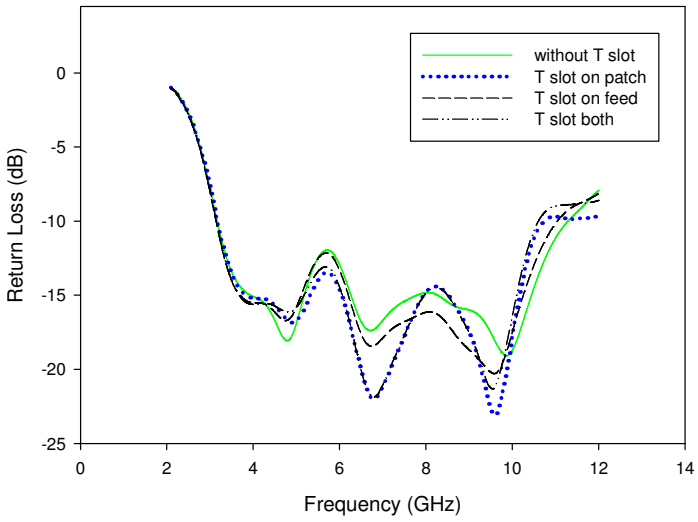

Figure 5.12: The simulated return loss of various T slots design for T slotted with slotted ground plane antenna

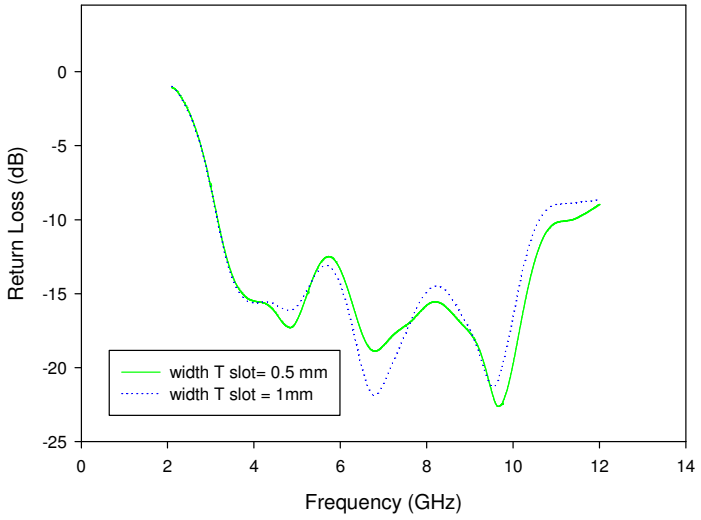

Figure 5.13: The simulated return loss of various width of T slots design

Figure 5.13 shows the return loss of T slots with 0.5 mm and 1 mm width, respectively. From the results, there is not a significant effect to the antenna's return loss performance by decreasing the slot width. The optimum width is found to 1 mm.

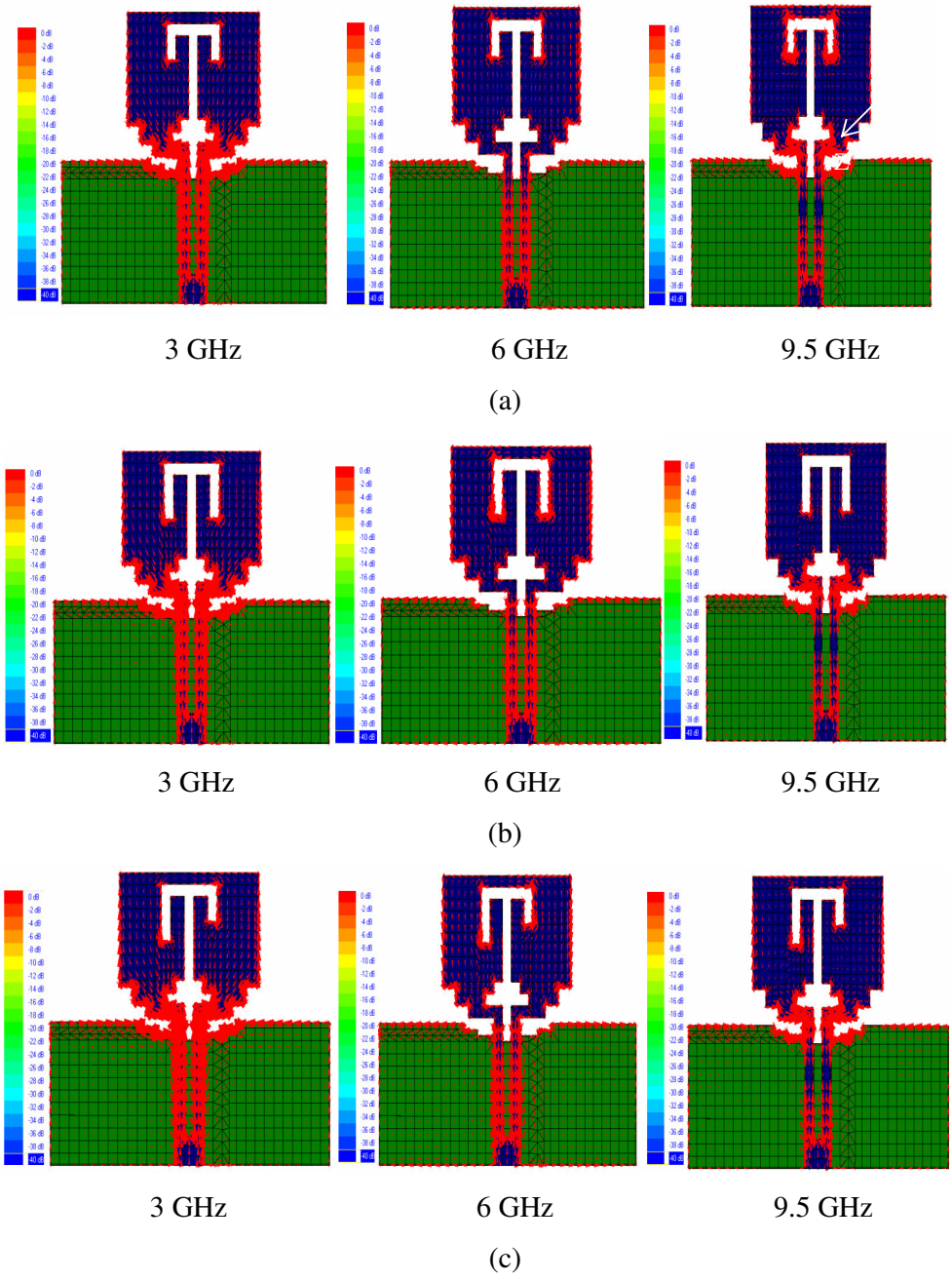

Figure 5.14: The simulated current distribution on the antenna by varying its height of T slot on the patch radiator for different frequency: (a) both length 3 mm, (b) both length 5 mm, and (c) length 4 and 3mm

Figure5.14 shows the current distribution on the antenna by varying its height of T slot on the patch radiator. The T slot height provides significantly effect to the return loss performance, as shown in Figure 5.15. From the simulation results, increasing the height of T slots results multiple resonance frequency. The lower edge resonance frequency is same for all T height at 5.2 GHz. Asymmetry heights of T slots does not give any return loss improvement, but degrade the return loss at around 8 GHz. The optimum height is found to be 2 to 3 mm.

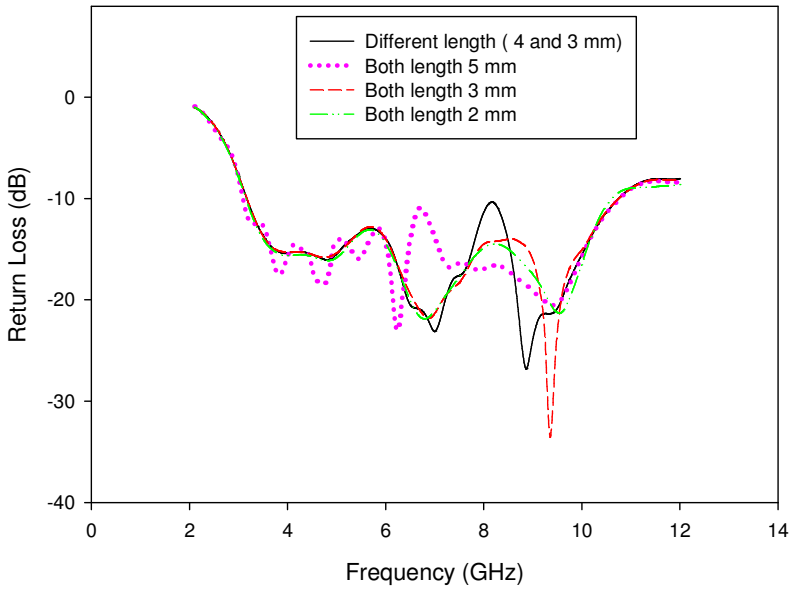

Figure 5.15: The simulated return loss of various heights for upper T slot

5.2.4.2 Various L and U Slot Design

The L and U slotted antenna with current distribution at 3, 6, and 9 GHz is presented in Figure 5.16. Individual L and U slotted antenna is depicted as well. It is shown in both figures; the vertical current is most concentrated near to the slots edges for all frequency range. It is noted for both L and U slots, the current distribution is less on the area between both slots. While for L slot only, the intensity current distribution decreases on the area below the L slot. The U slotted antenna has less current distribution on the area opposite to the U slot.

It has been investigated that by increasing the frequency caused decreasing the distributed current on the area between both L and U slots, below L slot and opposite the U slot. This is due to the current tends to distribute along the slot which correspondence to the resonance frequency.

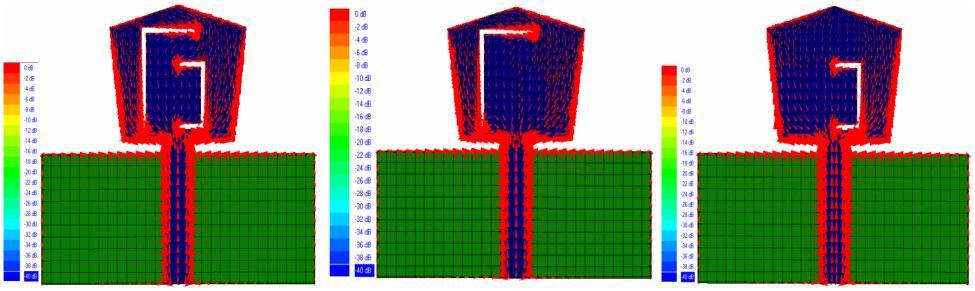

(a)

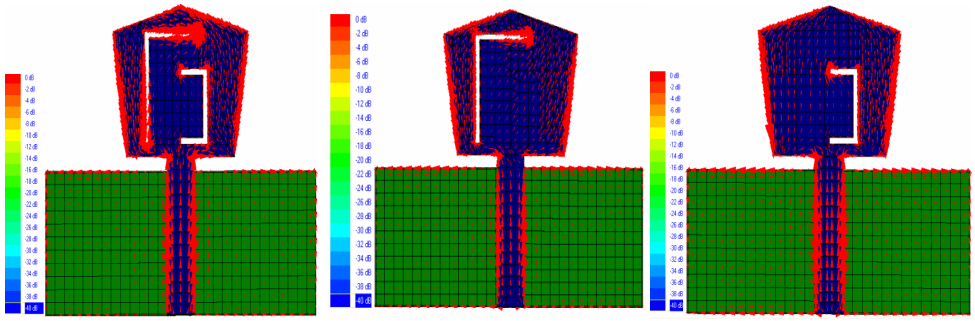

(b)

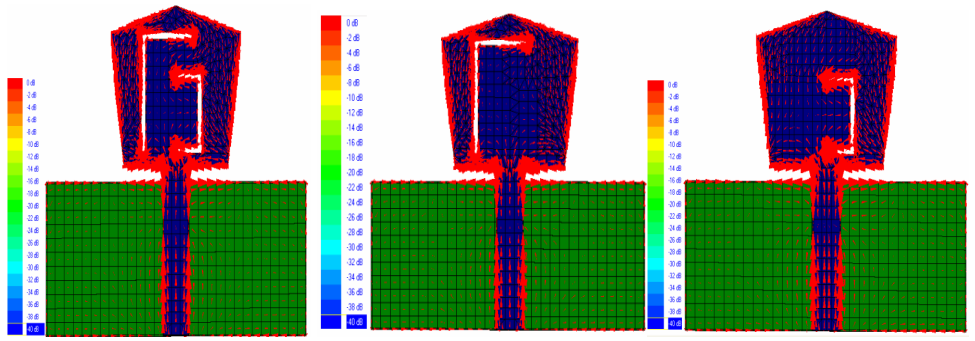

(c)

Figure 5.16: The simulated current distribution of 3, 6, and 9 GHz for L and U slotted antenna

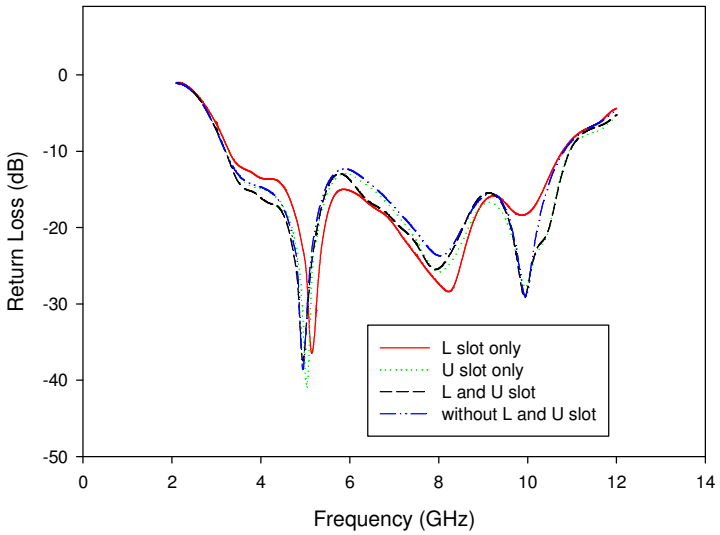

Figure 5.17: The simulated return loss of various L and U slots design for L and U slotted antenna

Figure 5.17 shows the return loss comparison between antenna with and without L and U slotted on patch radiator. The lower resonances for all antenna models are shifted slightly, but they are still around 5 GHz. The individual L slotted antenna has degraded the return loss at upper frequency rather than the individual U slotted antenna. It is clearly shown that L and U slotted antenna has a good return loss performance with respect to -10 dB.

Figure 5.18 is the simulated return loss of various width L and U slots design. By decreasing the width slot to 0.5 mm has improved the return loss especially at upper frequency and widened the impedance bandwidth.

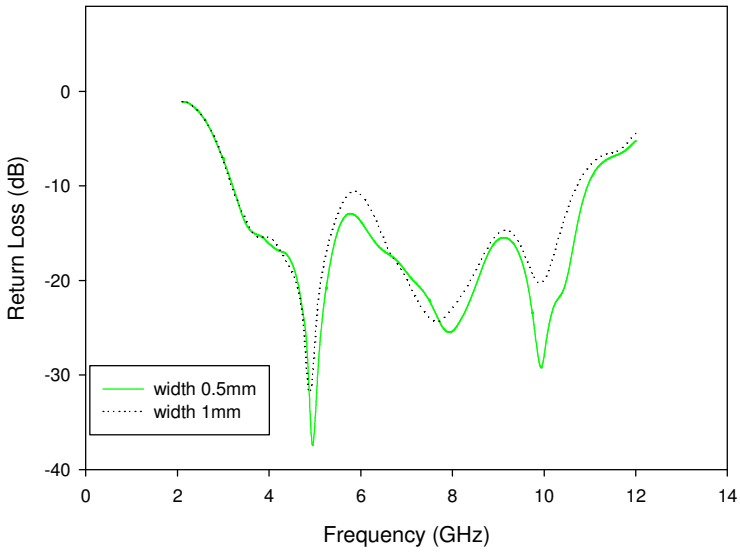

Figure 5.18: The simulated return loss of various width of L and U slots design

Figure 5.19 and Figure 5.20 show the current distribution of L and U slotted antenna with different length slot and their return loss performance, respectively. As mentioned previously, most current distributes near to the slots edges. Increasing the frequency has caused decreasing the distributed current on the area between both slots. It is noted from the results, varying the length slot of L or U slot only give a little impact to the antenna performance without affect the impedance bandwidth. The optimum length of slots is found as listed in Table 4.7.

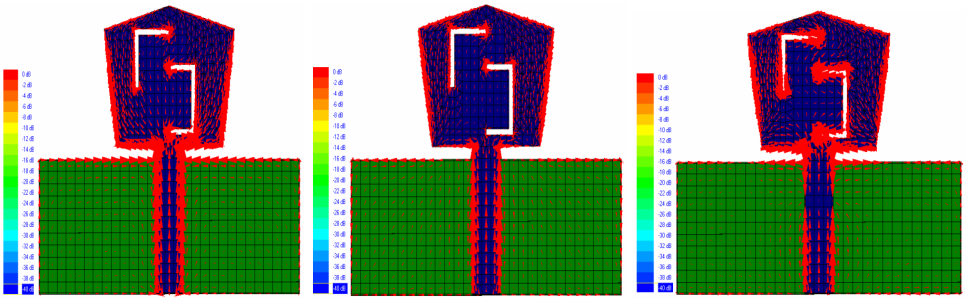

3 GHz 6 GHz 9 GHz

(a)

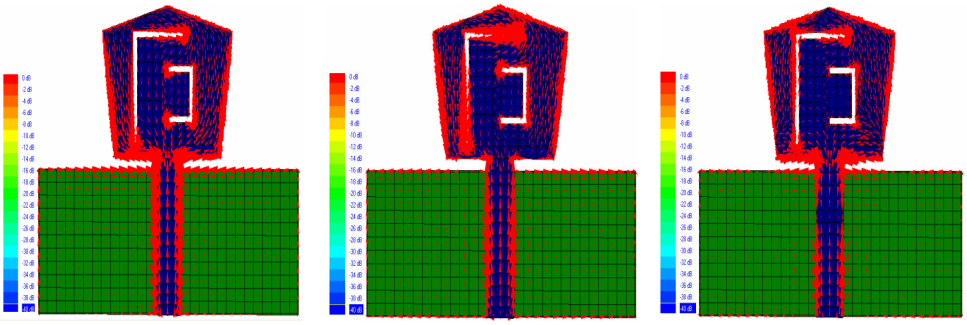

3 GHz 6 GHz 9 GHz

(b)

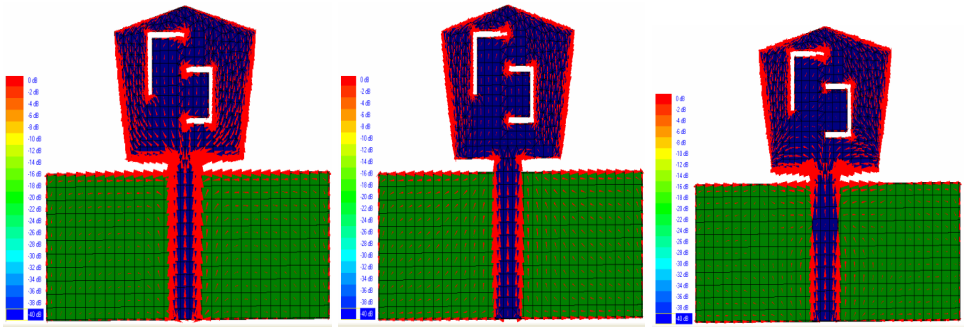

3 GHz 6 GHz 9 GHz

(c)

Figure 5.19: The simulated current distribution on the antenna by varying its length of L and U slot on the patch radiator for different frequency: (a) vary L, (b) vary U, and (c) vary both L and U

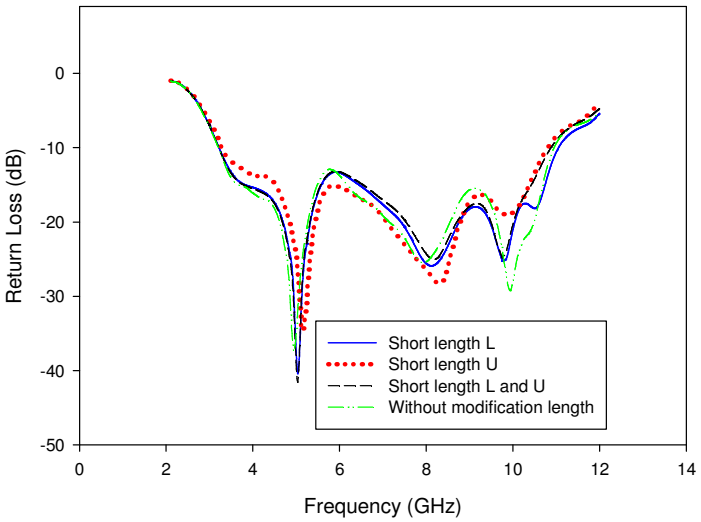

Figure 5.20: The simulated return loss of L and U slotted antenna with different length slot

5.3 Final Design of Reconfigurable Slotted UWB Antenna

Three prototypes resulted for each model of slotted UWB antenna. As mentioned before, there are two models such as T slotted antenna and L and U slotted antenna. Each prototype has capability to reject a certain frequency. Figure 5.21 shows the geometry of first model reconfigurable slotted UWB antenna and the photograph of prototypes. From the top left side of Figure 5.21(a) is a prototype which has band notched at FWA band. The top middle side and the top right side of Figure 5.21(a) are both prototypes have band notched bands at HIPERLAN and WLAN band, respectively. The same sequential are also applied to the Figure 5.21(b)

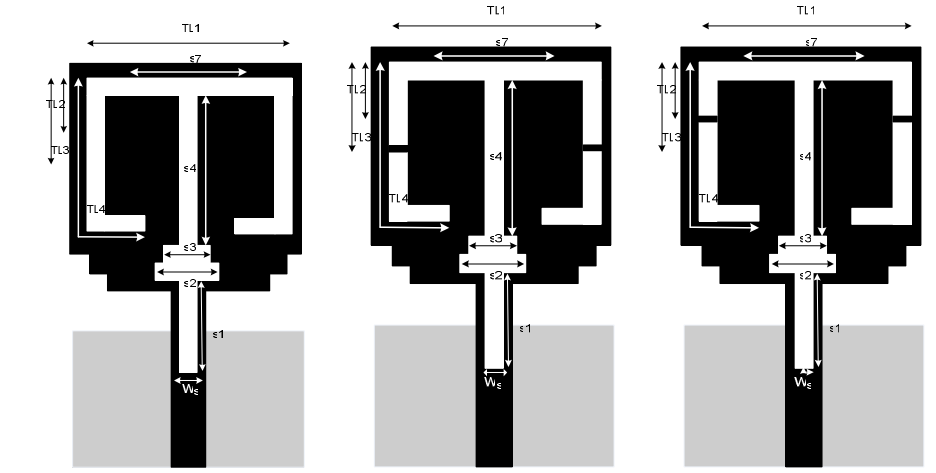

(a)

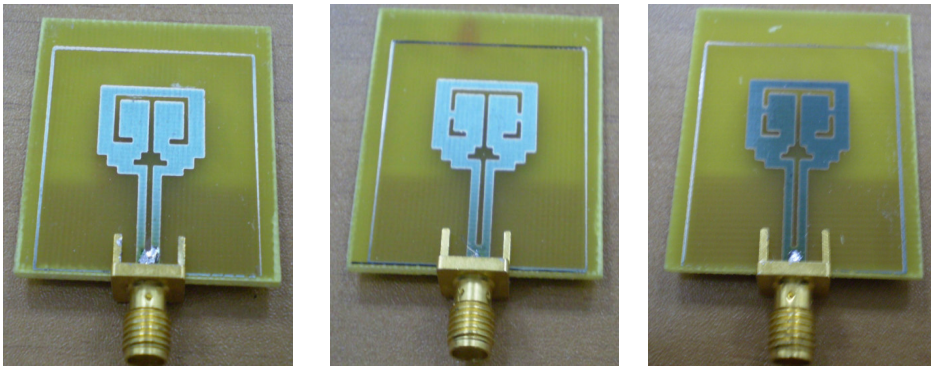

(b)

Figure 5.21: Three prototypes of T slotted antennas with notched band at FWA (left), notched at HIPERLAN (middle) and notched at WLAN (right): (a) geometry of reconfigurable T slotted antenna and (b) photograph of prototype

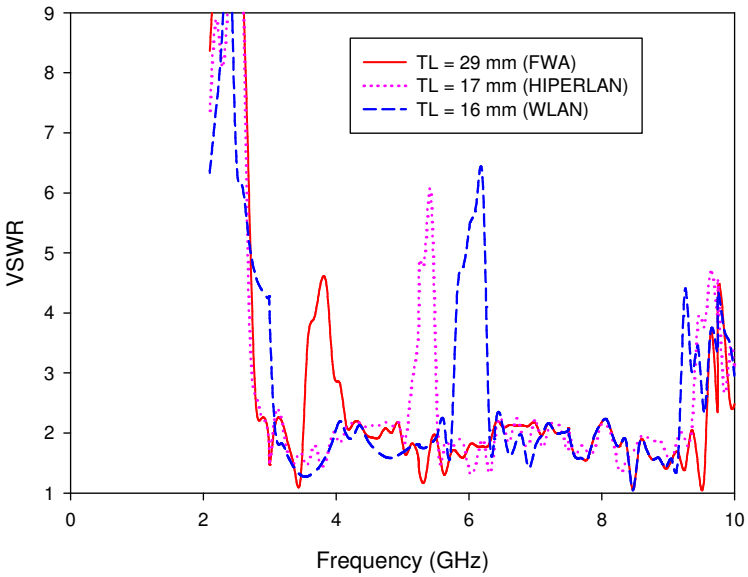

Figure 5.22: The measured VSWR for the three prototypes of modified T slotted antenna

Figure 5.22 shows the measured VSWR for three prototypes of modified T slotted antenna. The measured VSWR increased to 2.2 compared to the simulated result described in Chapter 4. The band notched curves for all frequency are also shifted. This is due to the imperfect matching in the coaxial feed during soldering and fabrication. For band notched at FWA band, the rejection covers from 3.56 GHz to 4.05 GHz, the rejection at HIPERLAN and WLAN are 5.13 GHz to 5.43 GHz and 5.82 GHz to 6.2 GHz, respectively. The VSWR beyond 9.3 GHz is getting worse.

Figure 5.23 shows the measured phase for the modified T slotted antenna which has the band notched at FWA band. It is shown that the phase almost constant over frequencies range, slightly shifted occurred. This nearly constant phase also occurs for others both prototypes. This constant phase and group delay is important to ensure the pulse transmitted are not distorted.

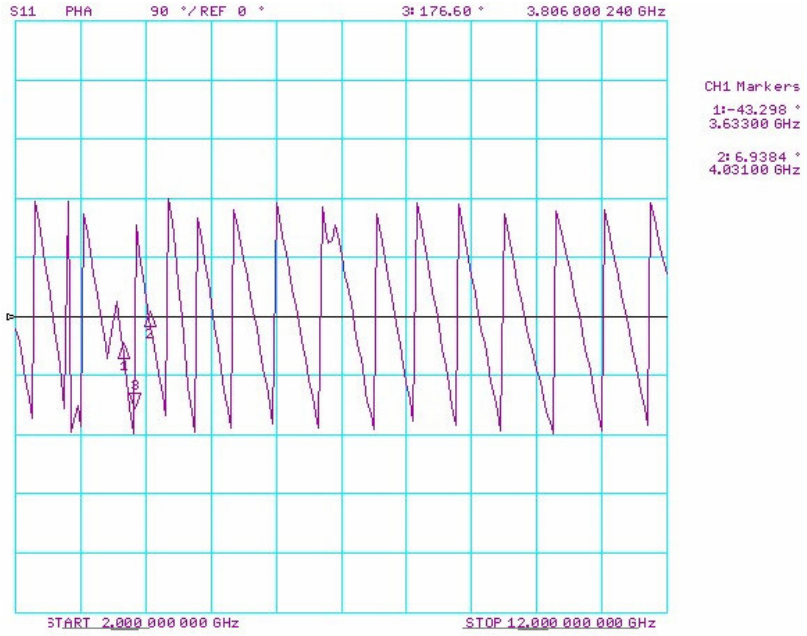

Figure 5.23: The measured phase for modified T slotted antenna

There are three prototypes have been developed for this modified L and U slotted antenna as shown in Figure 5.24. Figure shows the geometry and photograph of L and U slotted antenna. The top side of Figure 5.24(b) shows a prototype of band notched at 3 GHz, the left figure is a prototype of band notched at HIPERLAN and the right figure is a prototype of antenna band notched at WLAN. The geometry with respect to these configurations are shown in Figure 5.24(a). The measured VSWR for three prototypes of L and U slotted antenna are shown in Figure 5.25.

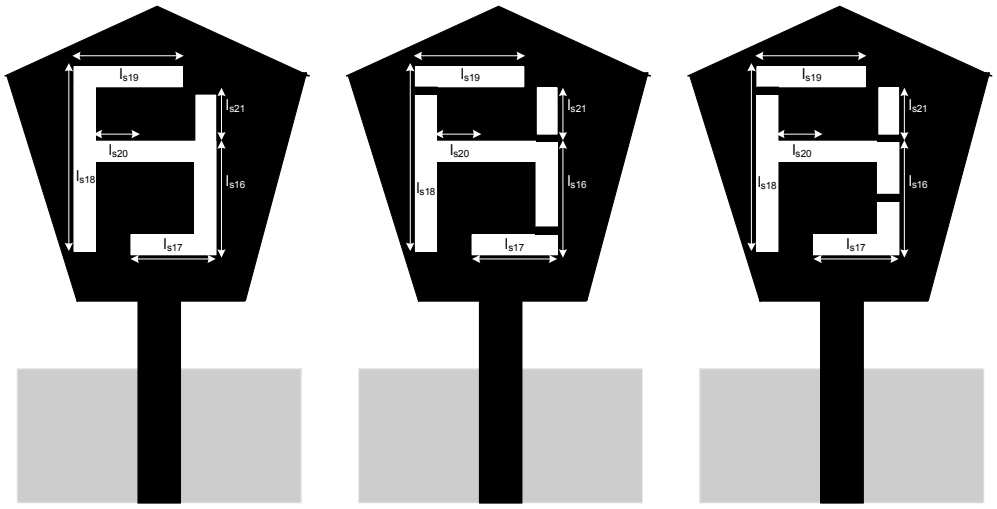

(a)

(b)

Figure 5.24: Three prototypes of modified L and U slotted antenna for band notched at FWA (top), at HIPERLAN (left) and at WLAN (right): (a) geometry and (b) photograph

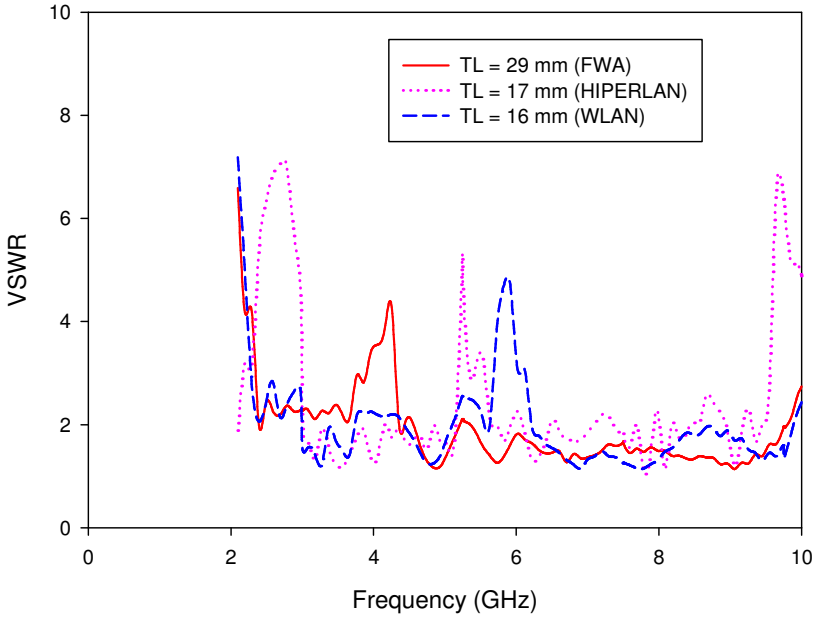

Figure 5.25: The measured VSWR for L and U slotted antenna

The measured VSWR for this type of antenna is shown in Figure 5.25. The VSWR is approximately less than 2.2 over 3 GHz to 10 GHz, except for antenna with band notched at HIPERLAN band. The VSWR beyond 9.5 GHz is getting worse. For band notched at FWA, the rejection is in the range of 3.76 GHz to 4.25 GHz, and the rejection of HIPERLAN is 5.23 GHz to 5.53 GHz. The antenna with band notched at WLAN band has rejection in the range of 5.72 GHz to 6.1 GHz. Even though the band notched slightly shifted from the required bands, but it still covers the rejection bandwidth.

Figure 5.26 presents the measured constant phase for the antenna with HIPERLAN rejection. The slightly distorted occurred over the frequency ranges. Both other prototypes have almost similar constant phase.

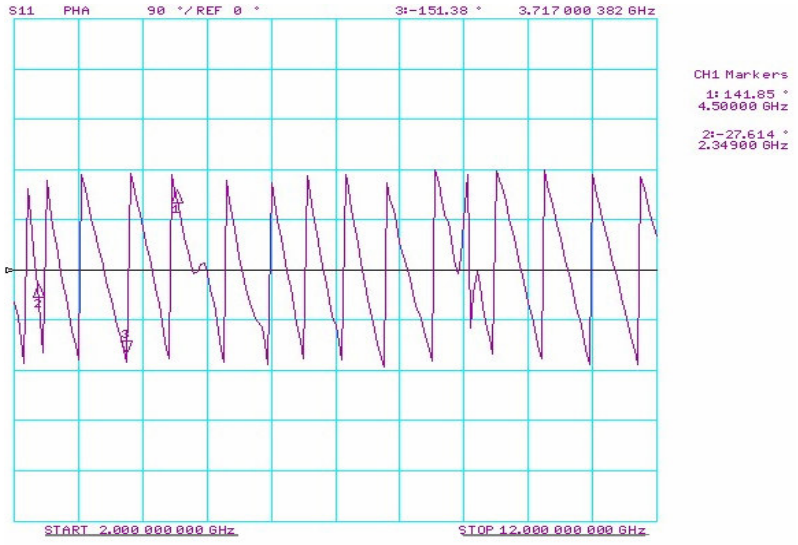

Figure 5.26: The measured phase of L and U slotted antenna with HIPERLAN notched band

5.4 Spherical Near Field Testing

Once the resonance frequencies were identified, principal radiation patterns were taken to characterize the operational performance of each antenna. These measurements were obtained using indoor anechoic chamber room. For these measurements, the chamber was arranged as shown in Figure 5.27.

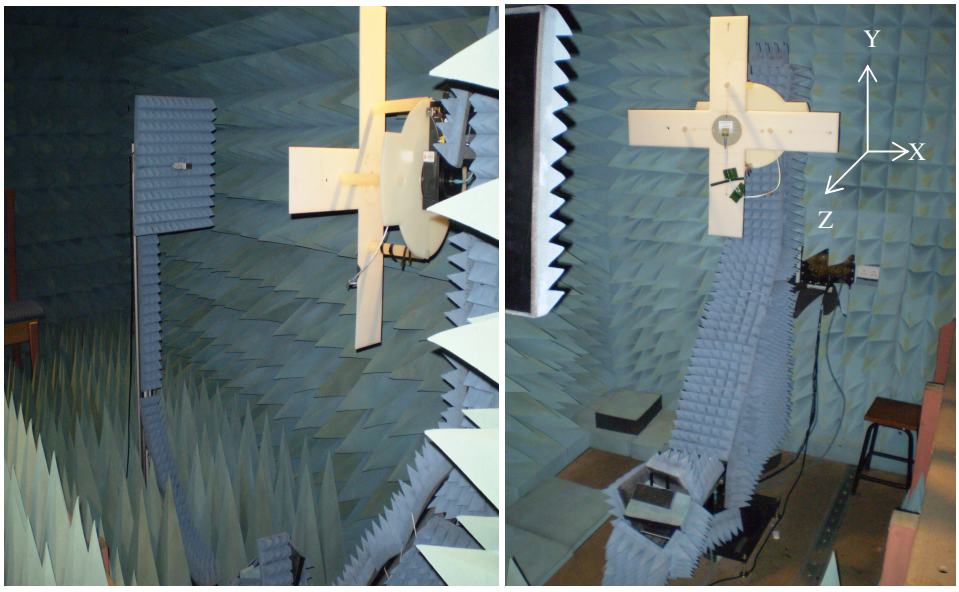

Figure 5.27: The radiation pattern measurement setup inside the anechoic chamber room

From Figure 5.27, it is shown the measurement setup for both antenna and probe which were mounted to the vertical positioner-holders. The probes available at the chamber are in the frequency ranges of 3.95 – 5.85 GHz and 8.95 – 12 GHz, respectively. Therefore, the radiation patterns were measured at 4 GHz, 5.8 GHz and 10.6 GHz. The measured radiation patterns were plotted into horizontal (H) and vertical (V) cuts. The H-cut is cut for the azimuth plane with fixed elevation angle at 0^0 and vary the azimuth angle. The V-cut is cut for the elevation plane with fixed azimuth angle at 0^0 and vary the elevation angle.

The existing chamber employed the spherical near field measurement as shown in Figure 5.28. By definition, near field tests are done by sampling the field very close to the antenna on a known surface. From the phase and amplitude data collected, the far field pattern must be computed in much the same fashion that theoretical patterns are computed from theoretical field distributions. The transformation used in the computation depends on the shape of the surface over which the measurements are taken with the scanning probe [155].

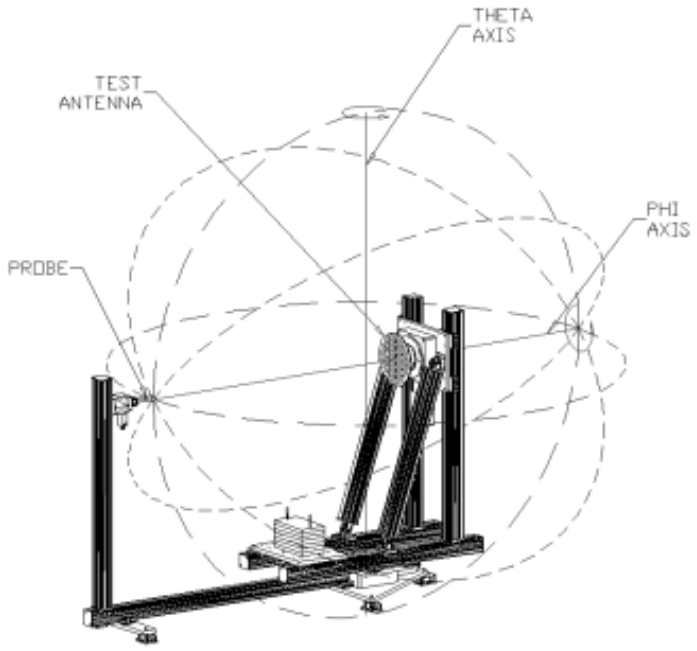

Figure 5.28: Coordinate system for typical spherical near-field rotator system [156]

This spherical system acquired a double data set on the antenna under test (AUT). The '360phi' data set is taken with full 360^0 phi rotation of the AUT, but with only $0 - 180^0$ motion in theta. In this mode, the AUT's Z axis will only be looking at one side of the chamber during the measurement [156]. The AUT was swept every 2^o increment in azimuth plane in order to reduce the aliasing errors. Data point spacing aliasing errors will occur for spherical near-field measurements if the data point spacing is not small enough to sample the highest spatial frequency components in the measured data [156].

5.4.1 Radiation Patterns of T Slotted Antenna with Slotted Ground Plane

Several requirements are needed to take into consideration during the measurement process. Obtaining true patterns depends primarily on accurately positioning the probe, accurately measuring the field, and eliminating distortions in

the field introduced by the room, track, or probe it self [155]. The room reflections must be lower than the basic sidelobe level, the probe it self must have low reflections. The probe position must be accurate to better that the tolerance corresponding to the sidelobe level. In a spherical near-field range, the spherical measurement surface will be imperfect due to inaccuracies of the positioners and misalignment of these positioners [156].

The elevation patterns for the antennas are simulated at the H-plane ($\varphi = 0^0$, yz-plane) and E-plane ($\varphi = 90^0$, xy-plane). The E-plane pattern is the radiation pattern measured in a plane containing feed, and the H-plane pattern is the radiation pattern in a plane orthogonal to the E-plane. These both simulated results are compared to the measured H-plane and E-plane for the three differences frequencies of 4 GHz, 5.8 GHz and 10.6 GHz, as shown in Figure 5.29 to Figure 5.31, respectively.

The results show that the radiation patterns are changing as the frequency increases. The measured H-planes show omnidirectional radiation pattern over the frequencies. The patterns resulted from the measurements have many ripples in amplitude due to many reflections into the field between the AUT and probe. The reflections may come from the room (floor and ceiling), chamber scattering, antenna holder it self and track inside the anechoic chamber. It is shown in Figure 5.27, the antenna size is very small compared to its huge holder, and also the floor and the track surrounding the antenna tower are not all covered by absorber. If moved sideways, the ripples due to the track to move about half cycle. If moved vertically, the ceiling and floor reflections are indicated. Various types of leakage occur are also considered as pattern degradation. The most significantly is probably from improper cable connectors allowing excitation of the outside surface [155]. Leakage will be added to the measured pattern as degradation.

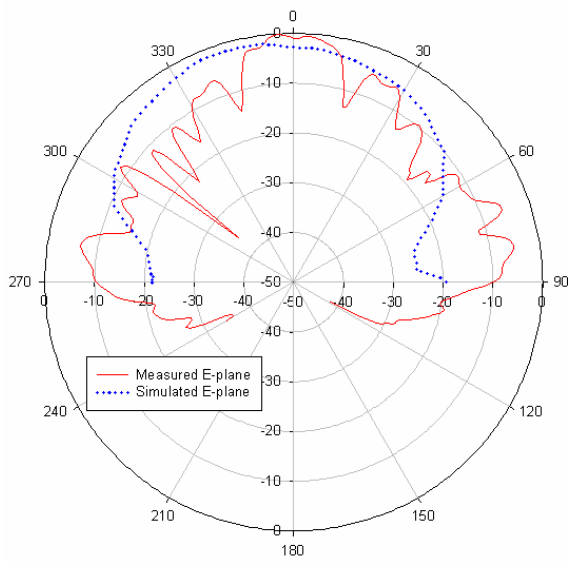

(a)

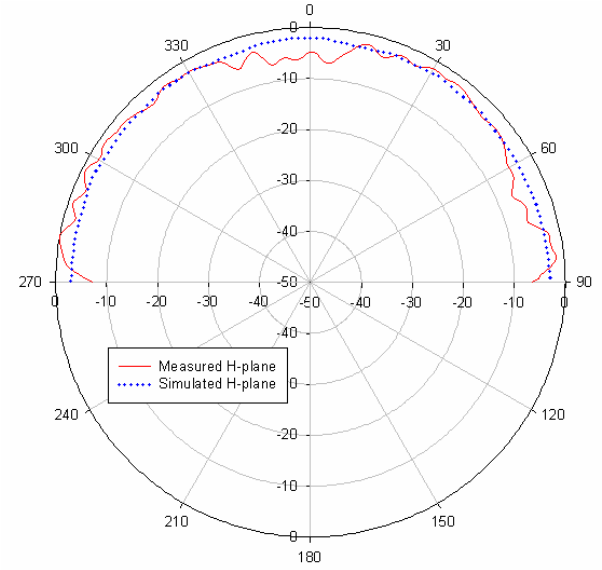

(b)

Figure 5.29: The measured and simulated E and H planes at 4 GHz: (a) measured and simulated E-planes and (b) measured and simulated H-planes

It is observed that the measured and simulated elevation patterns for the E and H planes are relatively broad. The antenna tends to radiate energy equally to all direction. The measured radiation patterns demonstrate that at the low end of the operating band, the currents are well distributed over the patch antenna plate so the patterns are nearly omnidirectional. But at high end of the operating band, the currents are concentrated near the slot, thus the fields radiate mainly through the slot.

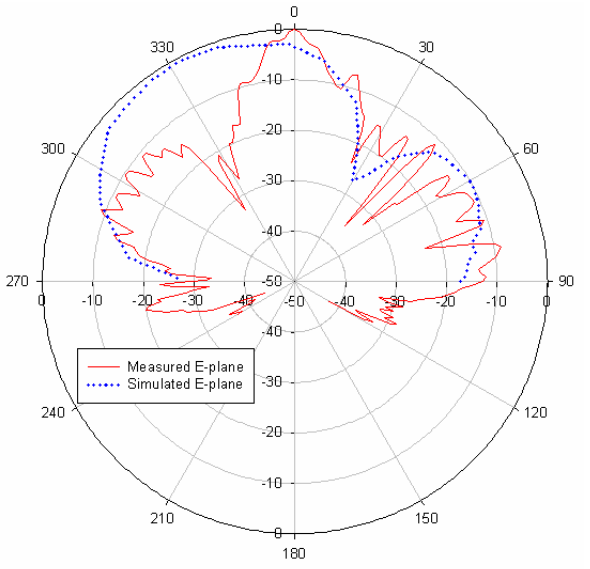

(a)

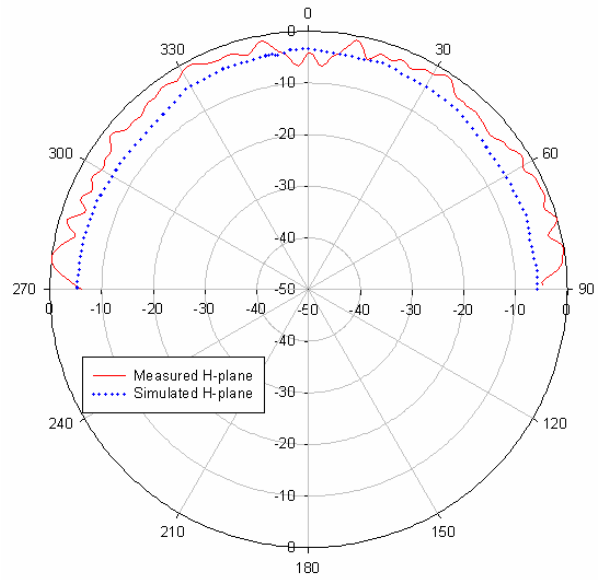

Figure 5.30: The measured and simulated E and H planes at 5.8 GHz: (a) measured and simulated E-planes and (b) measured and simulated H-planes

It is also noted from Figure 5.30 that with increasing frequency to 5.8 GHz, the E-plane patterns become smaller. Many ripples occurred in this frequency. The dips also present for various different angles. Even though the measured radiation patterns are slightly difference to the simulated ones, since their patterns are nearly omni directional and their return losses are less than -10 dB, this proposed antenna meets the UWB requirements.

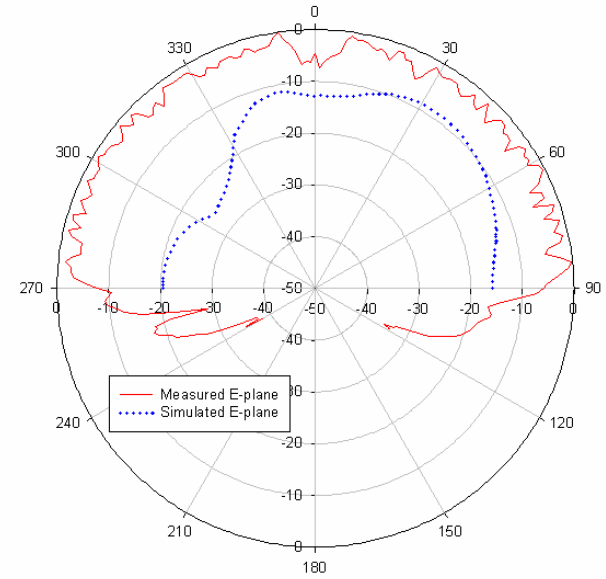

(a)

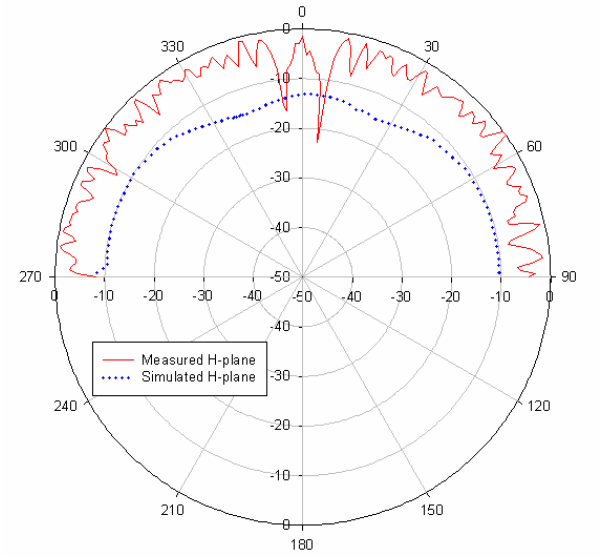

(b)

Figure 5.31: The measured and simulated E and H planes at 10.6 GHz: (a) measured and simulated E-planes and (b) measured and simulated H-planes

Figure 5.31 shows the E and H-planes for simulated and measured results. Slightly degradation at boresight occurs in measured H-plane. It is shown from both figures that both measured planes are wider than both simulated planes. The E-plane pattern seems tend to omnidirectional, which is similar to the H-plane. The degradation at boresight is due to misalignment of the AUT.

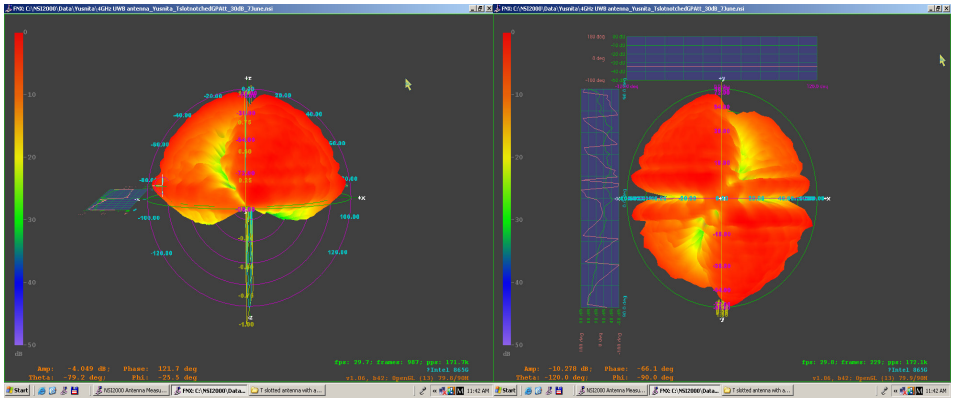

(a)

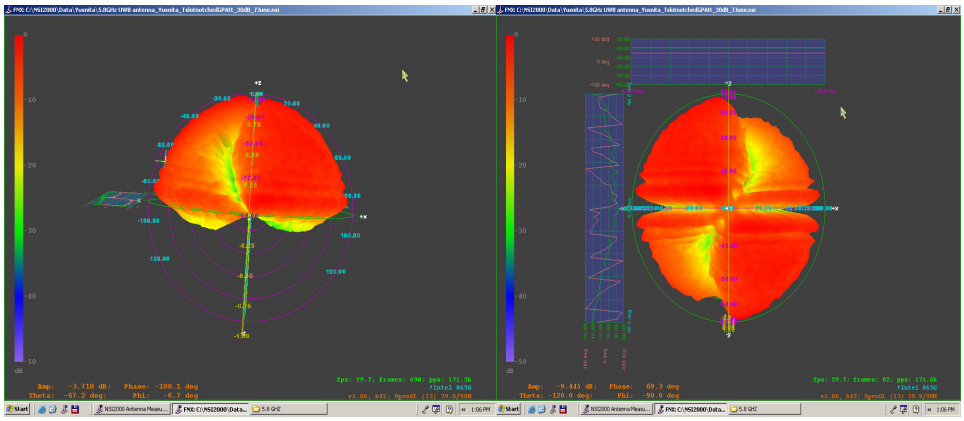

(b)

Figure 5.32: The measured 3D radiation pattern: (a) 4 GHz and (b) 5.8 GHz

Figure 5.32 and Figure 5.33 present the measured 3D radiation patterns for 4 GHz, 5.8 GHz and 10.6 GHz. This 3D graphical radiation patterns show clearly the nearly omni directional pattern for each frequency. The pattern types are almost similar. The 3D radiation patterns are plotted from top and side views.

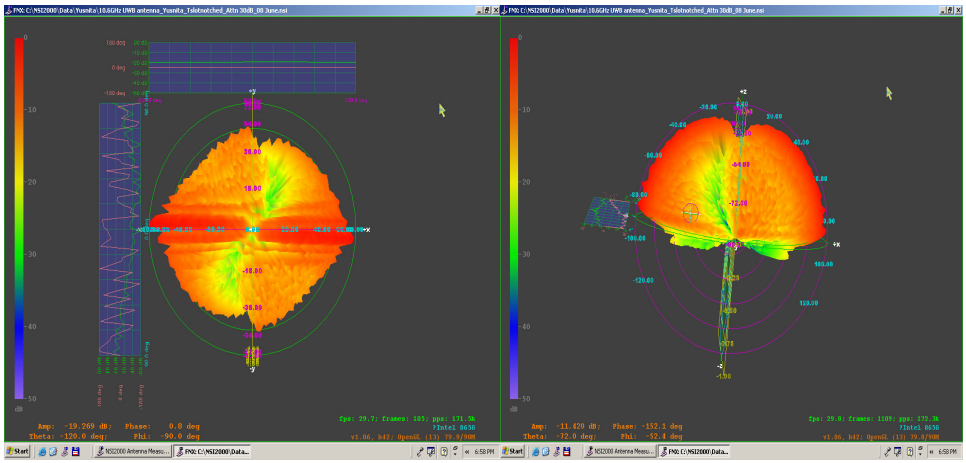

Figure 5.33: The measured 3D radiation pattern at 10.6 GHz: (a) side view and (b) top view

5.4.2 Radiation Patterns of L and U Slotted Antenna

Figure 5.34 to Figure 5.36 present the measured and simulated radiation pattern for E and H planes of 4 GHz, 5.8 GHz and 10.6 GHz, respectively. An important feature that is highly desirable of proposed UWB antennas are the nearly omni directional radiation patterns as demonstrated by the fact that the H plane patterns are not significant different for all frequencies. The E-plane pattern for 10.6 GHz is very broad and tends to nearly omnidirectional.

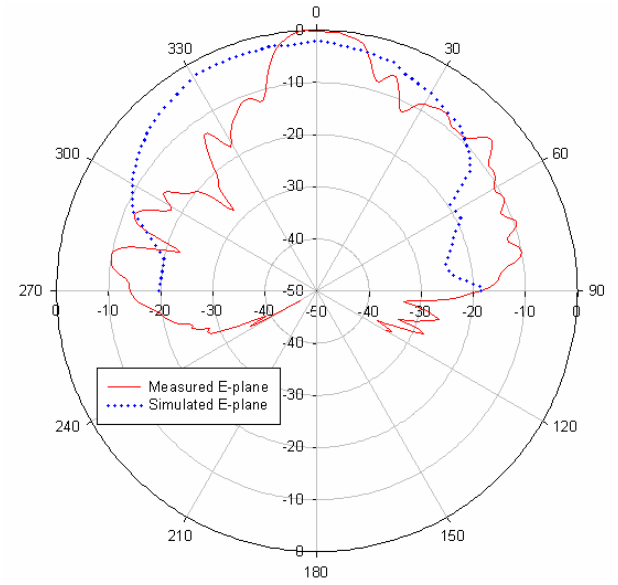

(a)

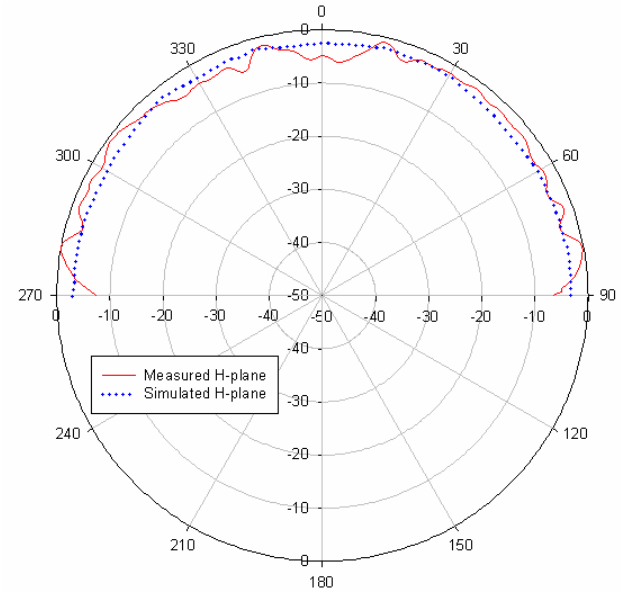

(b)

Figure 5.34: The measured and simulated E and H planes at 4 GHz: (a) measured and simulated E-planes and (b) measured and simulated H-planes

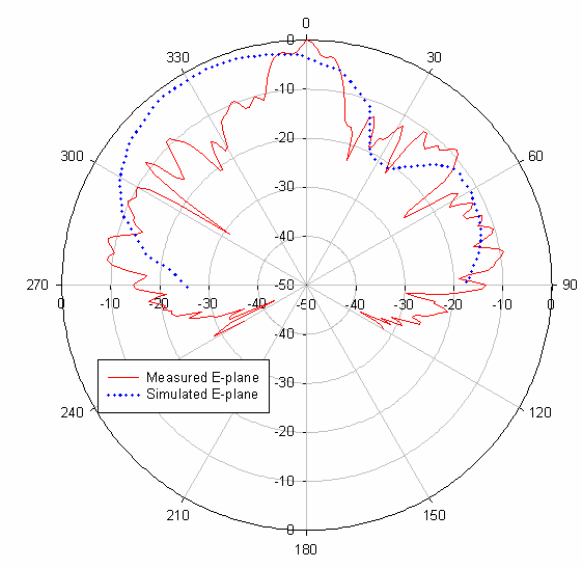

(a)

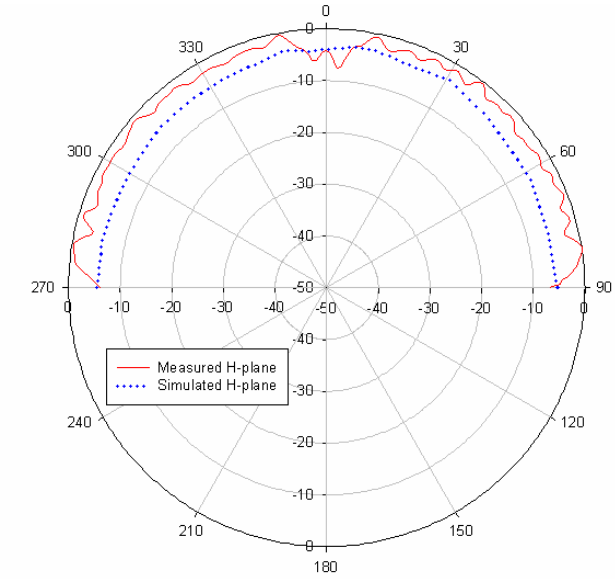

(b)

Figure 5.35: The measured and simulated E and H planes at 5.8 GHz: (a) measured and simulated E-plane and (b) measured and simulated H-planes

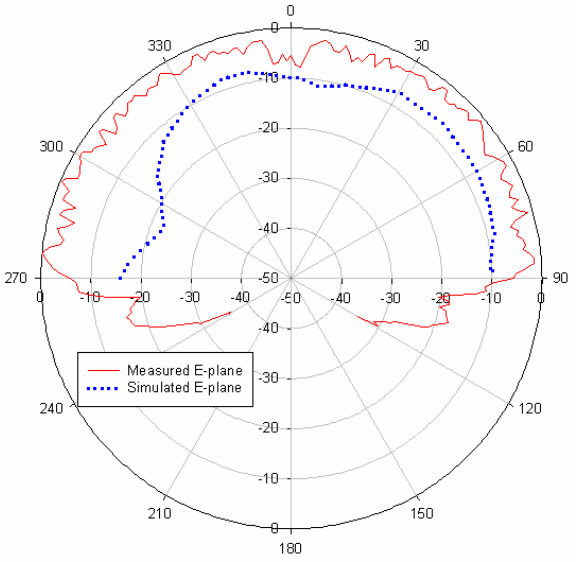

(a)

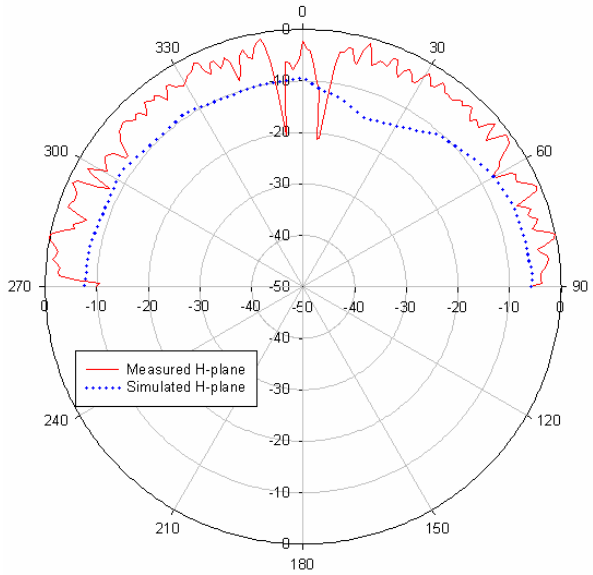

(b)

Figure 5.36: The measured and simulated E and H planes at 10.6 GHz: (a) measured and simulated E-planes and (b) measured and simulated H-planes

From the measured results obtained, the E and H planes for the T slotted antenna and this antenna have nearly similar patterns. The H planes are remaining omnidirectional along the bandwidth. The ripples problem still occurs for all frequencies range. This is due to imperfect system inside the anechoic chamber where is difficult to obtain the true patterns. However, the mathematical error computed by simulation software are very small in error, the largest sources of error are experimental. The antenna misalignment also directly contributes to the boresight errors.

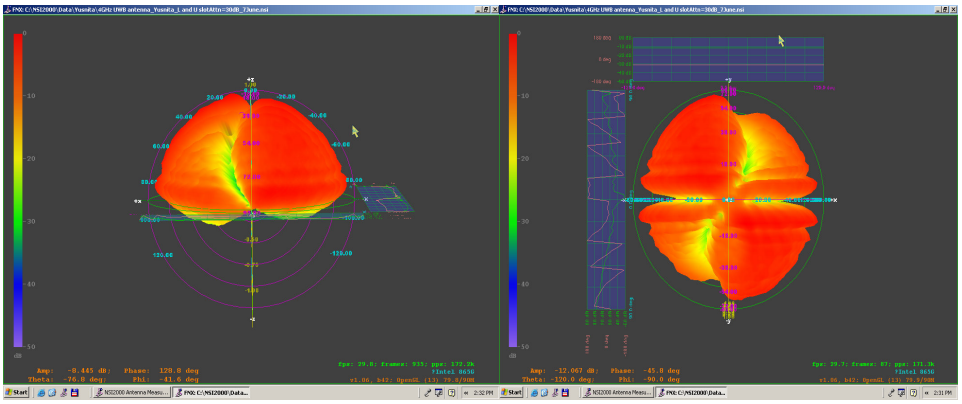

(a)

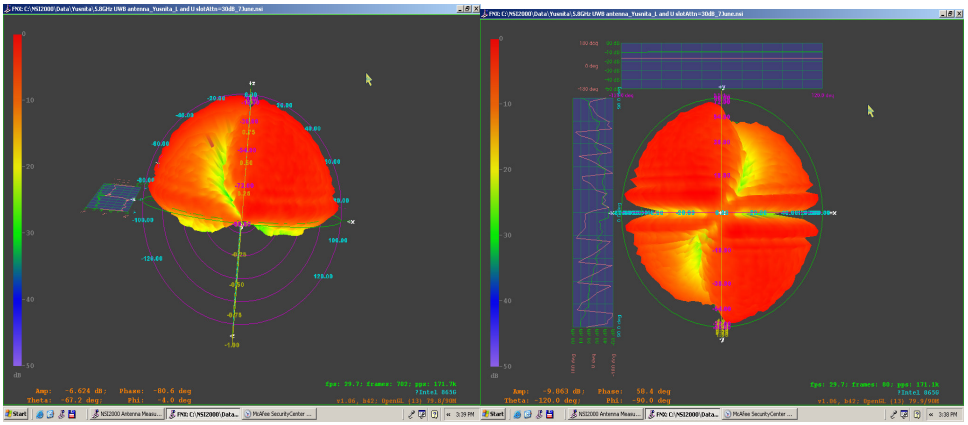

(b)

Figure 5.37: The measured 3D radiation pattern: (a) 4 GHz (b) 5.8 GHz

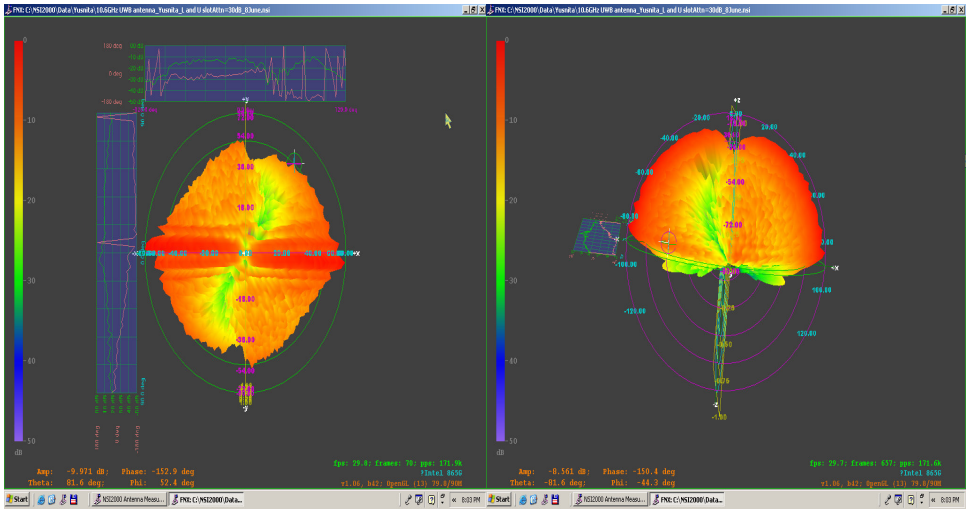

Figure 5.38: The measured 3D radiation pattern at 10.6 GHz

The 3D graphical radiation patterns are presented in Figure 5.37 and Figure 5.38 for 4 GHz, 5.8 GHz and 10.6 GHz. These patterns are seen from top view and side view. It is noticed that the patterns behavior of this antenna show very closely with the T slotted antenna.

5.4.3 Radiation Patterns of Reconfigurable T slotted UWB Antenna

This thesis is also investigated the effect of frequency notched to the radiation pattern at 4 GHz and 5.8 GHz. Figure 5.39 presents the measured and simulated radiation patterns for antenna having frequency notched at FWA. Comparison between the reconfigurable modified T slot antenna and UWB T slotted antenna without frequency notch function, in terms of radiation patterns, have been done. It is found that the radiation pattern at 4 GHz of notched band at FWA has a dip towards null at 30^0 in E plane. This dip is smaller than the dip occurs at 49^0 for antenna without notch function. For radiation pattern at 5.8 GHz, more distortions occur for the E-plane rather than the E-plane pattern of previous frequency. Both the E planes for both frequencies are relative broad. The measured H planes for both frequencies

are remaining omnidirectional behaviors. The E plane at 5.8 GHz has a dip to null at -30^0.

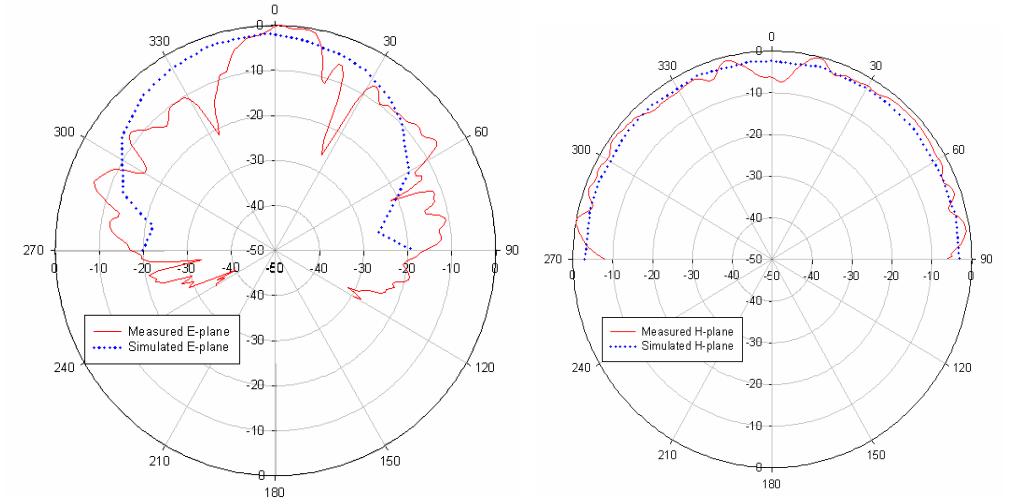

(a)

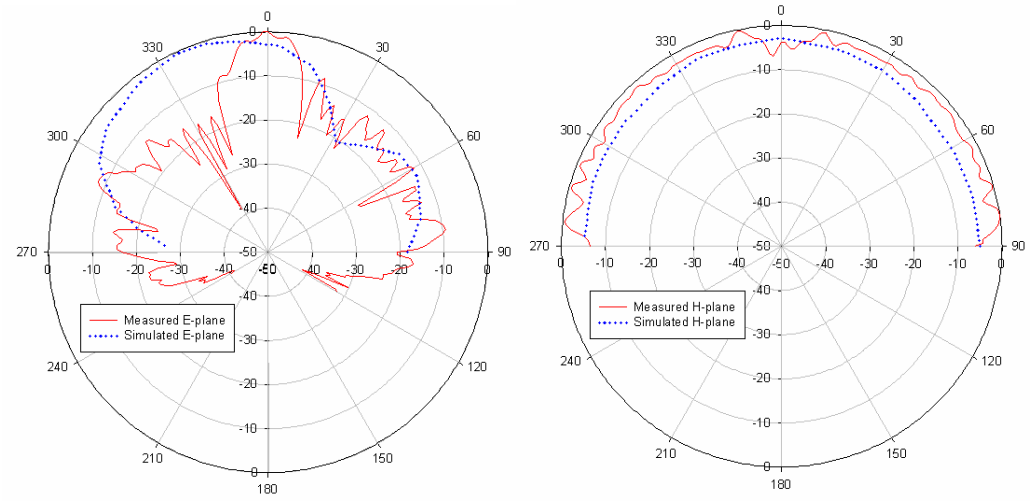

(b)

Figure 5.39: The measured and simulated E and H-planes for T slotted antenna notched at FWA: (a) 4 GHz and (b) 5.8 GHz

Figure 5.40 shows the measured and simulated radiation pattern for antenna with notched band at HIPERLAN band. It is observed that the E-pattern of 5.8 GHz is smaller than E-pattern of 4 GHz, while both H-planes are omnidirectional. It is noticed that the notched band does not affect to the radiation pattern. This is

investigated by comparing between these characteristic patterns with the previous characteristics without notched function. Both characteristics are mostly similar each other. A dip occurs at -60^0 for E-plane of 5.8 GHz pattern. E-plane pattern of 4GHz has no dip toward null, it is broad and the ripples still occur in the pattern due to the uncertainties. The uncertainties of the far-field patterns caused by any errors, as mentioned in previous chapter, contribute to the radiation pattern degradation.

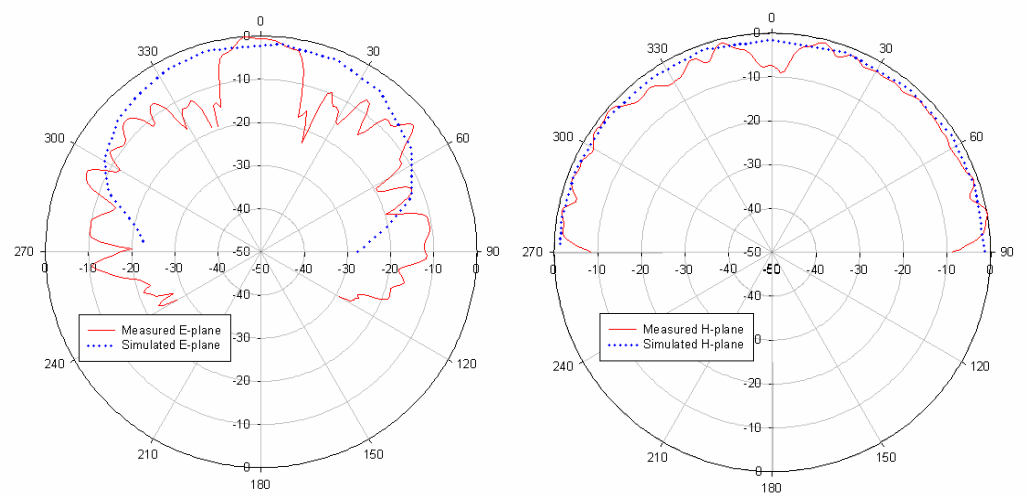

(a)

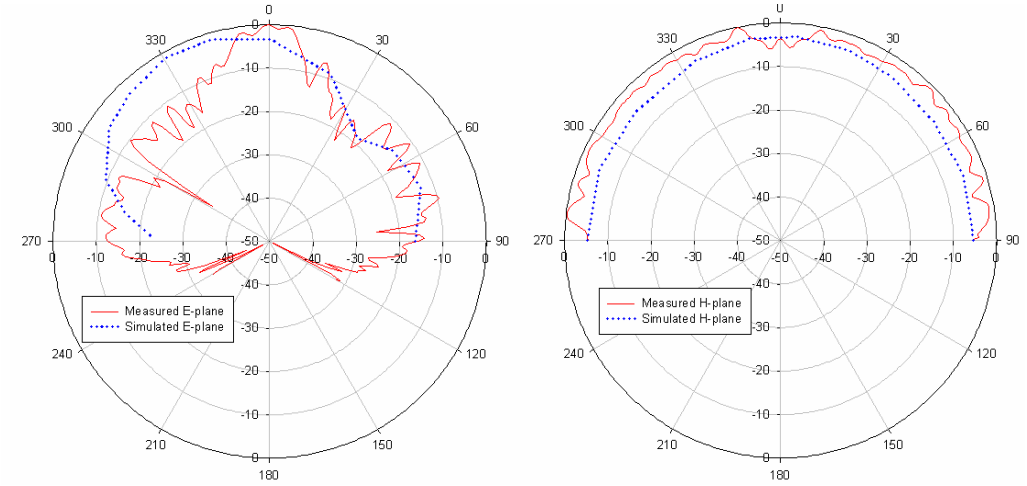

(b)

Figure 5.40: The measured and simulated E and H planes for T slotted antenna notched at HIPERLAN: (a) 4 GHz and (b) 5.8 GHz

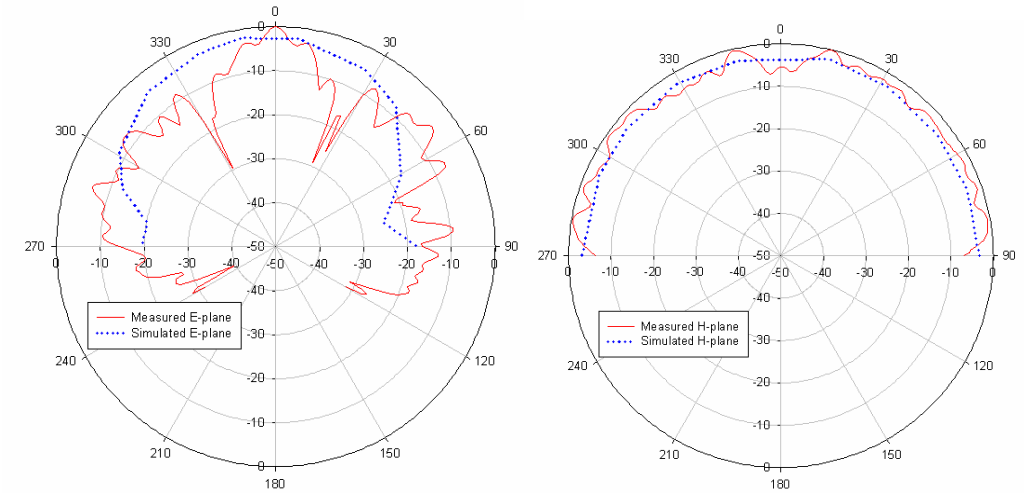

(a)

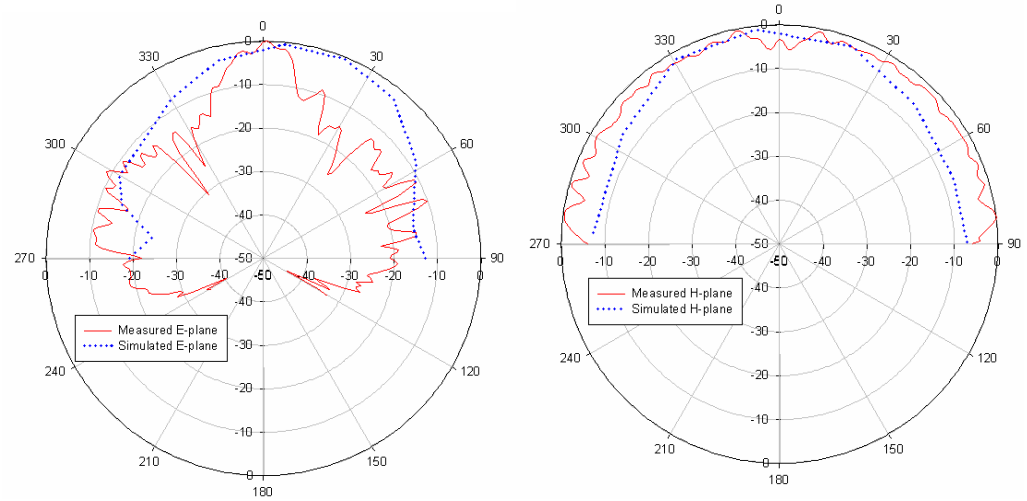

(b)

Figure 5.41: The measured and simulated E and H planes for T slotted antenna notched at WLAN: (a) 4 GHz and (b) 5.8 GHz

The measured radiation patterns for antenna notched band at WLAN band are shown in Figure 5.41. The patterns behavior is almost same with the measured radiation pattern for others both prototypes. The H planes for both frequencies are having omnidirectional while the E planes are relative broad. Two dips occur at $\pm 30^0$ at E-plane pattern of 4GHz. The measured 3D radiation patterns for those antennas

are shown in Figure 5.42 and Figure 5.43 from the side view. It is clearly shown the omnidirectional pattern over the bandwidth.

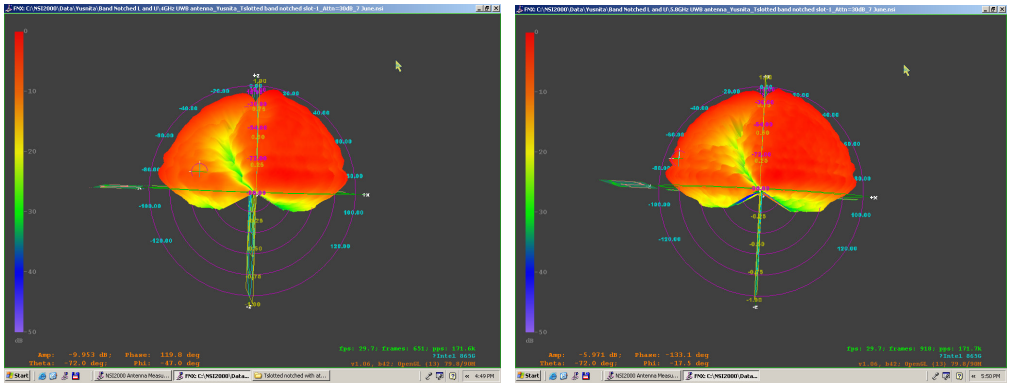

4 GHz 5.8 GHz

(a)

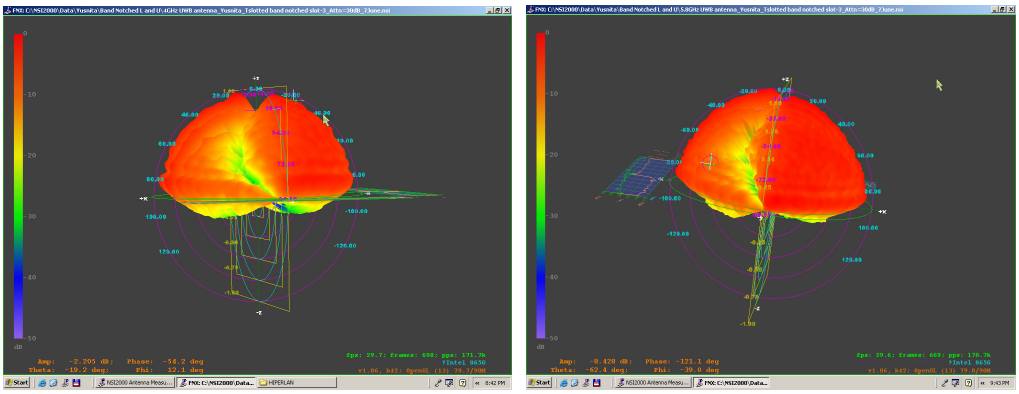

4GHz 5.8 GHz

(b)

Figure 5.42: The measured 3D radiation patterns for T slotted notched band antenna: (a) band notched at FWA and (b) band notched at HIPERLAN

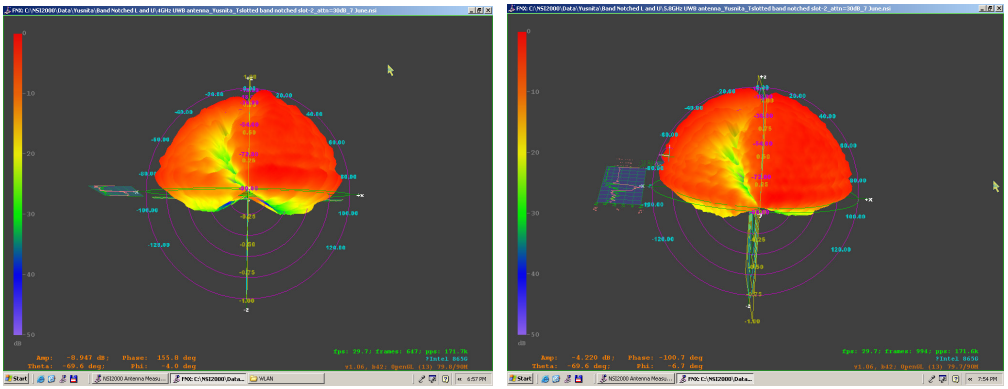

4GHz 5.8 GHz

Figure 5.43: The measured 3D radiation patterns for T slotted notched band at WLAN

5.4.4 Radiation Patterns of Reconfigurable L and U Slotted Antenna

Comparison between measured and simulated radiation patterns for these proposed antennas are plotted in Figure 5.44 to Figure 5.46. There are slightly backlobe presents at the E-planes for both frequencies, as illustrated in Figure 5.44. The frequency notched at FWA has shown no significant variation to the radiation pattern from the previous antenna model. The measured and simulated radiation patterns at 4 GHz and 5.8 GHz for both antennas with frequency notched bands at HIPERLAN and WLAN are shown in Figure 5.45 and Figure 5.46, respectively. Both H-planes are omnidirectional with slightly gain decreased at boresight direction. There are more distortions in the measured patterns compared with the simulated ones due to an enhanced perturbing effect on the antenna performance caused by the feeding structure and cable at these frequencies. Though the overall radiation pattern of the antenna has gone through a notable transformation, the H-planes patterns retain a satisfactory omnidirectionality (less than 10 dB gain variation in most directions) over the entire bandwidth in both simulation and experimental.

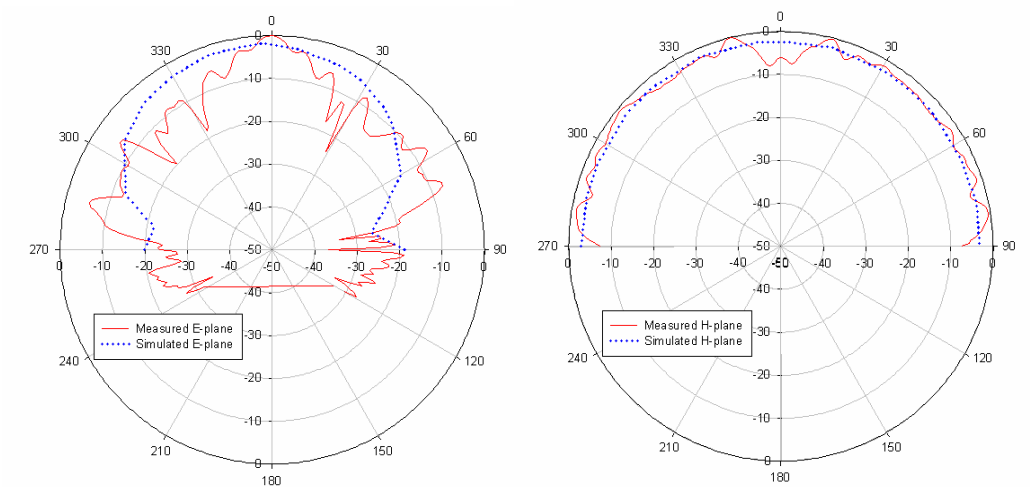

(a)

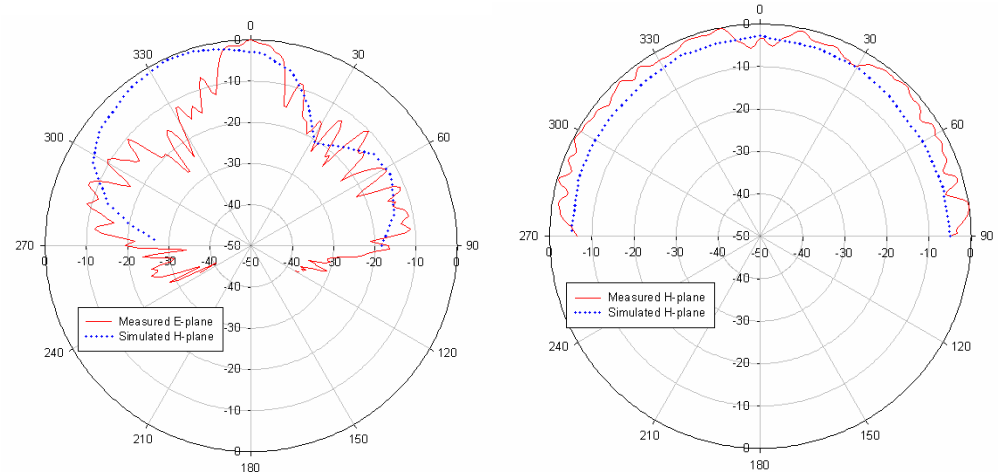

(b)

Figure 5.44: The measured and simulated E and H planes for L and U slotted notched antenna at FWA (a) 4 GHz and (b) 5.8 GHz

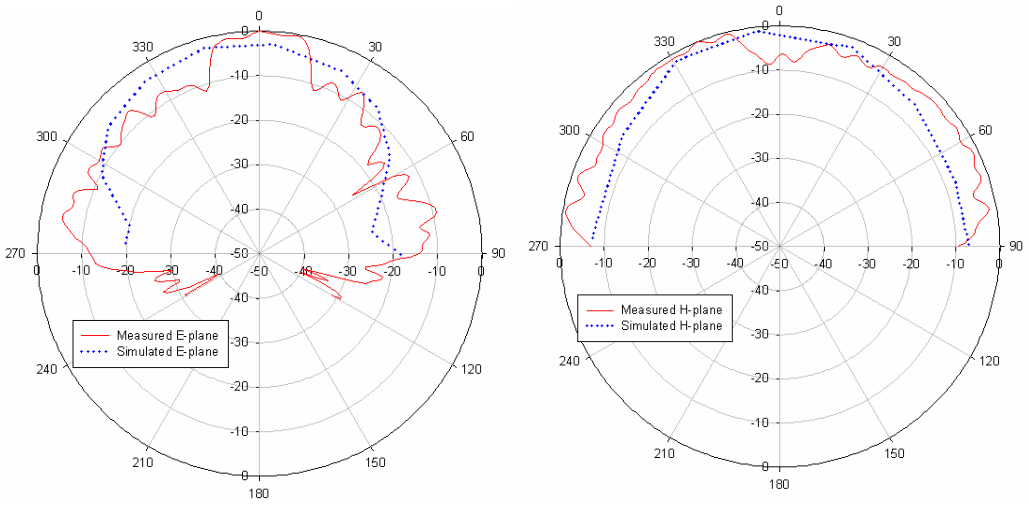

(a)

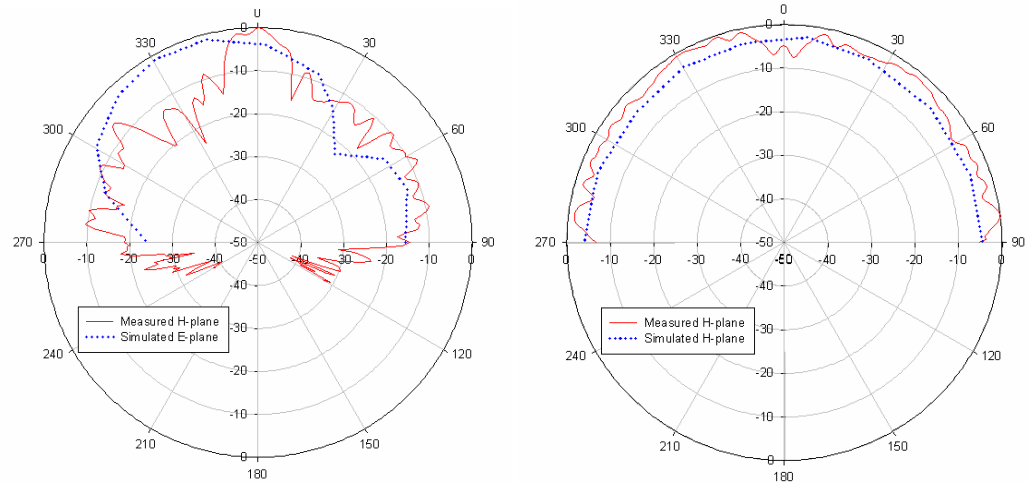

(b)

Figure 5.45: The measured and simulated E and H planes for L and U slotted antenna notched at HIPERLAN: (a) 4GHz and (b) 5.8 GHz

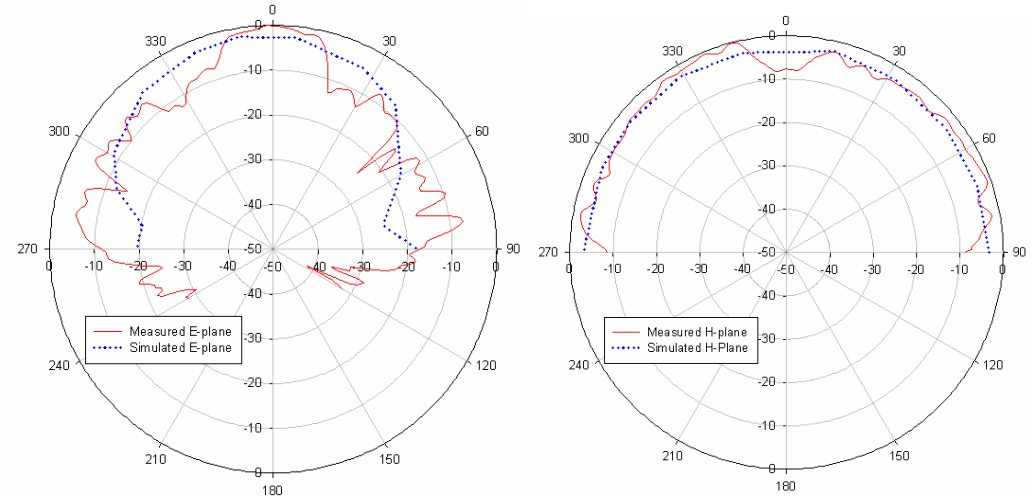

(a)

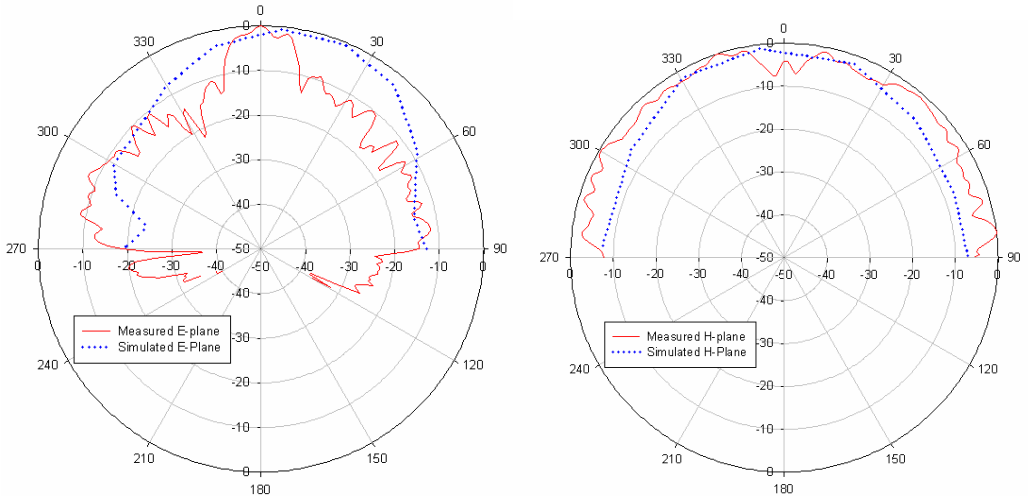

(b)

Figure 5.46: The measured and simulated E and H planes for L and U slotted antenna notched at WLAN: (a) 4 GHz and (b) 5.8 GHz

The 3D radiation patterns are shown in Figure 5.47 to Figure 5.49, respectively for all types of this modified L and U slotted antenna. From the 3D patterns, it is clearly shown that the antennas have omnidirectionality behavior. The patterns are presented from side and top views.

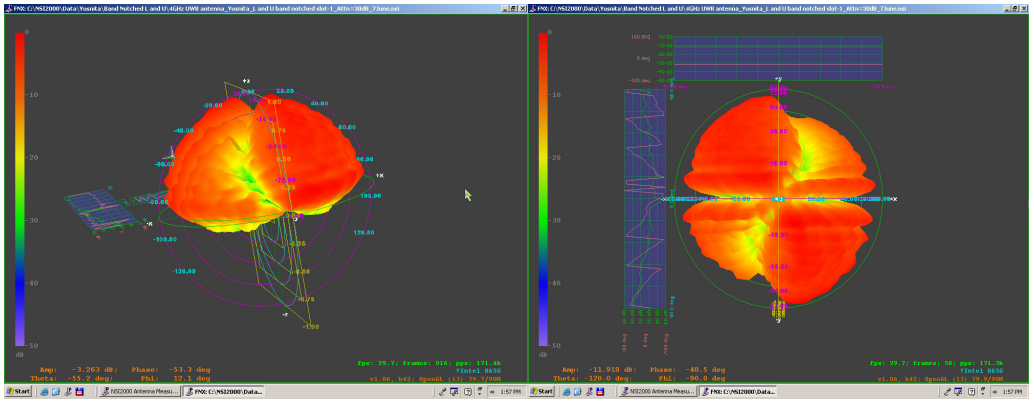

(a)

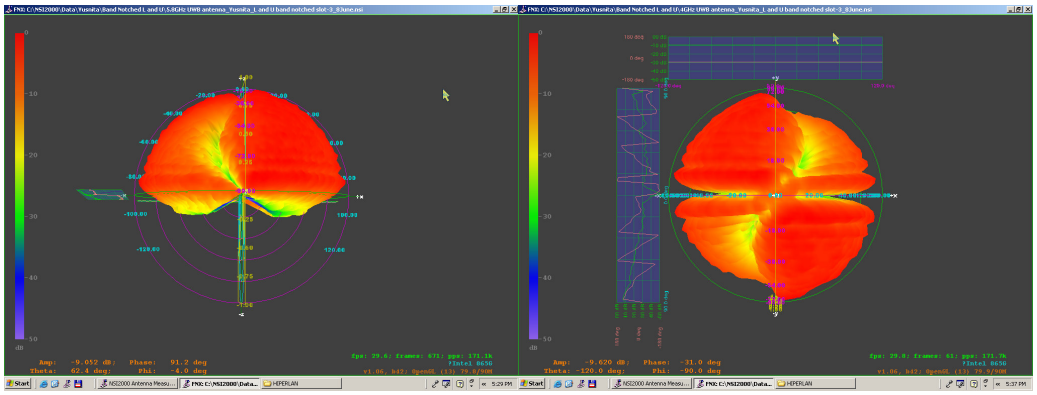

(b)

Figure 5.47: The measured 3D radiation patterns for L and U slotted antenna notched band at FWA: (a) 4 GHz and (b) 5.8 GHz

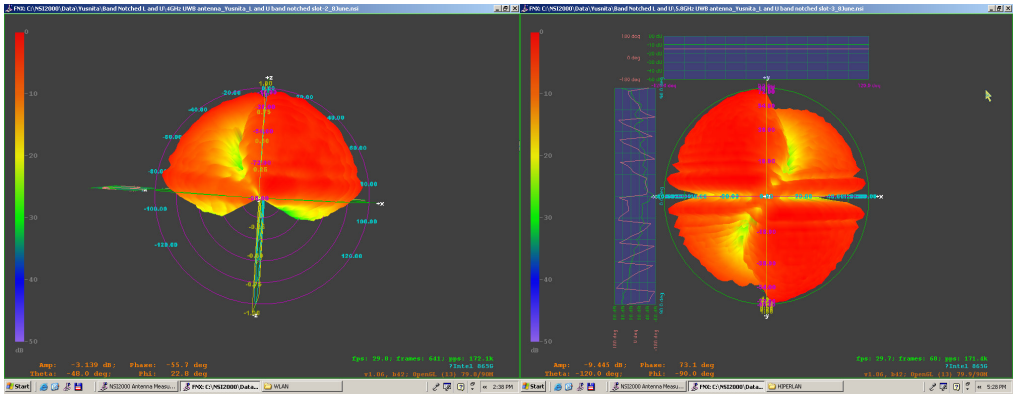

(a)

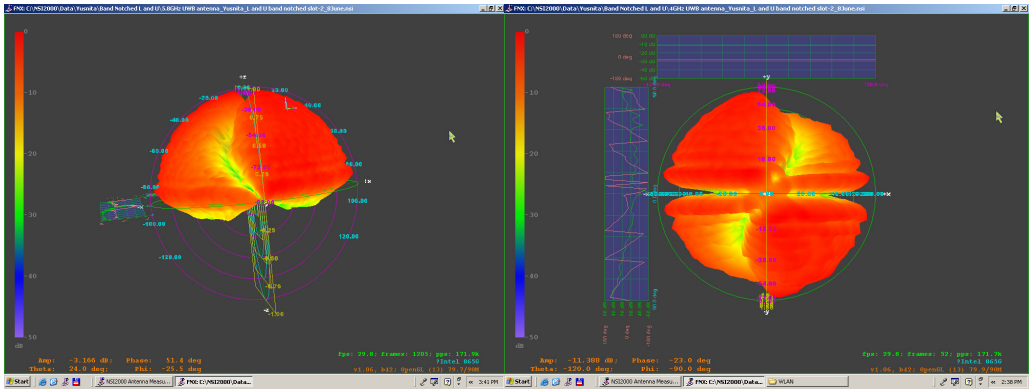

(b)

Figure 5.48: The measured 3D radiation patterns for L and U slotted antenna notched band at HIPERLAN: (a) 4 GHz and (b) 5.8 GHz

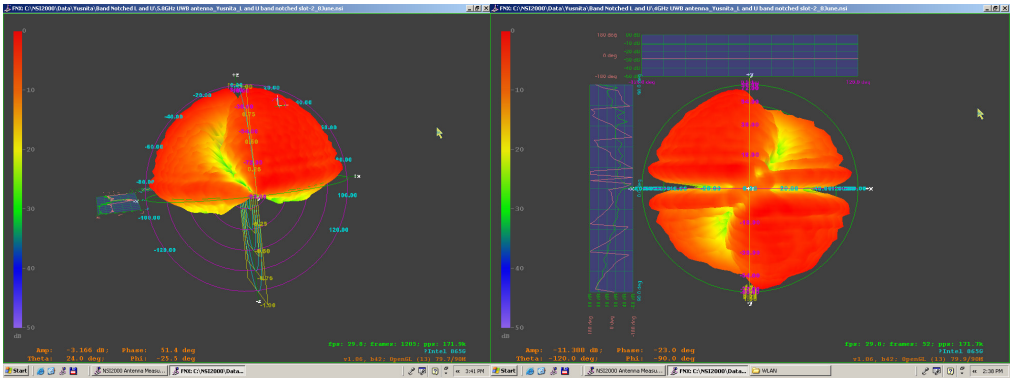

(a)

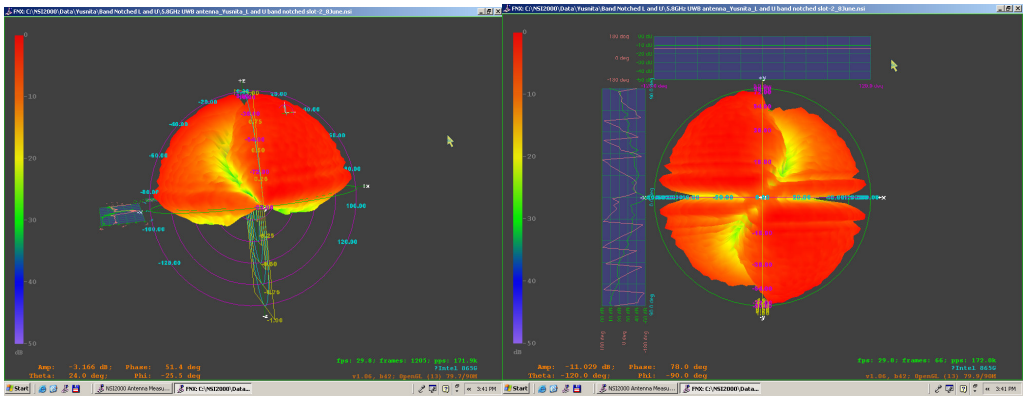

(b)

Figure 5.49: The measured 3D radiation patterns for L and U slotted antenna notched band at WLAN: (a) 4 GHz and (b) 5.8 GHz

5.5 Estimating Error Analysis in Radiation Pattern Measurement

Since the measured radiation patterns obtained have many ripples and dips for the E-planes, the error analysis has been done to estimate the uncertainty and the caused of the error. The development of analysis and measurements to estimate the error during measurement in spherical near-field has been conducted in [156] – [157]. These are summarized in Table 5.5. Each error give affect to the antenna

performance and some corrections have been taken to ensure the correct results achieved.

Table 5.5: Near field error analysis for spherical measurement [156] – [157].

No.	Error terms	Far-field parameters affected
1	Multiple reflection	Gain, side lobe, cross-pol, pointing
2	AUT alignment	Pointing, pattern comparisons
3	Rotator alignment and position errors	Gain, side lobe, cross-pol, pointing
4	Drift correction	Gain, pointing
5	Probe rotary joint	Gain, side lobe, cross-pol, pointing
6	Room scattering	Gain, side lobe, cross-pol, pointing
7	Random errors in amplitude/phase	Gain, side lobe, cross-pol, pointing

Table 5.5 lists the possible errors occur during the measurement procedures. The multiple reflections, rotator alignment, probe rotary joint and room scattering are shown as primary sources of errors that cause degradation in measured radiation pattern.

Multiple reflections between the AUT and probe produce the ripple in the measured data. The correction is difficult to do due to the need a series of near-field measurements at Z-positions separated by λ/8. The far-fields are then calculated for each and averaged [126]. In the case of multiple reflections and random errors, multiple measurements are required.

Figure 5.50 shows the example of the random errors presented during measurement. These measured patterns are from repeated measurement at 5.8 GHz for L and U slotted antenna. Some corrections on the AUT alignments have also been done. From the pattern comparison graphics show the random error occurs in amplitude and phase during multiple measurements.

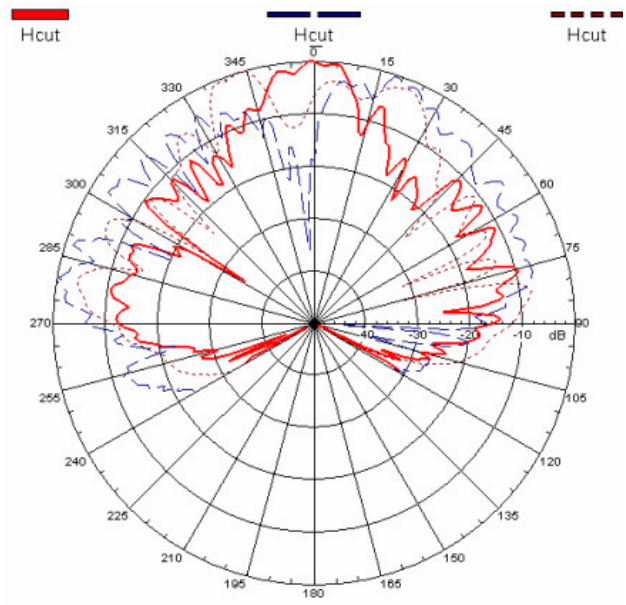

Figure 5.50: An Example of results of random errors for L and U slotted antenna at 5.8 GHz

When the AUT is not precisely aligned to reference coordinate system, vector components or coordinate angles may change for some rotation. This correction can be done by realigned the AUT position.

The rotator alignment for spherical is a special case of position errors. The orthogonallity and intersection of the theta and phi axes and the coincidence of the phi and probe polarization axes can be checked by measuring and comparing near-field cuts at $\theta = 0$ and 180 degrees. The misalignment can be corrected by adjustments of the mechanical system. However, the difference values still present at those near-field cuts of measured data.

The thermal drift during measurements can cause changes in the transmission lines as well as the alignment of the AUT. It is usually have little effect on the far-field patterns.

The probe rotary joints associated with the theta and phi rotators produce some amplitude and phase variations as it is moved and this is as a function of theta and phi. The error can be observed from the measured data by comparing the amplitudes and phases of the two components at (θ, φ) coordinates, (0, 0) and (0,180) [157]. At these points, the amplitude should be identical and the phases should be either identical or 180 degrees different. This error is more important at high frequencies where rotary joints may not be as accurate. From the measured data obtained, it is observed that the variations have presented in amplitudes and phases for those points of both proposed antennas. Thus, this error contributes to the uncertainty in far-field results.

Both probe and room scattering can produce higher spatial frequencies in the data. The smaller data point spacing is needed to avoid the aliasing errors. The room scattering effect can be more severe when low gain AUT's are being measured [157]. In this measurement, the 2^0 data point spacing is used for scanner movement. Scattering from structures and absorber introduces an error that is difficult to estimate. This is because the procedure is demanding and time consuming. The AUT and probe must be translated together in a combination of X, Y and Z movements while maintaining precise angular alignment. The translations should be at least multiple wavelengths in dimension and the AUT must be realigned in the new position. Comparison of the patterns from the two locations provides an estimate of the room scattering but it is difficult to distinguish from alignment differences, probe/AUT multiple reflections and system drift [157].

5.6 Key contributions

The major contributions in the thesis are detailed below:

Firstly, the mechanism which leads to UWB characteristics were proposed based on the further insight of the operations of UWB various monopoles with and without slots. The overlapping of multiple resonances which are evenly and closely spaced accounts for the UWB characteristics. Various slot types are designed by studying their current behaviors, with much effect to the impedance bandwidth. In addition, the UWB antennas designed with novelty slot type has produced a new structure in antenna type.

Secondly, the miniaturization of vertical type T slotted antenna and L and U slotted antenna was realized by narrowing the patch and inserting the slots while retaining the UWB characteristics. The proposed antennas are simple in design, small in size and easy to manufacture. Their sizes are considerable small compared to the existing UWB antenna in the reference listed.

Thirdly, printed two UWB antennas with asymmetry slots were proposed. One is T slotted antenna with slotted ground plane and second is L and U slotted antenna. Both of them feature small size, ease of fabrication, low profile and compatibility with printed circuit board. Both of them are fed by a SMA coaxial port.

Fourthly, six printed reconfigurable UWB slotted antenna were realized. The reconfigurable behaviors on the notched band for each antenna were proposed by varying the length of slots. All proposed antennas exhibits nearly omnidirectional radiation patterns and broad bandwidth.

Lastly, the reconfigurable antenna with notched band at FWA band assigned by MCMC Malaysia is as primary contribution in this type of antenna. This characteristic is obtained with this small slotted UWB antenna by retaining their UWB performance. All of these antennas proposed in the thesis can provide ultra wide bandwidth with nearly omni-directional radiation patterns which make them very suitable for the future UWB applications.

5.7 Summary

This chapter presents the slotted and reconfigurable UWB antenna results with experimental verifications. Both simulated and experimental results are closely to each other. Slotted UWB antennas show a good impedance matching covering the UWB requirements. The reconfigurable characteristic for proposed UWB antennas has been done by inserting the half-wavelength slot to the patch. These proposed types of antennas are variation from the previous models. The reconfigurability behaviors are achieved by shortened or widened the slot. The switching is model as a small patch of 0.7 mm x 1 mm instead of PIN diodes. It has been demonstrated that the measured results closely to the simulated results. Event though the rejected band slightly shifted from the expected one but it still covers the frequency range.

The radiation patterns are also studied for notched band characteristics. It is found that the notched bands do not give any significant effect to the antenna radiation performance. The uncertainties due to errors in measurements are also presented as ripples in the patterns.

The imperfect of the anechoic chamber system cause some ripples occurring in the measured radiation patterns. This is due to many reflections absorbed from surrounding. Analysis on possible errors occurred during measurement has been done. The measured relative gain for slotted UWB antennas are given from the H-plane plots of measured radiation patterns. The simulated gain and directivity for both antennas are also presented as well. Thus, these antennas are very promising for UWB application which is small, compact and has a good performance.

CHAPTER 6

CONCLUSIONS AND FUTURE WORKS

6.1 Conclusions

The UWB technology will be the key solution for the future WPAN systems. This is due to its ability to achieve very high data rate which results from the large frequency spectrum occupied. Besides, extremely low power emission level will prevent UWB systems from causing severe interference with other wireless systems. As the only non-digital part of a UWB system, antenna remains as a particular challenging topic because there are more stringent requirements for a suitable UWB antenna compared with a narrowband antenna. Therefore, the antenna design and analysis for UWB systems were carried out in this thesis.

Rectangular planar monopole antenna is chosen as conventional structure, this is due to a simple structure, low profile, easy to fabricate and UWB characteristics with nearly omni-directional radiation patterns. T slotted antenna and L and U slotted antenna originates from a conventional rectangular monopole by modifying the bottom patch with beveling and notches. Various antenna configurations with various forms of notch and bevel have also analyzed in order to form the novelty structure. Slots insertion and truncation ground plane are added to further improve the impedance bandwidth.

Studies indicate that the UWB characteristic is obtained by proper selection in the size of notch and bevel and the distance between the bottom patch to the ground plane. In a broad sense, the ground plane serves as an impedance matching circuit, and it tunes the input impedance and hence changes the operating bandwidth when the feed gap is varied. Therefore, it is essential to design a smooth transition between the feeding line and the antenna for good impedance matching over the entire operational bandwidth.

Investigations have also been carried out in this thesis to analyze the current distribution of antennas. The dimension of the antenna also has an impact on the antenna performance because the current is mainly distributed along the edge on the antenna. Thus, it will be possible to fix which elements will act on each characteristic. By varying the edges closed to the feeding point means modifying the current path on the antenna. In addition, the current distributions along the neutral zone do not much influence to the antenna performance, due to the current levels are not too strong. Consequently, antenna with neutral zone slot insertion exhibits the similar characteristics as its antenna without neutral zone slot, as long as the size and the position of the neutral zone are precisely determined.

The current distributions on various slots of rectangular with two notches and pentagonal antennas have investigated in this thesis. It is shown that with increasing the frequency the current much concentrated along the slot edges. The slot also appears to introduce a capacitive reactance which counteracts the inductive reactance of the feed. Thus, the slot wideband behavior is due to the fact that the currents along the edges of the slot introduce the same resonance frequencies, which, in conjunction with the resonance of the main patch, produce an overall broadband frequency response characteristic.

The T slotted antenna with slotted ground plane has shown the return loss varies from -15 dB to -20 dB. However, during fabrication process, the slightly shifted impedance bandwidth has occurred. This is due to the antenna with slotted ground plane need very accuracy in alignment between the slotted ground plane and patch on both sided of substrate. The distance of patch to the ground plane is also very small of 0.5 mm, where is this distance as the impedance matching.

L and U slotted antenna has performed UWB characteristics with feed gap of 1.5 mm to the ground plane. Adding slotted ground plane to this antenna did not give any improvement to the bandwidth. Therefore, in this antenna, the slotted ground plane is out of design consideration. From the measurement results, T slotted antenna and L and U slotted antenna have shown much closed to the simulated one in terms of the return loss and radiation patterns. Ripples and dips occur on the patterns are due to the uncertainties caused by any errors during measurement. However, the omnidirectional patterns exhibit for the H-planes, and the E-planes are relative broad over the entire bandwidth. It has been shown that the operating bandwidth meets the FCC requirements.

Reconfigurable UWB antennas with band notched characteristics have been investigated. There are three models resulted for each antenna model, T slotted antenna and L and U slotted antenna. The VSWR, radiation patterns and gain are evaluated. Three notched bands required are FWA assigned by MCMC, HIPERLAN, and WLAN. This thesis primary contributes to design and develop UWB antenna with notched band at FWA assigned by MCMC Malaysia. By modifying the length of slots, the required notched bands are obtained. The measured radiation patterns show agree well with the simulated one.

6.2 Future Work

Based on the conclusions drawn and the limitations of the work presented, future work can be carried out in the following areas:

Firstly, it has been shown that both UWB antennas with asymmetry slots operate over UWB bandwidth. A more detailed understanding of the current distribution mode mechanism and the impedance variations caused by the asymmetry slot could lead to improved design of UWB antennas.

Secondly, further study is also needed for this proposed UWB antenna with different feeding applied, such as coplanar waveguide (CPW). This is useful for the

future antenna design, in order to reduce the error due to misalignment between patch and ground plane printed on both substrates during fabrication process.

Thirdly, in this thesis, all of the antenna measurements are carried out inside an anechoic chamber. However, imperfect existing antenna holder and far field measurement systems have led degradation to the radiation patterns. Because of this antenna is very small, it needs special handling in measurement procedures to avoid multiple reflections from other sources.

Fourthly, in the future UWB systems, antenna might be embedded inside a laptop or other devices. Thus, the devices' effects on the antenna performances need to be investigated. When the antenna is built on a portable device, the impact from human body should also be considered.

Fifthly, to ensure the performance of UWB antenna, time domain measurement needs to be evaluated. This is to evaluate how good this antenna transmits or received the pulse without any distortion and delay.

Sixthly, UWB systems operate at extremely low power level which limits its transmission range. In order to enhance the quality of the communication link and improve channel capacity and range, directional systems with high gain are required for some applications. Therefore, research on UWB directional antenna and antenna array could be carried out.

Seventhly, inserting the real PIN diodes into antenna structure need to be developed to ensure the antennas have the required notched bands. A more studies on electronic drive circuit and the effect of switching to the electromagnetic waves on antenna need to be investigated. A programmed microcontroller to control the current source of PIN diodes is needed in order to randomly on/or state the switching.

Lastly, gain measurement need to be carried out to complete the overall performance of UWB antennas.

REFERENCES

1. Celine Foong Leng Lew. *Inverted Trapezoidal Antenna for Pulsed Application*. B.Eng. Thesis. The University of Queensland; 2003.
2. I. Oppermann, M. Hamalainen and J. Iinatti. *UWB Theory and Applications*. John Wiley & Sons Ltd. 2004.
3. Pulse LINK, Inc. http://www.fantasma.net
4. Federal Communications Commission (FCC). *Revision of Part 15 of the Commission's Rules Regarding Ultra-Wideband Transmission Systems*. First Report and Order, ET Docket 98-153, FCC 02-48. April, 2002. http://www.fcc.gov
5. Zhi Ning Chen et al. Considerations for Source Pulses and Antennas in UWB Radio Systems. *IEEE Transactions on Antennas and Propagation*. July, 2004. Vol. 52(7).
6. Liang Jianxin. *Antenna Study and Design for Ultra Wideband Communication Applications*. Ph.D. Thesis. Queen Mary, University of London; 2006.
7. M. A. Peyrot Solis, G. M. Galvan Tejada, and H. Jardon Aguilar. State of the Art in Ultra-Wideband Antennas. *2nd International Conference on Electrical and Electronics Engineering (ICEEE) and XI Conference on Electrical Engineering (CIE 2005)*. Mexico City, Mexico. September 7-9, 2005. 101 – 105.
8. Kamya, Y.Y., and Ryuji Kohno. Ultra Wideband Antenna. *IEEE Radio Communications*. June, 2004.
9. J. F. Zurcher and F. E. Gardiol. Broadband Patch Antenna. Norwood, MA: Artech House. 1995.
10. R. Garg *et al*. *Microstrip Antenna Design Handbook.* Ed. Artech House. 2001.
11. Albert K. Y. Lai *et al*. A Novel Antenna for Ultra-Wideband Application. *IEEE Transactions on Antennas and Propagation*. July, 1992. Vol. 40(7).

12. Seok H. Choi *et al*. A New Ultra-Wideband Antenna for UWB Application. *Microwave and Optical Technology Letters*. March 5, 2004. Vol. 40(5).
13. E. Guillanton *et al.* A New Design Tapered Slot Antenna for Ultra-Wideband Applications. *Microwave Opt. Technol. Lett*. 1998. Vol. 19: 286-289.
14. N. P. Agrawall, G. Kumar, and K. P. Ray. Wide-Band Planar Monopole Antennas. *IEEE Transactions on Antennas and Propagation*. Feb., 1998. Vol. 46(2): 294-295.
15. Chun Yih Wu, Chia Lun Tang and An Chia Chen. UWB Chip Antenna Design using LTCC Multilayer Technology for Mobile Applications. *Asia Pacific Microwave Conference (APMC)*, Dec 4-7, 2005. Suzhou, China. 2005.
16. Zhi Ning Chen *et al*. *Planar Antennas*. IEEE Microwave Magazine. December, 2006.
17. T. Yang and W. A. Davis. Planar Half-Disk Antenna Structures for Ultra Wideband Communications. *IEEE Antenna Propagat. Soc. Int. Symp. Dig*. 2004. Vol. 3: 2508-2511.
18. S. H. Lee, J. K. Park, and J. N. Lee. A Novel CPW-Fed Ultra Wideband Antenna Design. *Microwave Opt. Technol. Lett*. 2005. Vol. 44: 393-396.
19. K. L. Wong, T. C. Tseng, and P. L. Teng. Low Profile Ultra Wideband Antenna for Mobile Phone Applications, *Microwave Opt. Technol. Lett*. 2004. Vol. 43: 7-9.
20. Ian Oppermann. *The Role of UWB in 4G, Wireless Personal Communication*. Kluwer Academic Publishers. 2004. 121-133.
21. Haruki Kamiya *et al*. Evaluation of Interference between MB-OFDM UWB and WLAN Systems using a GTEM Cell. *2008 Asia-Pacific Symposium on Electromagnetic Compatibility & 19th International Zurich Symposium on Electromagnetic Compatibility.* Singapore. May 19-22, 2008. 100 – 103.
22. M. Yamada et al. Evaluation of Electromagnetic Interference between UWB System and WLAN using GTEM Cell. *IEEE International Electromagnetic Compatibility Symposium.* July, 2007.
23. Kenneth C. L. Chan and Yi Huang. A Compact Semi-Circular Disk Dipole with Notched Band for UWB applications. *The Institution of Engineering and Technology Seminar on Ultra Wideband Systems, Technologies and Applications*. 2006. 226-230.

24. Kyungho Chung, Jaemoung Kim, and Jaehoon Choi. Wideband Microstrip-Fed Monopole Antenna Having Frequency Band Notch Function. *IEEE Microwave and Wireless Components Letters.* November, 2005. Vol. 15(11).
25. H. G. Schant, G. Wolenec, and E. M. Myszka. Frequency Notched UWB Antenna. *Proc. IEEE Conference on Ultra Wideband Sys and Tech*. 2003. 214-218.
26. Y. Kim and D. H. Kwon. CPW-Fed Planar Ultra-Wideband Antenna Having a Frequency Band Notch Function. *Electronics Letters*. April, 2004. Vol. 40(7): 403-405.
27. S. W. Su, K. L. Wong, and F. S. Chang. Compact Printed Ultra-Wideband Slot Antenna with a Band Notched Operation. *Microwave & Optical Techni. Letters*. April, 2005. Vol. 45(2): 128-130.
28. W. Choi *et al*. Compact Ultra-Wideband Printed Antenna with Band Rejection Characteristics. *Electronics Letters*. September, 2005. Vol. 41(18): 990-991.
29. Yongjin Kim, and Do Hoon Kwon. Planar Ultra Wideband Slot Antenna with Frequency Band Notch Function, *Antennas and Propagation Society International Symposium*. IEEE. 2004.
30. H. Yoon *et al*. A Study of the UWB Antenna with Band Rejection Characteristic. *Proc. IEEE APS Int. Symp*. June, 2004. 1784-1787.
31. S. Y. Suh *et al*. A UWB Antenna with a Stop-Band Notch in the 5 GHz WLAN Band. *Proc. IEEE/ACES International Conference*. April, 2005. 203-207.
32. W. J. Lui *et al*. Frequency Notched Ultra-Wideband Microstrip Slot Antenna with Fractal Tuning Stub. *Electronics Letters*. March, 2005. Vol. 41(6): 294-296.
33. K. H. Kim *et al*. Band-Notched UWB Planar Monopole Antenna with Two Parasitic Patches. *Electronics Letters*. July, 2005. Vol. 41(14): 783-785.
34. W. J. Lui, C. H. Cheng, and H. B. Zhu. Frequency Notched Printed Slot Antenna with Parasitic Open-Circuit Stub. *Electronics Letters*. September, 2005. Vol. 41(20): 1094-1095.
35. Zhi Ning Chen, Terence S. P. See, and Xianming Qing. Small Ground-Independent Planar UWB Antenna. *Antennas and Propagation Society International Symposium 2006.* IEEE. 2006.1635-1638.
36. N. Askar. Overview of General Atomics PHY Proposal to the IEEE 802.15.3a. *IEEE P 802.15*. March, 2003.

37. R. J. Fontana. Recent System Applications of Short-Pulse UWB Technology. *IEEE Transactions on Microwave Theory and Techniques*. September, 2004. Vol. 52(9): 2087-2104.

38. R. J. Fontana. *A Brief History of UWB Communications*. Multispectral Solutions Inc. Kluwer Academic/Plenum Publishers. 2000. http://www.multispectral.com/history.html

39. Harmuth, H. F. *Transmission of Information by Orthogonal Functions*. 2nd. ed. New York: Springer. 1969.

40. Harmuth, H. F. *Transmission of Information by Orthogonal Functions*, 3rd. ed. New York: Springer. 1972.

41. Harmuth, H. F. Range-Doppler Resolution of Electromagnetic Walsh Waves in Radar. *IEEE Transactions on Electromagnetic Compatibility*. EMC-17.1975. 106-111.

42. Harmuth, H. F. Selective Reception of Periodic Electromagnetic Waves With General Time Variation. *IEEE Transactions on Electromagnetic Compatibility*. EMC-19. 1977. 137-144.

43. Harmuth, H. F. *Sequency Theory*. New York: Academic Press. 1977.

44. Harmuth, H. F. *Nonsinusoidal Waves for Radar and Radio Communication*. New York: Academic Press. 1981.

45. Harmuth, H. F. *Antennas and Waveguides for Nonsinusoidal* Waves. New York: Academic Press. 1984.

46. Robbins, K.W. *Short Baseband Pulse Receiver*. U. S. Patent 3,662,316. May 9, 1972.

47. Robbins, K.W., and Robbins, G. F. *Stable Baseband Super Regenerative Selective Receiver*. U. S. Patent 3,794,996. Feb. 26, 1974.

48. Ross, G. F. *Transmission and Reception System for Generating and Receiving Baseband Duration Pulse Signals for Short Baseband Pulse Communication System*. U. S. Patent 3,728,632. Apr. 17, 1973.

49. Ross, G. F. *Energy Amplifying Selector Gate for Baseband Signals*. U. S. Patent 3,750,025. July 31, 1973.

50. Ross, G. F., and Lamensdorf, D. *Balanced Radiator System*. U. S. Patent 3,659,203. Apr. 25, 1972.

51. Ross, G. F., and Mara, R. M. *Coherent Processing Tunnel Diode Ultra Wideband Receiver*. U. S. Patent 5,337,054. Aug. 9, 1994.

52. Ross, G. F., and Robbins, K.W. *Baseband Radiation and Reception System.* U. S. Patent 3,739,392. June 12, 1973.
53. Ross, G. F., and Robbins, K.W. *Narrow Range-Gate Baseband Receiver.* U. S. Patent 4,695,752. Sep. 22, 1987.
54. Morey, R. N. *Geophysical Survey System Employing Electromagnetic Impulse.* U. S. Patent 3,806,795. April, 1974.
55. Kazimierz Siwiak and Debra Mc. Keown. *Ultra-Wideband Radio Technology*. John Wiley & Sons, Ltd. 2004.
56. Domenico Porcino. UWB Regulations & Coexistence: From the FCC First Report and Order to the Path to Approval in Europe. *Tutorial at International Workshop on Ultra Wideband Systems*. June, 2003. Oulu, Finland. 2003.
57. European Telecommunications Standards Institute (ETSI). *Technical Report, Technical Characteristics for Short Range Devices Communication Equipment using Ultra-Wideband Technology.* TR 101 994-1, V1.0.0. August, 2003.
58. Hailiang Mei. *Modeling and Performance Evaluation of a BPPM UWB System.* Msc. Thesis. Delf University of Technology; July 2003.
59. Nicholas Cravotta. Ultrawideband: The Next Wireless Panacea. October 17, 2002. EDN. www.edn.com
60. Electronic Communications Committee (ECC) Report 64. *The Protection Requirements of Radio Communications Systems below 10.6 GHz from Generic UWB Applications*. February, 2005.
61. William Webb. Ultra Wideband-The Final Few Regulatory Processes. *2006 IET Seminar on Ultra Wideband Systems, Technologies and Applications*. London, U. K. April, 2006.
62. Ryuji Kohno and Kenichi Takizawa. Overview of Research and Development Activities in NICT UWB Consortium. 2005 *IEEE International Conference on Ultra-Wideband*. Zurich, Switzerland. September 5-8, 2005. 735-740.
63. Hans Gregory Schantz. A Brief History of UWB Antennas. *IEEE Aerospace and Electonics System Magazine.* Vol; 19 (4): 22-26. April, 2004.
64. Alexander Vorobyov. *Planar Elliptically Shaped Dipole Antenna for UWB Impulse Radio*. Ph.D. Thesis. Delf Technical University, Netherlands; 2008.
65. P. S. Carter. *Short Wave Antenna*. U. S Patent 2,175,252. October 10, 1939.
66. P. S. Carter. *Wide Band, Short Wave Antenna and Transmission Line System.* U. S Patent 2,181,870. December 5, 1939.

67. Stratton and Chu. *Journal of Applied Physics*. March, 1941.

68. S. Ramo and J. R. Whinnery. *Fields and Waves in Modern Radio*. New York. 1944. 480-482.

69. W. L. Stutzman and G. A. Thiele. *Antenna and Theory and Design*. 2nd. ed. New York: John Wiley & Sons. 1998.

70. Schelkunoff. *Electromagnetic Waves*. Van Nostrand, 1943.

71. Johnna Powel. *Antenna Design for Ultra wideband Radio*. MSc Thesis. Massachusetts Institute of Technology (M. I. T); May 7, 2004.

72. V. H. Rumsey. Frequency Independent Antennas. *1957 IRE National Convention.* 1957.

73. J. D. Dyson. The Equiangular Spiral Antenna. *IRE Transactions on Antennas & Propagations*. April, 1959. Vol. AP-7: 181-187.

74. M. Kanda. Transients in a Resistively Loaded Linear Antennas Compared with those in a Conical Antenna and a TEM Horn. *IEEE Transactions on Antennas and Propagations.* Jan, 1980. Vol. 28(1): 132–136.

75. K. L. Shlager, G. S. Smith, and J. G. Maloney. Accurate Analysis of TEM Horn Antennas for Pulse Radiation. *IEEE Trans. Electromagn. Compat.* Aug., 1996. Vol. 38(3): 414–423.

76. B. Scheers, M. Acheroy, and A. Vander Vorst. Time-Domain Simulation and Characterisation of TEM Horns using a Normalised Impulse Response. *Proc. Inst. Elect. Eng. Microw. Antennas Propagat.* Dec., 2000. Vol. 147(6): 463–468.

77. L. T. Chang and W. D. Burnside. An Ultrawide-Bandwidth Tapered Resistive TEM Horn Antenna. *IEEE Trans. Antennas Propagat.* Dec., 2000. Vol. 48(12): 1848–1857.

78. Jennifer T. Bernhard. *Reconfigurable Antenna*. Morgan & Claypool Publisher. 2007.

79. R. T. Lee and G. S. Smith. On The Characteristic Impedance of the TEM Horn Antenna. *IEEE Trans. Antennas Propagat.* Jan., 2004. Vol. 52(1): 315–318.

80. P. E. Mayes. Frequency-Independent Antennas and Broad-band Derivatives thereof. *Proceeding of The IEEE.* Jan., 1992. Vol. 80(1): 103–112.

81. T. W. Hertel and G. S. Smith. On the Dispersive Properties of the Conical Spiral Antenna and Its Use for Pulsed Radiation. *IEEE Trans. Antennas Propagat.* July, 2003. Vol. 51(7): 1426–1433.

82. T. T. Wu and R.W. P. King. The Cylindrical Antenna with Non-Reflecting Resistive Loading. *IEEE Trans. Antennas Propagat.* May, 1965. Vol. 13(3): 369–373.

83. D. L. Senguta and Y. P. Liu. Analytical Investigation of Waveforms Radiated by a Resistively Loaded Linear Antenna Excited by a Gaussian Pulse. *Radio Sci.* June, 1974. Vol. 9(3): 621–630.

84. J. G. Maloney and G. S. Smith. A Study of Transient Radiation from the Wu-King Resistive Monopole-FDTD Analysis and Experimental Measurements. *IEEE Trans. Antennas Propagat.* May, 1993. Vol. 41(5): 668–676.

85. R. H. Duhamel. *Dual Polarized Sinuous Antennas*. U. S. Patent 4,658,262. April 14, 1987.

86. S. Honda *et al*. A Disc Monopole Antenna with 1:8 Impedance Bandwidth and Omni-Directional Radiation Pattern. *Proceedings of the 1992 ISAP*. September 1992. Sapporo, Japan. 1992. 1145-1148.

87. P. P. Hammoud and F. Colomel. Matching the Input Impedance of a Broadband Disc Monopole. *Electronics Letters*. Feb., 1993. Vol. 29: 406-407.

88. J. A. Evans and M. J. Ammann. Planar Trapezoidal and Pentagonal Monopoles with Impedance Bandwidth in Excess of 10:1. *IEEE International Symposium Digest*. 1999. Orlando. Vol. 3: 1558-1559.

89. R. M. Taylor. A broadband Omni-Directional Antenna. *IEEE Antennas and Propagation Society International Symposium Digest*. June, 1994. Vol. 2: 1294–1297.

90. Anatoliy Boryssenko. Time Domain Studies of Ultra Wideband Antennas. *Proceedings of the 1999 IEEE Canadian Conference on Electrical and Computer Engineering*. May 9-12, 1999. Shaw Conference Center, Edmonton, Alberta, Canada. IEEE. 1999.

91. J. R. Nealy. *Foursquare Antenna Radiating Element*. U. S. Patent 5,926,137. July 20, 1999. VTIP Ref. 96-056. http://www.vtip.org

92. Randall Nealy *et al*. *Improvements to the Foursquare Radiating Element-Trimmed Foursquare*. U. S. Patent 6,057,802. May 2, 2000. VTIP Ref. 98-001. http://www.vtip.org

93. M. Z. Win and R. A. Scholtz. Impulse Radio: How It Works. *IEEE Comm. Letters*. January, 1998. Vol. 2(1): 36-38.

94. J. Joe. Cellonics UWB Pulse Generators. *International Workshop on Ultra Wideband Systems*. June, 2003. Oulu, Finland. 2003.

95. http://cpk.auc.dk/FACE/overview.html

96. C. L. Bennett and G. F. Ross. Time-Domain Electromagnetic and Its Applications. *Proceedings of The. IEEE*. March, 1978. Vol. 66(3): 299-318.

97. J. D. Taylor. *Introduction to Ultra-Wideband Radar Systems*. Boca Raton: CRC Press. 1995.

98. J. D. Taylor. Ultra-Wideband Radar Technology. Boca Raton: CRC Press. 2001.

99. R. Fontana. Recent Advances in Ultra Wideband Communications Systems. *IEEE Conference on Ultra Wideband Systems and Technologies (UWBST)*. May, 2002.

100. K. Siwiak. Ultra-Wide Band Radio: Introducing a New Technology. *IEEE Vehicular Tech. Conference (VTC)-Plenary session*. May, 2001.

101. K. Siwiak. Ultra-Wide Band Radio: The Emergence of an Important RF Technology. *Proc. IEEE Vehicular Tech. Conference (VTC)*. May, 2001.

102. J. Farserotu *et al*. UWB Transmission and MIMO Antenna Systems for Nomadic User and Mobile PAN. *Wireless Personal Communications*. 2002. Vol. 22: 197-317.

103. Hans Gregory Schantz. Plenary Talk: Introduction to Ultra Wideband Antennas. *IEEE UWBST*. November, 2003.

104. K. Siwiak. Impact of UWB Transmission on Generic Receiver. *Proc. IEEE Vehicular Tech. Conference (VTC)*. May, 2001.

105. Kazuhiro Hirasawa and Misao Haneishi. Analysis, Design, and Measurement of Small and Low Profile Antennas. Boston, London: Artech House. 1992.

106. Giuseppe Ruvio and Max. J. Ammann. A Novel Small Wideband Monopole Antenna. *LAPC 2006*. April 11-12, 2006.

107. Hassan Ghannoum, Serge Bories, and Raffaele D'Errico. Small Size UWB Planar Antenna and Its Behaviour in WBAN/WPAN Applications. *IET seminar on Ultra wideband System, Technologies and Applications.* April, 2006.

108. Serge Boris, Christophe Roblin, and Alan Sibille. Dual Stripline Fed Metal Sheet Monopoles for UWB Terminal Applications. *ANTEM*. Saint Malo, France. June 15-17, 2005.

109. T. Huynh and K. F. Lee. Single-Layer Single-Patch Wideband Microstrip Antenna. *Electronics Letters*. August 3, 1995. Vol. 31(16).

110. Mayhew Ridgers, G. Wideband Probe-Feed Microstrip Patch Antennas and Modeling Techniques. Ph.D Thesis. University of Pretoria; 2004.

111. Y.X. Guo *et al*. Double U-Slot Rectangular Patch Antenna. *Electronics Letters*. September 17, 1998. Vol. 34(19).

112. A. A. Eldek. Numerical Analysis of a Small Ultra Wideband Microstrip-Fed Tap Monopole Antenna. *Progress in Electromagnetic Research*, PIER 65. 2006. 59-69.

113. Moteco Group website. *Antenna Basics*. http://www.moteco.com

114. F. T. Ulaby. *Fundamentals of Applied Electromagnetic*. 2nd. ed. Prentice Hall. 1999.

115. Constantine A. Balanis. *Antenna Theory: Analysis and Design*. 2nd. ed. John Wiley & Sons, Inc. 1997.

116. Antenna Standards Committee of the IEEE Antennas and Propagation Society. *IEEE Standard Definitions of Terms for Antennas*. IEEE std. 145-1993. New York: The Institute of Electrical and Electronics Engineers Inc. 1993.

117. Hans Gregory Schantz. Dispersion and UWB Antennas. *IEEE IWUWBS/*UWBST. May, 2004.

118. Guofeng Lu, Predrag Spasojevic, and Larry Greenstein. *Antenna and Pulse Designs for Meeting UWB Spectrum Density Requirements*. WINLAB, ECE Department, Rutgers University.

119. Debatosh Guha. Broadband Design of Microstrip Antenna: Recent Trends and Developments. *Facta Universitatis, series: Mechanics, Automatic Control and Robotics.* 2003. Vol. 3(15): 1083-1088.

120. Marta Cabedo Fabres *et al. On The Influence of the Shape of Planar Monopole Antennas in the Impedance Bandwidth Performance*. International Union of Radio Science (URSI). 2005.

121. M. J. Ammann and Z. N. Chen. A Wideband Shorted Planar Monopole with Bevel. *IEEE Trans. Antennas and Propagat*. 2003. Vol. 51(4): 901-903.

122. M. J. Ammann and Z. N. Chen. An Asymmetrical Feed Arrangement for Improved Impedance Bandwidth of Planar Monopole Antennas. *Microw. Opt. Tech. Letters*. 2004. Vol. 40(2): 156–159.

123. M. J. Ammann. Control of the Impedance Bandwidth of Wideband Planar Monopole Antennas using a Beveling Technique. *Microw. Opt. Tech. Letters*. July, 2001. Vol. 30(4): 229–232.

124. A. Cai, T. S. P. See, and Z. N. Chen. Study of Human Head Effects on UWB Antenna. *in Proc. IEEE Intl. Workshop on Antenna Technology (iWAT)*. Singapore. Mar. 7–9, 2005. 310–313.

125. E. Lee, P. S. Hall, and P. Gardner. Compact Wideband Planar Monopole Antenna. *Electron. Let.* Dec., 1999. Vol. 35(25): 2157–2158.

126. E. Antonino-Daviu *et al*. Wideband Double-Fed Planar Monopole Antennas. *Electron. Lett.* Nov., 2003. Vol. 39(23): 1635–1636.

127. Z. N. Chen *et al.* Circular Annular Planar Monopoles with EM Coupling. *Proc. Inst. Elect. Eng. Microw Antennas, Propagat.* Aug., 2003. Vol. 150(4): 269–273.

128. Christophe Roblin *et al*. Antenna Design, Analysis and Numerical Modeling for Impulse UWB. *International Symposium on Wireless Personal Multimedia Communication (WPMC) 2004 (Ultrawaves invited communication)*. Abano Terme, Italy. Sept. 12–15, 2004.

129. E. Antonino-Daviu *et al*. Wideband Double–Fed Planar Monopole Antennas. *Electronics Letters*. September 13, 2003. Vol. 39(23).

130. Eva Antonino *et al*. Design of Very Wide-Band Linear-Polarized Antennas. Zeland Publication. 2004.

131. E. Gueguen, F. Thudor, and P. Chambelin. A Low Cost UWB Printed Dipole Antenna with High Performance. *IEEE International Conference on Ultra Wideband (ICU)*. Zurich. Sept. 5-8, 2005.

132. Z. N. Chen, M. Y. W. Chia, and M. J. Ammann. Optimization and Comparison of Broadband Monopoles. *IEE Proc. Microw. Antenna Propag*. December, 2003. Vol. 150(6): 429-435.

133. Daniel Valderas *et al*. Design of UWB Folded-Plate Monopole Antennas Based on TLM. *IEEE Transactions on Antennas and Propagation.* June, 2006. Vol. 54(6): 1676-1687.

134. A. J. Kerkhoff. The Use of Genetic Algorithm Approach in the Design of Ultra-Wide Band Antennas. *Proceedings of IEEE Radio and Wireless Conference (RAWCON) 2001*. Boston, MA. August 19-22, 2001.

135. R. Holtzman *et al*. Ultra Wideband Antenna Design Using the Green's Function Method (GFM) ABC with Genetic Algorithm. *Antennas and Propagation Society International Symposium*. IEEE. 2001.

136. A. J. Kerkhoff, Robert L. Rogers, and Hao Ling. Design and Analysis of Planar Monopole Antennas Using a Genetic Algorithm Approach. *IEEE Transactions on Antennas and Propagation*. October, 2004. Vol. 52(10): 2709-2718.

137. Shaqiu Xiao *et al*. Reconfigurable Microstrip Antenna Design Based on Genetic Algorithm. *Antennas and Propagation Society International Symposium*. IEEE. 2003.

138. H. Choo and H. Ling. Design of Broadband and Dual-Band Microstrip Antennas on a High-Dielectric Substrate Using a Genetic Algorithm. *IEE Proc. Microwave Antenna Propagation*. June, 2003. Vol. 150(3).

139. Boti, M., Dussopt, L., and Laheurte, J. M. Circularly Polarized Antenna with Switchable Polarization Sense. Aug., 2000. *Electronics Letters*. Vol. 36: 1518-1519.

140. Nikolau, S. *et al*. Pattern and Frequency Reconfigurable Annular Slot Antenna Using PIN Diodes. IEEE Transactions on Antenna and Propagation. Feb., 2006. Vol. 54: 439-448.

141. J. Kim, C. S. Cho, and J. W. Lee. 5.2 GHz Notched Ultra-Wideband Antenna Using Slot-Type SRR. *Electronics Letters*. March 16, 2007. Vol. 42(6).

142. Wang-Sang Lee, Won-Gyu Lim, and Jong Won Yu. Multiple Band-Notched Planar Monopole Antenna for Multiband Wireless Systems. *IEEE Microwave and Wireless Components Letters*. Sept., 2005. Vol. 15(9).

143. Wang-Sang Lee *et al*. Compact Frequency-Notched Wideband Planar Monopole Antenna with L-Shape Ground Plane. *Microwave and Optical Technology Letters*. Aug. 20, 2005. Vol. 46(4).

144. Seokjin Hong, Kyungho Chung, and Jaehoon Choi. Design of a Band-Notched Wideband Antenna for UWB Applications. Antenna. *Antennas and Propagation Society International Symposium*. IEEE. 2006.

145. R. F. Harrington and J. R Mautz. Theory of Characteristic Modes for Conducting Bodies. IEEE Trans. Antenna Propagat. Sept., 1971. Vol. AP-19: 622-628.

146. Pele. I. *et al*. Antenna Design with Control of Radiation Pattern and Frequency Bandwidth. *Antennas and Propagation Society International Symposium*. IEEE. 2004.

147. Daniel Valderas et al. Design of UWB Folded-Plate Monopole Antenna Based on TLM. *IEEE Transaction on Antenna and Propagation*. June, 2006. Vol. 54(6).

148. Zeland Software, Inc. Fidelity Manual: Getting Started, EM Analysis and Simulation. Zeland Software, Inc. 8th. ed. April, 2006.

149. Gh. Z. Rafi and L. Shafai. Wideband V-Slotted Diamond-Shaped Microstrip Patch Antenna. *Electronics Letters*. September 16, 2004. Vol. 40(19).

150. R. Bhalla and L. Shafai. Resonance Behavior of Single U Slot and Dual U Slot Antenna. *Antennas and Propagation Society International Symposium*. IEEE. 2001.

151. P. K. Singhal, Bhawana Dhaniram, and Smita Banerjee. A Stacked Square Patch Slotted Broadband Microstrip Antenna**.** *Journal of Microwaves and Optoelectronics.* August, 2003. Vol. 3(2).

152. Verma Y. K. and Verma A. K. Accurate Determination of Dielectric Constant of Substrate Materials Using Modified Wolff Model. *Microwave Symposium Digest 2000.* IEEE MTT-S International. 2000.

153. Schaubert, D. H., Pozar, D. M, and Adrian A. Effect of Microstrip Antenna Substrate Thickness and Permittivity: Comparison of Theories with Experiment. *IEEE Transactions on Antenna and Propagations*. June, 1989. Vol. 37(6): 677-682.

154. Nader Behdad and Kamal Sarabandi. A Compact Antenna for Ultra Wideband Applications. IEEE Transactions on Antenna and Propagation. Vol. 53(7). July 2005. 2185–2192.

155. Gary E. Evans. *Antenna Measurement Techniques*. Boston, London: Artech House. 1990.

156. Greg Hindman and Allen C. Newell. Simplified Spherical Near-Field Accuracy Assessment. *Technical Paper*. Nearfield System, Inc. 2004.

157. Allen Newell and Greg Hindman. Planar and Spherical Near-Field Range Comparison with -60 dB Residual Error Level. *Technical Paper*. Nearfield System, Inc. 2004.

158. Yusnita Rahayu et al. Ultra Wideband Technology and Its Applications. International Conference Wireless on Optical Communication Networks (WOCN), Surabaya. East Java, Indonesia. May 5th-7th, 2008.

LIST OF AUTHOR'S PUBLICATIONS

National and International Conference Paper

1. Yusnita Rahayu, Razali Ngah and Tharek A. Rahman," Simulation of Wideband Inverted Suspended Patch Antenna", Asia Pacific Conference on Applied Electromagnetics (APACE), Johor Bahru, Malaysia. 20-21 December 2005. IEEE Catalog Number: 05EX1185C. ISBN: 0-7803-9432-1.
2. Razali Ngah, Yusnita Rahayu, Teguh Prakoso, and Mohd. Shukri Othman, "Printed Square UWB Antenna", International Conference on Electrical Engineering and Informatics (ICEEI), Bandung Institute of Technology, Bandung, Indonesia, 17th – 19th June 2007. ISBN: 978-979-16338-0-2.
3. Yusnita Rahayu, Tharek Abd. Rahman, Razali Ngah, Peter S. Hall, "Slotted UWB Antenna for Bandwidth Enhancement", Loughborough Antenna and Propagation Conference (LAPC), Loughborough, UK, 17th – 18th March 2008. IEEE Catalog Number: CFP0869B-PRT. ISBN: 978-1-4244-1893-0
4. Yusnita Rahayu, Tharek Abd. Rahman, Razali Ngah, Peter S. Hall, "A Small Novel Ultra Wideband Antenna with Slotted Ground Plane", International Conference on Computer and Communication Engineering (ICCCE-2008), Kuala Lumpur, Malaysia, 13th – 15th May 2008.
5. Yusnita Rahayu, Tharek Abd. Rahman, Razali Ngah, Peter S. Hall, "Numerical Analysis of Small Slotted UWB Antenna Based on Current Distribution for Bandwidth Enhancement", European Electromagnetics (EUROEM) 2008, Switzerland, 21st – 25th July 2008.
6. Yusnita Rahayu, Tharek Abd. Rahman, Razali Ngah, Peter S. Hall, "Ultra Wideband Technology and Its Applications", International Conference Wireless on Optical Communication Networks (WOCN), Surabaya, East Java, Indonesia, 5th – 7th May 2008.

7. Yusnita Rahayu, Tharek Abdul Rahman, Razali Ngah, P.S. Hall, "Asymmetrical Slotted UWB Antenna", International Symposium on Antenna and Propagation (ISAP), Taipei, Taiwan , 27th–30th October 2008. (*Submitted*).

Journal Paper

1. Yusnita Rahayu, Tharek Abd. Rahman, Razali Ngah, Peter S. Hall, "Numerical Analysis of the Beveled Polygonal UWB Monopole Antennas", Journal IET Electronics Letters, 2008. (*Submitted*).
2. Yusnita Rahayu, Tharek Abd. Rahman, RAzali Ngah, P.S. Hall, "Reconfigurable Slotted UWB Antenna with Band Notched Characteristics", IEEE Antenna Transactions and Propagations, 2008. (*Submitted*).
3. Yusnita Rahayu, Tharek Abd. Rahman, RAzali Ngah, P.S. Hall, "Reconfigurable T Slotted UWB Antenna with Band Notched Characteristics", Progress in Electromagnetic Research (PIER), MIT, 2008. (*Submitted*).

Paper in a Book

1. Yusnita Rahayu, Tharek Abd. Rahman, RAzali Ngah, P.S. Hall, "Numerical Analysis of Small Slotted Ultra Wideband Antenna Based on Current Distribution for Bandwidth Enhancement", Springer Publication, 2008. (*Accepted*).